eLife

Reviewed Preprint
v2 • September 23, 2025
Revised by authors

Reviewed Preprint
v1 • April 9, 2024

Neuroscience

# LRRK2 regulates synaptic function through modulation of actin cytoskeletal dynamics

**Giulia Tombesi, Shiva Kompella, Giulia Favetta, Chuyu Chen, Marta Ornaghi, Yibo Zhao, Ester Morosin, Martina Sevegnani, Adriano Lama, Antonella Marte, Ilaria Battisti, Lucia Iannotta, Nicoletta Plotegher, Laura Civiero, Franco Onofri, Britta J Eickholt, Giovanni Piccoli, Giorgio Arrigoni, Dayne Beccano-Kelly, Claudia Manzoni, Loukia Parisiadou, Elisa Greggio**

Department of Biology, University of Padova, Padua, Italy • School of Pharmacy and UK Dementia Research Institute, Cardiff University, Cardiff, United Kingdom • Northwest University, Chicago, United States • Institute for Biochemistry, Charité Universitätsmedizin Berlin, Berlin, Germany • Freie Universität Berlin, Berlin, Germany • School of Pharmacy, University College London, London, United Kingdom • CIBIO, University of Trento, Trento, Italy • Experimental Medicine, University of Genova, Genoa, Italy • IRCCS, Ospedale Policlinico San Martino, Genova, Italy • Department of Biomedical Sciences, University of Padova, Padua, Italy • Centro Studi per la Neurodegenerazione (CESNE), University of Padova, Padua, Italy • IRCCS San Camillo Hospital, Venice, Italy



**eLife Assessment**

This **important** work begins to understand how BDNF regulates the phosphorylation and activity of LRRK2. The overall strength of evidence has been assessed as **compelling**, though some claims are only partially supported. The work will be of interest for those that might pursue specific LRRK2 interactions and mutational effects on these pathways as the work continues to develop.

https://doi.org/10.7554/eLife.95987.2.sa3

## Abstract

Parkinson's disease (PD) is a multisystemic disorder that manifests through motor and non-motor symptoms. Motor dysfunction is the most debilitating and it is caused by the degeneration of dopamine-producing neurons in the substantia nigra pars compacta (SNpc). Increasing evidence suggests that synapse dysfunction precedes neuronal loss by years. Still, early synaptic alterations in PD remain poorly understood.

Here we integrate literature meta-analysis, proteomics and phosphoproteomics with biochemical, imaging and electrophysiological measurements in neurons and brains from knockout and knockin Lrrk2 mouse models, as well as human iPSC-derived neurons lacking LRRK2. We demonstrate that phosphorylation of LRRK2 at Ser935 and of RAB proteins is induced by brain-derived neurotrophic factor (BDNF) stimulation in differentiated SH-SY5Y cells and primary mouse neurons. Affinity-purification coupled with mass spectrometry (AP-MS/MS) revealed a significant remodelling of the LRRK2 interactome following BDNF treatment, with enhanced association of LRRK2 to a network of actin cytoskeleton-related

proteins. Gene-ontology analyses of both literature-curated LRRK2 interactors and phosphoproteome from striatal tissues with elevated LRRK2 activity (G2019S knockin mice) highlight synapse-actin remodelling as major affected pathways.

We further observed that loss of LRRK2 impairs BDNF signaling and alters postsynaptic density architecture. One month-old *Lrrk2* knockout mice display structural alterations in dendritic protrusions, a phenotype that normalizes with age. In human iPSC-derived neurons, BDNF enhances the frequency of miniature excitatory post-synaptic currents (mEPSC) in wild-type but not in LRRK2 knockout neurons, which appear to bypass this regulation through developmental compensation.

Taken together, our study discloses a critical role of LRRK2 in BDNF-dependent synaptic modulation and identifies the synaptic actin cytoskeleton as a convergent site of LRRK2's pathophysiological activity.

## Introduction

Synaptic damage and connectome dysfunction are emerging as early pathological events preceding neurodegeneration and the manifestation of clinical symptoms in multiple neurodegenerative disorders, including Parkinson's disease (PD).[1–5] PD is an age-related motor disorder for which no cure is available. The motor symptoms typically manifest as a consequence of the progressive loss of the dopaminergic neurons of the Substantia Nigra pars compacta (SNpc) projecting to the striatum.[6] The degeneration of the nigrostriatal projections precedes the loss of the dopaminergic cell bodies in the SNpc and synaptic failure may be the triggering cause of axonal deterioration.[5,7] Pre- and postsynaptic alterations were described in PD animal models.[5] For example, PD pathology was reported as associated with an evident striatal spine loss, that appeared to be correlated with the degree of dopamine denervation prevalently due to glutamate excitotoxicity in striatal neurons.[8,9]

Accumulating evidence indicate that more than half of the causative genes and risk factors for PD have a function at the synapse. Mutations in *LRRK2* gene represent the most common cause of autosomal dominant late onset familial PD and variations around the *LRRK2* locus increase lifetime risk for PD.[10] Pathogenic mutations are clustered into the enzymatic core of the LRRK2 protein, composed by a Roc/GTPase and a kinase domain, bridged by a COR scaffold.[11–13] The most frequent mutation (G2019S) located in the kinase domain results in a protein with a gain of kinase activity, associated with increased cellular toxicity.[11] Previous findings from our team and other laboratories suggested that LRRK2 sits at the crossroads between cytoskeletal dynamics and vesicular trafficking. LRRK2 activity seems to be modulated by interactions with a diverse array of cytoskeletal and vesicle-associated proteins, and it regulates membrane-trafficking events *via* phosphorylation of a subset of Rab GTPases, including RAB3, RAB8, RAB10, RAB12, RAB35 and RAB43 (reviewed in [14]).[15,16] LRRK2 subcellular localization is dynamically controlled by phosphorylation/dephosphorylation of a cluster of N-terminal serine residues (e.g. Ser935 and Ser910), which determines 14-3-3 protein binding.[17] Phosphorylation of LRRK2 Ser935 and Ser910 is regulated by multiple kinases, including casein kinase 1 alpha (CK1a), IKKs and protein kinase A (PKA),[18–20] and serves as a scaffold for 14-3-3 protein binding and LRRK2 subcellular localization.[17,21] In immune cells, extracellular signals such as Toll-like receptor 4 (TLR4) agonists stimulate LRRK2 Ser935 and Ser910 phosphorylation to positively modulate immune-related responses.[18,22] In contrast, the extracellular signals that orchestrate Ser935 phosphorylation enhancing LRRK2 activity in neurons are still unknown.

The ability of the neurons to relocate LRRK2 within or nearby the synapse could be particularly important as LRRK2 was suggested to provide the scaffold for the assembly of the signalling cascade effectors to sustain synaptic functions[15,23,24] In particular, LRRK2 has been shown

to regulate synaptic vesicles cycling at the presynaptic site through interaction and phosphorylation of a panel of pre-synaptic proteins,[25] such as NSF,[26] synapsin I,[27] EndophylinA,[28] synaptojanin-1[29] and DNAJC6/Auxilin.[30] Interestingly, recent literature supports a role for LRRK2 in the dendritic spine compartment, where it was suggested to influence AMPA receptor trafficking,[31,32] spine morphology and functionality in developing brains.[33–35]

Here, starting from the observation that brain derived neurotrophic factor (BDNF) stimulates LRRK2 Ser935 and RABs phosphorylations in neurons, we used unbiased protein-protein interaction (PPI) and phosphoproteomic investigations to disclose a novel function of LRRK2 in regulating actin-dependent synaptic dynamics in complementary neuronal models.

# Results

## BDNF treatment rapidly increases LRRK2 phosphorylation at Ser935

Neurotrophic factors plastically shape neuronal activity by binding to their cognate receptor tyrosine kinases.[36] Brain-derived neurotrophic factor (BDNF) is particularly important to modulate neurotransmission in the cortico-striatal circuitry.[37] This circuitry is relevant for PD and presents with the highest LRRK2 expression in comparison with the rest of the brain.[38,39] To address whether LRRK2 activity is stimulated by BDNF, we prepared primary mouse cortical neurons from C57BL/6J wild-type mice and stimulated them with 100 ng/ml of BDNF at days *in vitro* 14 (DIV14) when synapses are fully functional (**Fig. 1A**) and LRRK2 expression is detectable.[40] Western blot analysis revealed a rapid and transient increase of Ser935 phosphorylation after BDNF treatment (**Fig. 1B** and **1C**). Of interest, BDNF failed to stimulate Ser935 phosphorylation when neurons were pretreated with the LRRK2 inhibitor MLi-2, indicating that either LRRK2 kinase activity controls the upstream kinases activated by BDNF or that the binding with MLi-2, a type I inhibitor, locks the kinase in a conformation that favors dephosphorylation/hinders phosphorylation during the stimulus.[41]

To gain mechanistic insights into the effects of BDNF stimulation on LRRK2 function, we differentiated neuroblastoma SH-SY5Y cells with 10 μM retinoic acid (RA) treatment for 6 days[42] and measured BDNF response by monitoring Tropomyosin receptor kinase B (TrkB) levels and phosphorylation of AKT and ERK1/2, two major downstream effector pathways of BDNF/TrkB signaling (**Fig. 1D**).[43] Expression of TrkB was undetectable in undifferentiated SH-SY5Y cells but was induced upon RA differentiation (**Fig. 1E**). Accordingly, differentiated SH-SY5Y cells respond to 100 ng/ml BDNF stimulation, as evidenced by increased phosphorylation of ERK1/2 and AKT (**Fig. 1F-G**). LRRK2 expression, low in undifferentiated cells, also increased upon differentiation (**Fig. S1A**), indicating that this is a suitable neuronal model to study endogenous LRRK2. Notably, BDNF stimulation enhanced Ser935 phosphorylation with kinetics comparable with that observed in primary neurons (**Fig. 1H** and **1I**). To determine whether BDNF-induced Ser935 phosphorylation reflects LRRK2 kinase activation, we assessed phosphorylation of RAB10 at Thr73, an established LRRK2 substrate. As illustrated in **Fig. 1J** and **1K**, BDNF treatment significantly increased RAB10 phosphorylation, supporting the role of BDNF as a physiological activator of LRRK2.

## BDNF promotes LRRK2 interaction with actin cytoskeleton components enriched at the postsynapse

To clarify the implications of BDNF-mediated LRRK2-activation on neuronal function, we used affinity purification coupled with mass spectrometry (AP-MS/MS). As the yields of endogenous LRRK2 purification were insufficient for AP-MS/MS analysis, we generated polyclonal SH-SY5Y

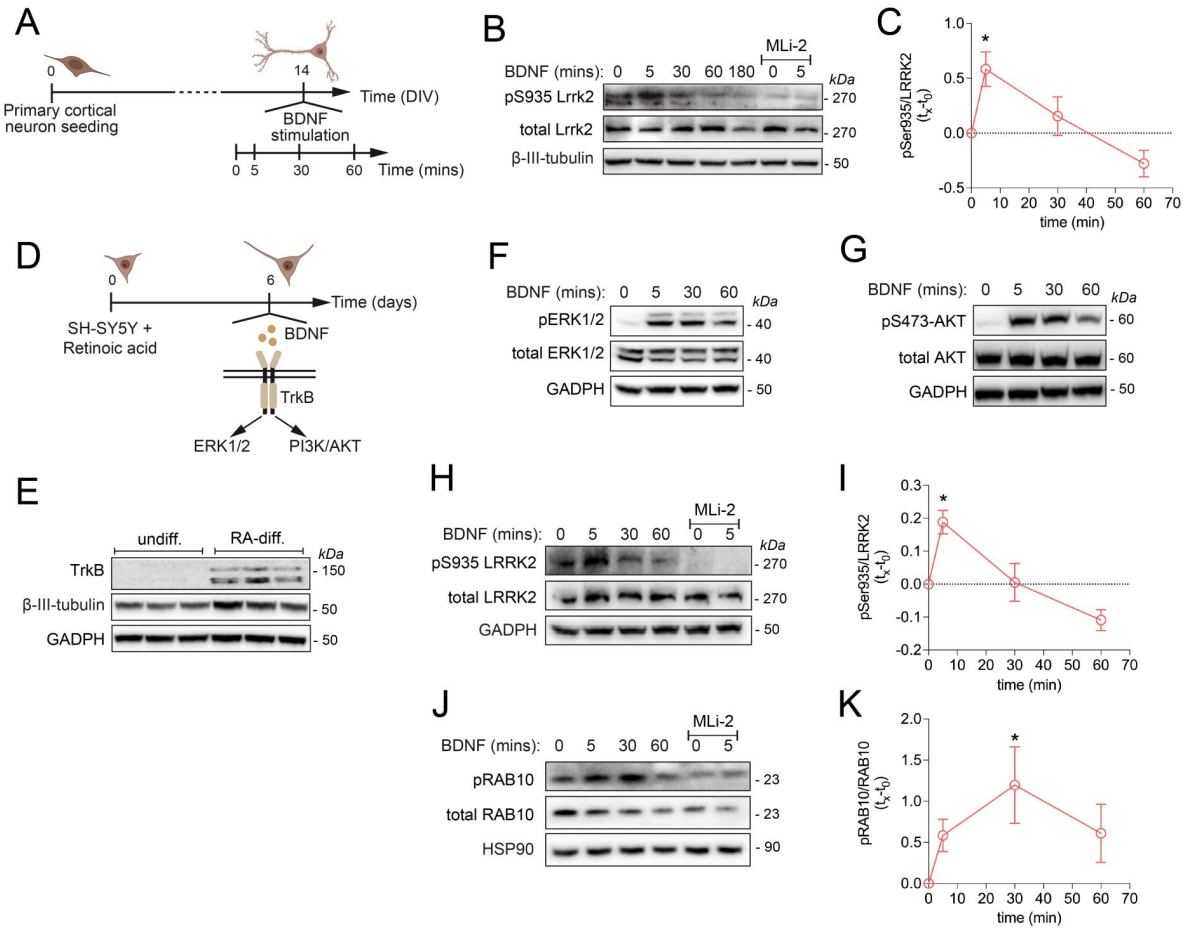


## Figure 1.

### LRRK2 phosphorylation at ser935 rapidly and transiently increases upon BDNF stimulation in primary mouse cortical neurons and differentiated SH-SY5Y cells.

**(A)** Schematic representation of the experimental setting of (B). **(B)** Phospho-Ser935 and total Lrrk2 protein levels of primary cortical neurons at DIV14 treated with 100 ng/mL BDNF for 0, 5, 30, 60 180 mins. MLi-2 was used at 500 nM for 90 mins to inhibit Lrrk2 kinase activity. **(C)** Quantification of n=6 independent experiments of (B). One-way ANOVA (***$P < 0.001$), Dunnett's multiple comparison test (t=0 compared with different time points, *$P < 0.05$ t=0 vs. t=5'). **(D)** Schematic representation of the experimental setting of (F) and (G). **(E)** TrkB protein levels in undifferentiated or retinoic acid-differentiated SH-SY5Y cells. **(F)** Phospho Thr202/185 ERK1/2, total ERK1/2 and **(G)** phospho Ser473 AKT, total AKT protein levels of retinoic acid-differentiated SH-SY5Y cells stimulated with 100 ng/mL BDNF for 0, 5, 30, 60 mins. **(H)** Phospho-Ser935 and total LRRK2 protein levels of retinoic acid-differentiated SH-SY5Y cells stimulated with 100 ng/mL BDNF for 0, 5, 30, 60 mins. MLi-2 was used at 500 nM for 90 mins to inhibit LRRK2 kinase activity. **(I)** Quantification of (H) (n=4 independent experiments). One-way ANOVA (**$P < 0.01$), Dunnett's multiple comparison test (*$P < 0.05$ t=0 vs. t=5'). **(J)** Phospho-T73 and total RAB10 protein levels of retinoic acid-differentiated SH-SY5Y cells stimulated with 100 ng/mL BDNF for 0, 5, 30, 60 mins. MLi-2 was used at 500 nM for 90 mins to inhibit LRRK2 kinase activity. **(K)** Quantification of (J) (n=4 independent experiments). One-way ANOVA ($P > 0.5$), Dunnett's multiple comparison test (*$P < 0.05$ t=0 vs. t=30').

cells stably expressing GFP-LRRK2 wild-type or GFP control. Notably, in this model, Ser935 phosphorylation showed only a modest increase upon BDNF treatment (**Fig. S1B**), and prolonged stimulation led to a reduction of Ser935 phosphorylation below baseline levels (**Fig. 1B–C** and **Fig. 1H-I**). We hypothesized that this apparent limited response could be due to high basal levels of Ser935 phosphorylation, approaching a ceiling effect under resting conditions. This is consistent with previous mass spectrometry analyses reporting that Ser935 is nearly fully phosphorylated (~100%) in the brain under basal conditions.[44] To test whether high basal phosphorylation masks BDNF-induced increases, we pretreated the cells with MLi-2 for 90 minutes to lower Ser935 phosphorylation. After inhibitor washout, cells were stimulated with BDNF at multiple time points. In these conditions, BDNF robustly increased both Ser935 and RAB phosphorylation, peaking at 5–15 minutes and returning to baseline by 60–180 minutes (**Fig. S1C**). Notably, while the magnitude of pSer935 phosphorylation at the peak was similar to untreated controls - supporting the idea that Ser935 is near saturation under basal conditions - RAB phosphorylation levels significantly exceeded those of untreated cells. This indicates that, unlike Ser935, RAB phosphorylation remains far from saturated under basal conditions and serves as a more dynamic readout of LRRK2 kinase activity. These data further support BDNF as a physiological activator of LRRK2 and validate GFP-LRRK2 SH-SY5Y cells for interrogating stimulus-induced changes in LRRK2 signaling and protein interactions.

Next, we used GFP-trap purification to isolate GFP or GFP-LRRK2 from RA-differentiated cells unstimulated or stimulated with BDNF for 15 mins prior to MS analysis. The unstimulated LRRK2 interactome (GFP-LRRK2 vs. GFP) is large (207 significant hits) and consistent with previous computational analysis of LRRK2 PPIs (**Fig. 2A**),[45,46] In particular, we confirmed interactions with known LRRK2 binders including 14-3-3 proteins, cytoskeletal proteins and protein translation factors (Supplementary.xls **table 1**). Since BDNF is synaptically released and influences pre- and post-synaptic mechanisms, we used SynGO[47] to search for LRRK2 interactors that are enriched at the synapse. About one-third (35%) of LRRK2 PPI under unstimulated conditions are SynGO annotated genes; among them, 33% are presynaptic proteins and 66% are post-synaptic proteins (**Fig. 2B**). The most significant enriched categories were pre- and post-synaptic ribosome and post-synaptic actin cytoskeleton (**Fig. 2B**).

We next compared unstimulated vs. BDNF-stimulated LRRK2 interactome. As shown in **Fig. 2C**, 15 minutes of BDNF stimulation reshapes LRRK2 PPI, with a group of interactors increasing binding with LRRK2 (blue dots) and another group decreasing binding (orange dots). Inclusion criteria were: (i) *P* value < 0.05 and fold change (FC) > 0.5 or FC < -0.5, or (ii) absolute fold change (|FC|) > 1 regardless of the *P* value. In this way, we increased the discovery power for gene ontology analysis. SynGO gene ontology revealed that 10 out of 19 hits with increased binding after BDNF [BDNF(+)] and 21 out of 50 hits with decreased binding [BDNF(-)] are synaptic proteins (**Fig. 2C** inset). Among synaptic interactors, the BDNF(+) binders are enriched in actin-cytoskeleton-related GO:BP categories while the BDNF(-) binders are enriched in protein translation GO:BP categories (**Fig. 2D**). Furthermore, 80% of synaptic BDNF(+) LRRK2 binders (DBN1, ARPC2, ACTR2, ACTR3, CFL1, CALD1, ACTN1, FLNA) and 62% of synaptic BDNF(-) binders (RPS2, RPS4X, RPS7, RPS9, RPS11, RPS13, RPS15A, RPL13, RPL23, RPL26, RPL27A, TUFM, EEF1A2, PCBP1) form functional and physical interaction networks (**Fig. 2E-F**).

To validate these findings, we performed western blot analysis on the AP samples analyzed by MS. We selected drebrin, encoded by *DBN1*, because it sits at the center of the BDNF(+) network (**Fig. 2E**, inset SynGO) and, in DIV14 primary neurons, it colocalizes with PSD95, a postsynaptic marker (**Fig. S2A**), confirming previous observations.[48] As predicted, BDNF treatment increases LRRK2:drebrin interaction by approximately twofold (**Fig. 2G** and **Fig. S2B**). To further characterize this interaction, we performed co-immunoprecipitation in HEK293T cells co-expressing Flag-LRRK2 and either full-length YFP-drebrin, its N-terminal (1-256 aa), or C-terminal (256-649 aa) fragments. These experiments confirmed a direct interaction between LRRK2 and drebrin, with the N-terminal domain appearing to mediate the majority of the binding (**Fig.**

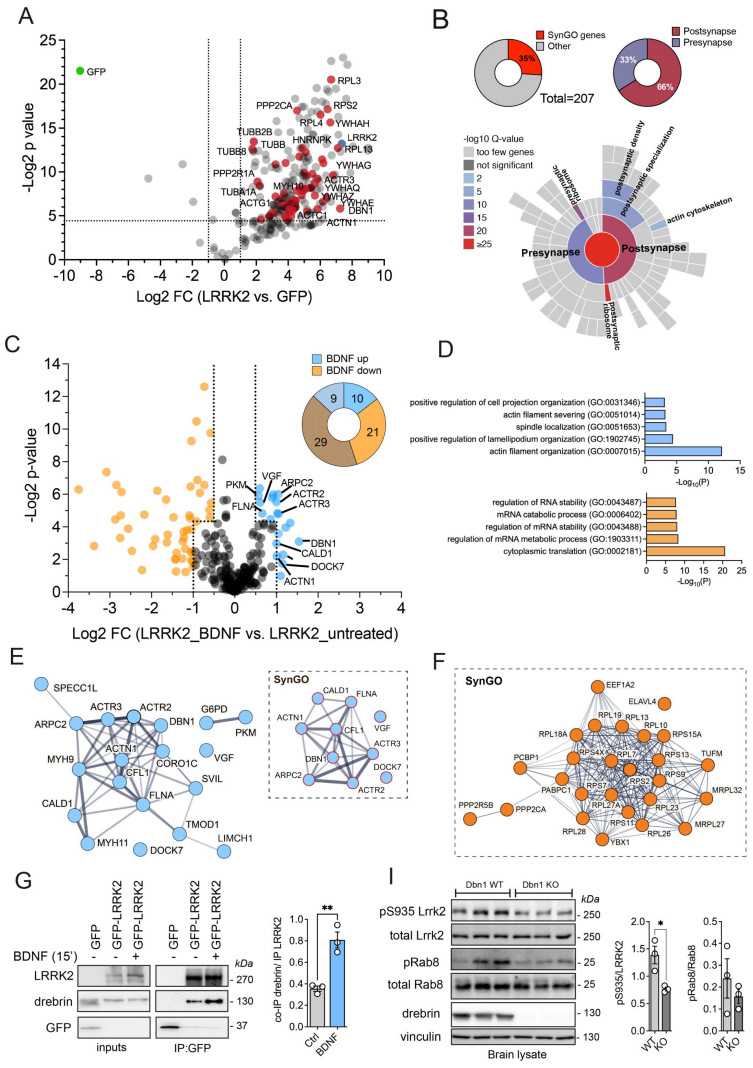


## Figure 2.

### BDNF promotes LRRK2 interaction with post-synaptic actin cytoskeleton components.

**(A)** Volcano plot of GFP-LRRK2 versus GFP enriched interactors from differentiated SH-SY5Y cells (n=6 replicates: n=3 independent experiments each with 2 technical replicates). Interactors that were considered for SynGO analysis have adjusted *P* value < 0.05 and FC > 2. (red dots). **(B)** Donut charts with % of SynGO genes among the total 207 LRRK2 interactors (A) and with % of presynaptic and postsynaptic proteins among SynGO genes. SynGO-CC terms visualized with a sunburst plot showing significant categories (below). **(C)** Volcano plot of GFP-LRRK2 +/-BDNF enriched interactors from differentiated SH-SY5Y cells (n=6 replicates: n=3 independent experiments each with 2 technical replicates). Interactors selected for pathway enrichment analysis fall into two categories: (i) adjusted *P* value < 0.05 and FC > 0.5 or FC < -0.5, or (ii) |FC| > 1 regardless of the *P* value. Proteins with increased interaction upon BDNF stimulation are blue-labeled, proteins with decreased interaction are orange-labeled. Donut chart showing the number of SynGO annotated genes versus non synaptic proteins in BDNF-up versus BDNF-down interactors (top right). **(D)** G:profiler g:GOSt pathway enrichment analysis showing the top 5 enriched biological processes (BP) categories of BDNF-increased interactors (top, blue bar graph) versus BDNF-decreased interactors (bottom, orange bar graph). GO analysis was performed with g:Profiler on 04/14/2025 (version e112_eg59_p19_25aa4782, database updated on 03/02/2025); enriched terms determined using g:SCS correction an size terms set to <500 to increase specificity. **(E)** Protein-Protein Interaction Networks built with STRING (*https://string-db.org/*) of all BDNF(+) interactors and SynGO BDNF-increased interactors (inset) and **(F)** of SynGO BDNF-decreased interactors. **(G)** Validation of increased drebrin:LRRK2 interaction upon BDNF treatment (15 mins) and quantification (one sample t-test, *P*<0.01). Samples are the same analyzed in the three rounds of MS (A). **(H)** Western blot analysis of brain samples from WT and *Dbn1* (drebrin) KO mice assessing Lrrk2 Ser935 and Rab8 (pan Rabs) phosphorylation Differences between the two genotypes have been evaluated using Student's t-test (significance *$P$<0.05 pSer935), *n*=3 animals per genotype per age.

| Capacitance | | | | Access Resistance | | | |
|---|---|---|---|---|---|---|---|
| **50 DIV** | | | | **50 DIV** | | | |
| | Mean (pF) | SEM | n | | Mean (MΩ) | SEM | n |
| WT -BDNF | 14.14 | 1.858 | 12 | WT -BDNF | 18.54 | 1.312 | 12 |
| WT +BDNF | 15.1 | 1.331 | 12 | WT +BDNF | 18.27 | 1.053 | 12 |
| KO -BDNF | 16.21 | 2.299 | 9 | KO -BDNF | 20.11 | 1.467 | 9 |
| KO +BDNF | 14.66 | 1.295 | 11 | KO +BDNF | 18.71 | 1.884 | 11 |
| **70 DIV** | | | | **70 DIV** | | | |
| | Mean (pF) | SEM | n | | Mean (MΩ) | SEM | n |
| WT -BDNF | 23 | 2.177 | 16 | WT -BDNF | 21.18 | 1.372 | 16 |
| WT +BDNF | 22.4 | 2.579 | 12 | WT +BDNF | 21.6 | 1.273 | 12 |
| KO -BDNF | 24.64 | 2.555 | 13 | KO -BDNF | 22.36 | 1.835 | 13 |
| KO +BDNF | 20.03 | 2.232 | 13 | KO +BDNF | 15.1 | 1.122 | 13 |
| **90 DIV** | | | | **90 DIV** | | | |
| | Mean (pF) | SEM | n | | Mean (MΩ) | SEM | n |
| WT -BDNF | 12.51 | 1.994 | 8 | WT -BDNF | 17.6 | 2.221 | 8 |
| WT +BDNF | 20.9 | 6.365 | 7 | WT +BDNF | 18.64 | 1.68 | 7 |
| KO -BDNF | 24.23 | 3.062 | 7 | KO -BDNF | 16.66 | 1.609 | 9 |
| KO +BDNF | 24.96 | 6.49 | 8 | KO +BDNF | 14.64 | 1.591 | 8 |

**Table 1.**

**Capacitance and access resistance of LRRK2 KO and WT cortical neurons at 50, 70 and 90 DIV with or without BDNF stimulation.**

**S2C**). Notably, this region contains both the ADF-H (actin-depolymerizing factor homology) domain and a coiled-coil motif known to associate with actin.[48,49] Finally, we observed a significant decrease in Ser935 phosphorylation and a trend decrease in Rab phosphorylation in *Dbn1* KO mouse brains (**Fig. 2I**). This finding further strengthen the notion that drebrin forms a complex with LRRK2 that is important for its activity, e.g. upon BDNF stimulation.

We conclude that BDNF stimulation engages LRRK2 into actin cytoskeleton dynamics via its interaction with actin-regulatory proteins. While SH-SY5Y cells may only contain sparse synapses[50], the enrichment of this BDNF-dependent protein network at synapses indicates that this site might be relevant for LRRK2 function. Our findings also suggest that a pool of LRRK2 binds protein translation factors under unstimulated conditions, which redistributes toward actin-rich domains upon BDNF-TrkB signaling.

## Convergence on actin and synaptic processes in literature-curated LRRK2 interactome and LRRK2 G2019S striatal phospho-proteome

We recently investigated the molecular environment surrounding LRRK2 specifically by constructing the protein-protein interaction (PPI) interactome around LRRK2 based on PPIs derived from peer reviewed literature. After filtering the LRRK2 PPIs for reproducibility (keeping only those interactions that have been reported at least twice in literature or at least replicated with 2 different interaction detection methods) we obtained the interactions linking across the LRRK2 interactors thus effectively building the LRRK2 protein interaction network ($LRRK2_{net}$) which describes the protein milieu around LRRK2 in the cellular context (see Zhao *et al.*[51] for details). The $LRRK2_{net}$ was topologically analyzed to identify the portions (clusters) of the network that are more densely connected locally in comparison with the overall connectivity of the entire network as these topological clusters are likely to represent functional units.[52] Among the 11 topological clusters identified in Zhao *et al.*[51], we further elaborated on one cluster in particular, containing 41 genes (**Fig. 3A**) and found that it exhibited significantly GO-BP enriched terms into semantic categories related to: actin polymerization (16 GO-BP terms), synaptic vesicles (5 GO-BP terms), postsynaptic actin-cytoskeleton (2 GO-BP terms), lamellipodium (6 GO-BP terms), cell-neuron projection/size (2 GO-BP terms), DNA recombination/repair (4 GO-BP terms) and uncategorized (6 GO-BP terms) (**Fig. 3B** and Supplementary.xls table 2). Out of the 41 proteins forming the cluster, 23 are proteins associated with the actin cytoskeleton including the 4 larger nodes (where the dimension of the nodes is directly proportional to the node degree/connections within the network): DBN1/drebrin, CAPZA2 and LIMA whose association with LRRK2 was identified in Meixner *et al.*[53] and IQGAP1 identified in Liu *et al.*[54] (**Fig. 3C**). Given the overrepresentation of synapse-related GO-BP terms, we further performed GO functional enrichment using SynGO and mapped 16 synaptic proteins within the cluster (**Fig. 3C**). Remarkably, DBN1/drebrin is a key protein in the cluster, as it engages in multiple interactions (16 edges) and sits at the interface between the nodes involved in GO:BPs functions related to the actin cytoskeleton (blue-colored nodes) and to the synapse (red-colored nodes) (**Fig. 3C** and **Fig. S3**).

Given the multiple lines of evidence pointing to the synapse-actin couple as a key area for LRRK2 function, and based on the increased LRRK2 activity upon neurotrophin stimulation, we next asked whether LRRK2 kinase activity is also linked to synaptic function. To this aim, we performed an unbiased phospho-proteomic characterization of the striatum, using knockin mice expressing the hyperactive G2019S mutation to probe the contribution of kinase activity. We isolated total striatal proteins from WT and G2019S striata, enriched the phosphopeptides (**Fig. 3D**) (also see[55]), and normalized the $\log_2$ intensity of each phosphopeptide to the $\log_2$ intensity of its corresponding total protein. Comparing WT and G2019S samples, we identified 228 differentially regulated phosphopeptides ($P$ value < 0.05 and $|\text{Log}_2$ fold change (FC)$|$ > 2) (**Fig. 3E** and supplementary.xls table 3). Gene ontology analysis of differentially phosphorylated proteins, using stringent term size (<200 genes), revealed enrichment of post-synaptic spines and presynaptic

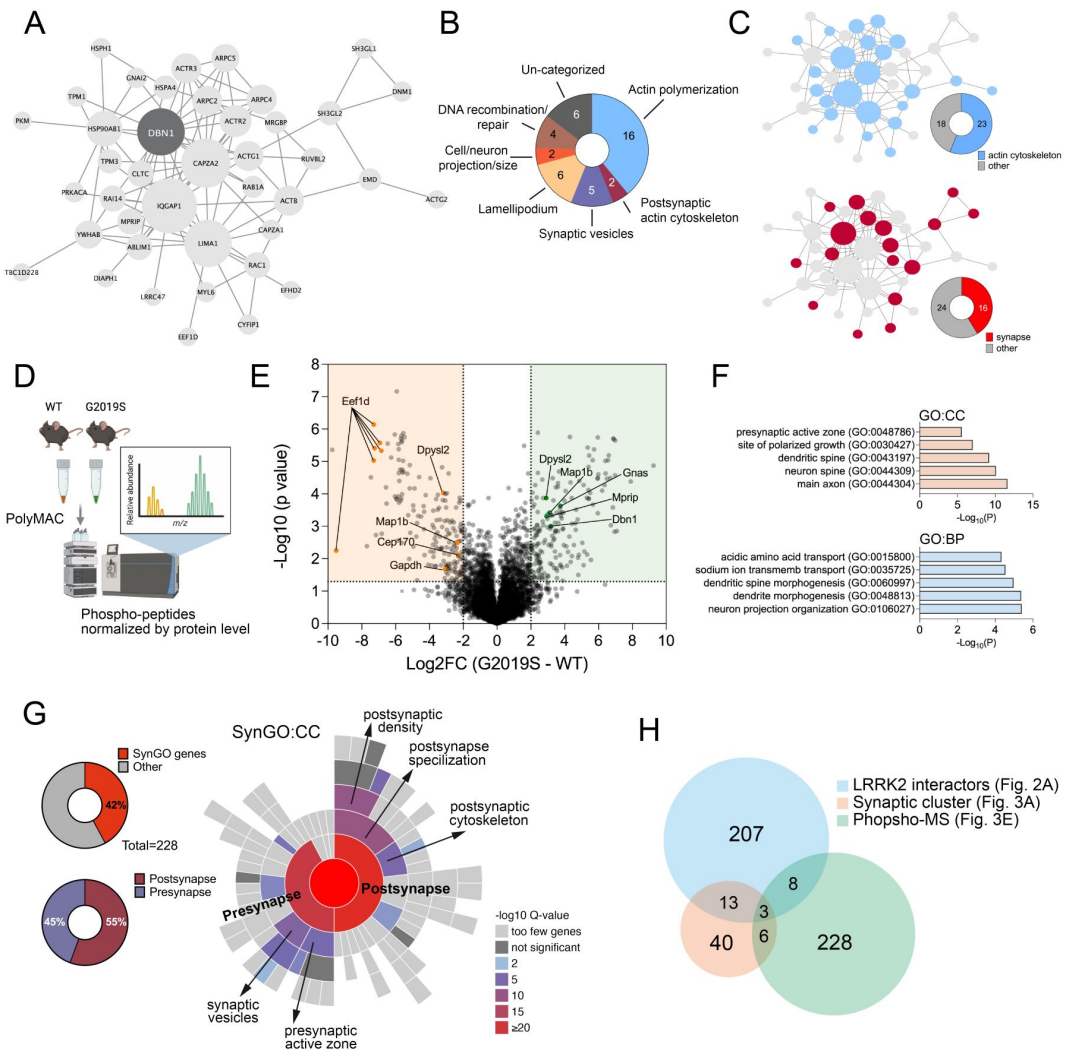


## Figure 3.

### Convergence on actin and synaptic processes in literature-curated LRRK2 interactors and the LRRK2 G2019S striatal phospho-proteome.

**(A)** Network graph showing one of the topological clusters extracted from the LRRK2 protein-protein interaction network. Proteins are represented as nodes while protein-protein interactions are represented as edges. Node size is proportional to the degree centrality: the larger the node, the higher the degree, the more interactions the node has in the network. **(B)** Gene Ontology biological-processes (GO-BPs) enrichment; the analysis was performed using g:Profiler, GO-BPs with term size >500 were discarded as general terms and the remaining terms was clustered based on semantics using the keywords: Postsynaptic (Actin) Cytoskeleton, Lamellipodium, Synaptic Vesicle, Actin Polymerization/Nucleation, DNA Recombination/Repair, Cell/Neuron Projection. **(C)** Upper network graph as in (A) highlighting actin cytoskeletal proteins in blue and the proportion over the total (pie chart) and lower network graph as in (A) highlighting synaptic proteins in red and the proportion over the total (pie chart). (**D**) Experimental design of phospho-proteomic analysis comparing WT and G2019S knockin mouse striata. Phosphopeptide abundances were normalized to total proteins levels. **(E)** Volcano plot of differentially enriched phosphopeptides, expressed as Log2 fold change (FC) between G2019S-KI versus WT. Highlighted peptides correspond to LRRK2 interactors discovered by MS in **Figure 2**. **(F)** GO enrichment analysis performed with g:Profiler (accessed on 01/23/2025; version e94_eg41_p11), filtering for GO terms with size <200 to avoid overly general categories. The top 5 most significant terms from the Cellular Component (CC) and Biological Process (BP) domains are shown. **(G)** Sunburst plot showing enriched SynGO cellular component (CC) categories and the percentage of SynGO genes among the differentially phosphorylated proteins. **(H)** Venn diagrams showing common and unique hits across the three datasets: GFP-LRRK2 interactomics, synaptic cluster and phospho-MS.

active zones (**Fig. 3F**). A SynGO analysis confirmed enrichment of both pre- and postsynaptic categories, with particular high significance for terms related to the postsynaptic cytoskeleton (**Fig. 3G**). Despite starting from whole striatal tissue - which contains a mix of different cellular populations - the strong synaptic enrichment of phosphorylation changes further supports the critical role of this compartment in LRRK2 brain function. By merging the three datasets (the LRRK2 interactome in SH-SY5Y cells, the literature-based synaptic/actin cluster and the phosphoproteomic dataset from G2019S striatum), we found three common hits: Dbn1/drebrin, Eef1d and Mprip (**Fig. 3H**). In particular, phosphorylation of drebrin at Ser339 was 3.7 fold higher in G2019S mice. This site is located in the N-terminal region of drebrin, which exhibited higher affinity for LRRK2 (**Fig. 3E** and **Fig. S2C**). To infer the potential physiological relevance of this phosphorylation, we examined its detection frequency in phosphoproteomic studies (67 observations, *https://www.phosphosite.org/proteinAction.action?id=2675&showAllSites=true*) and assessed its predicted pathogenicity using AlphaMissense.[56] Although the AlphaFold structural model has low confidence in this region of drebrin, amino acid substitutions at Ser339 are predicted to be non-pathogenic (**Fig. S4**), supporting the notion that LRRK2-mediated phosphorylation at this site acts as a regulatory modification for drebrin activity.

## BDNF-mediated signalling is impaired in LRRK2 knockout neurons

Having collected multiple lines of evidence linking LRRK2 to actin cytoskeletal proteins enriched at the synapse, and given that BDNF - a neurtrophin known to promote synaptic plasticity - activates LRRK2 (**Figure 1**), we next asked whether loss of LRRK2 could affect BDNF signalling. To this end, we generated LRRK2 knockout (KO) SH-SY5Y cells with CRISPR/Cas9 editing (**Fig. S5** and supplemental file 1), differentiated them with RA and assessed their response to BDNF stimulation. While application of BDNF increased AKT and ERK1/2 phosphorylation in naïve SH-SY5Y, as expected, LRRK2 KO cells exhibited a weaker response (**Fig. 4A-B**). These results indicate that LRRK2 acts downstream of TrkB and upstream of AKT and ERK1/2, in line with its rapid and transient phosphorylation kinetic upon BDNF stimulation (**Fig. 1B-C**).

Likewise, *Lrrk2* WT and KO primary cortical neurons at DIV14 were stimulated with BDNF at different timepoints. Similar to differentiated SH-SY5Y cells, *Lrrk2* WT neurons responded to BDNF by rapidly increasing Akt and Erk1/2 phosphorylation, whilst KO neurons exhibited a significantly reduced phosphorylation of Akt and Erk1 (**Fig. 4C-D**).

Considering that (i) BDNF induces dendritic spine formation, maturation and structural plasticity,[57,58] (ii) BDNF(+) LRRK2 interactors are actin-related proteins enriched at the postsynapse (**Fig. 2**) and (iii) loss of LRRK2 causes reduced phosphorylation of BDNF/TrkB downstream kinases AKT and ERK1/2 (**Fig. 4A-D**), we evaluated BDNF-induced PSD95 sites in the presence or absence of LRRK2, as a potential process affected by LRRK2 deletion. Primary cortical neurons were transfected with GFP filler at DIV4 and treated with BDNF for 24 h at DIV13 following previous protocols[59,60] (**Fig. 4E**). As shown in **figure 4F-G**, BDNF treatment significantly increased the density of PSD95-positive puncta in WT cultures ($P < 0.001$). In contrast, *Lrrk2* KO neurons did not exhibit increased PSD95 puncta upon BDNF. These findings further support a role for LRRK2 within the BDNF signalling cascade and show that the absence of LRRK2 impairs the remodelling of dendrite protrusions in response to BDNF stimulation.

## Morphological Alterations of Dendritic Protrusions in Young Lrrk2 Knockout Mice

Based on *in vitro* results indicating that BDNF stimulates LRRK2 activity and promotes its recruitment to the actin-cytoskeleton, enhancing the number of PSD95-positive dendritic protrusions, we next investigated whether loss of *Lrrk2* results in dendritic spine defects in the mouse brain. During development, dendritic spines are highly dynamic, with a rate of extension and retraction that allows proper and accurate synapse formation and neuronal circuit assembly.[61] By the adulthood, dendritic spines formation, motility, and pruning decrease

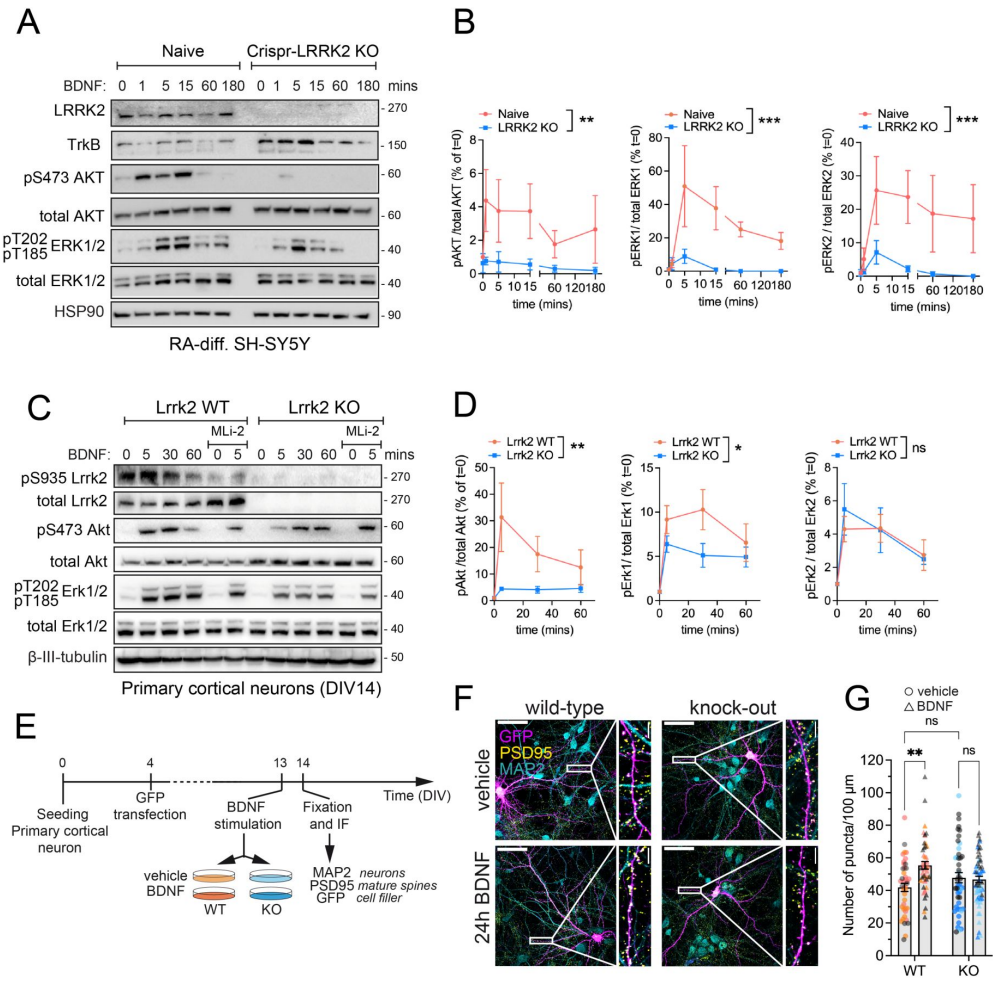


## Figure 4.

### BDNF signaling is impaired in *Lrrk2* knockout neurons.

**(A)** Six-day RA-differentiated SH-SY5Y naïve and CRISPR-LRRK2 KO cells stimulated with BDNF at different time points (0, 1, 5, 15, 60, 180 mins). Anti-TrkB antibodies were used to confirmed expression of BDNF receptor. To compare BDNF-induced signaling in naïve vs LRRK2-KO cells, phosphorylated Akt (S473) and Erk1/2 (T185/T202) were evaluated. **(B)** Quantification of phosphorylated proteins show from *n*=3 independent differentiation experiments. Two-way ANOVA; phospho-Akt: interaction *P*=0.7079, F (5, 24) = 0.5896; genotype: ***P*=0.0014, F (1, 24) = 13.07; time: *P*=0.5610, F (5, 24) = 0.7994. Phospho-Erk1: interaction *P*=0.0783, F (5, 24) = 2.284; genotype: ****P*=0.0003, F (1, 24) = 17.58; time: **P*=0.0244, F (5, 24) = 3.174. Phospho-Erk2: interaction: *P*=0.3725, F (5, 24) = 1.128; genotype: ****P*=0.0008 F (1, 24) = 14.59; time: *P*=0.1356, F (5, 24) = 1.879. **(C)** DIV14 primary cortical neurons from WT vs KO mice stimulated with BDNF at different time points (0, 5, 15, 30, 60 mins) in the presence or absence of LRRK2 inhibitor MLi-2 (90 min, 500 nM). To compare BDNF-induced signaling in WT vs KO neurons, phosphorylated Akt (S473) and Erk1/2 (T185/T202) were evaluated. Phosphorylated LRRK2 was assessed with pS935 antibodies. **(D)** Quantification of phosphorylated proteins show from *n*=9 independent cultures. Two-way ANOVA; phospho-Akt: interaction *P*=0.1186, F (3, 63) = 2.031; genotype: ***P*=0.0037, F (1, 63) = 9.101; time: *P*=0.0342, F (3, 63) = 3.069. Phospho-Erk1: interaction *P*=0.3256, F (3, 64) = 1.177; genotype: **P*=0.0201, F (1, 64) = 5.680; time: *****P*<0.0001, F (3, 64) = 10.04. Phospho-Erk2: interaction *P*=0.8524, F (3, 62) = 0.2622; genotype: *P*=0.7528, F (1, 62) = 0.1001; time: ****P*=0.0003, F (3, 62) = 7.428. **(E)** Overview of the experimental workflow to induce spine formation/maturation. **(F)** Representative confocal images of primary cortical neurons stimulated with 100 ng/ml of BDNF or vehicle control for 24 hours. GFP has been transfected at DIV4 to fill the neuroplasm and visualize individual dendrites, MAP2 is a neuronal marker and PSD95 is a marker of mature spines. **(G)** Quantification of the number of PSD-positive puncta per unit of length (100 µm). Dots represents individual segments (*nýý*20 neurites from *n*=5-6 neurons per replicate) and colors define neuronal cultures prepared in different days from pulled pups (*nýý*8 pups per culture per genotype, *n*=3 independent cultures). Two-way ANOVA; interaction ***P*=0.0038, F (1, 191) = 8.584; genotype: *P*=0.5833, F (1, 191) = 0.3020; treatment: **P*=0.0126, F (1, 191) = 6.346. Šídák's multiple comparisons test: vehicle vs. BDNF (WT) ****P*=0.0005; vehicle vs. BDNF (KO) *P*=0.9440; Vehicle (WT) vs. vehicle (KO) *P*= 0.3756.

reaching a relatively stable number of protrusions.[62] Since spines dynamics vary according to the stage of brain development, we performed a longitudinal analysis of young (1 month-old), adult (4 month-old) and aged (18 month-old) *Lrrk2* WT and KO mice in order to capture any age-dependent defect (**Fig. 5A**). We focused on the dorsal striatum, a region highly enriched in SPNs that receives excitatory afferents from the cortex and dopaminergic modulation from the SNpc. This region is relevant in the prodromal stages of PD neurodegeneration[63] and expresses high levels of LRRK2[38,64]. Moreover, several studies showed a key role of LRRK2 in shaping the structure and function of excitatory synapses in the striatum.[33,34,65,66] We evaluated the number and morphology of dendritic spines using Golgi-Cox staining (**Fig. 5B**). The total number of protrusions varied across ages, but there were no differences between the two genotypes (**Fig. 5C**). Instead, the width and the length of the protrusions were reduced in 1 month-old Lrrk2 KO striata with respect to WT. Specifically, the average neck height was 15% shorter and the average head width was 27% smaller, indicating that the protrusions are smaller in *Lrrk2* KO brains. No differences were observed at 4 and 18 months of age (**Fig. 5C**). We then classified the morphology of the protrusions into four categories: filopodia and thin protrusions (immature spines) and mushroom and branched protrusions (mature spines). One month-old *Lrrk2* KO animals exhibit a reduced number of filopodia and an increased quantity of thin protrusions, suggesting that loss of Lrrk2 may favor this transition. Instead, the proportion of mature spines (mushroom and branched) remained unaltered. No differences were observed in older mice (**Fig. S6**).

Since the overall width/height of *Lrrk2* KO protrusions is reduced (**Fig. 5C**), we next analyzed the postsynaptic ultrastructure using electron microscopy. To increase the experimental power, we used a separate group of animals. We measured the postsynaptic density (PSD) length as it directly correlates with the amount of postsynaptic receptors and signaling proteins, thus providing an indication of the synaptic strength (**Fig. 5D**). PSD is significantly shorter in 1 month-old *Lrrk2* KO animals compared to WT ($P < 0.001$), while no differences in PSD length are observed in 18 month-old KO mice (**Fig. 5E**). Taken all these data together, we conclude that subtle defects in the postsynaptic density are present in the striatum of postnatal *Lrrk2* KO mice, but these abnormalities appear to normalize with age.

To assess whether the loss of *Lrrk2* in young mice leads to reduced dendritic protrusion size and postsynaptic density through alterations in BDNF-TrkB signaling or postsynaptic scaffold expression, we measured transcript levels of *Bdnf*, *TrkB*, *Dbn1*, *Psd95* and *Shank3*. Neither *Bdnf* nor *TrkB* expression is altered in the striatum, cortex or midbrain of 1-month old *Lrrk2* KO as compared to WT mice (**Fig. 5F**), supporting a mechanism whereby LRRK2 acts downstream of BDNF signaling. Instead *Dbn1*, *Psd95* and *Shank3* expression levels are reduced in *Lrrk2* KO mice across most brain regions analyzed, with the most pronounced decrease observed in the midbrain (**Fig. 5F**).

Given (i) the central role of *Dbn1*/drebrin in the LRRK2 synaptic network (**Fig. 2**-**3**), (ii) its key function as an actin regulatory protein at the synapse and (iii) its expression highly enriched at dendritic spines (**Fig. S2A**), we assessed drebrin protein levels at the 3 stages of life in whole brain lysates. In agreement with the qPCR results, drebrin levels are significantly lower in 1 month-old *Lrrk2* KO mice but not in older animals (**Fig. 5G**), further linking altered spine maturation with improper actin-dynamics in the absence of LRRK2.

Taken together, our results indicate that LRRK2 influences dendritic spine structural dynamics during brain development.

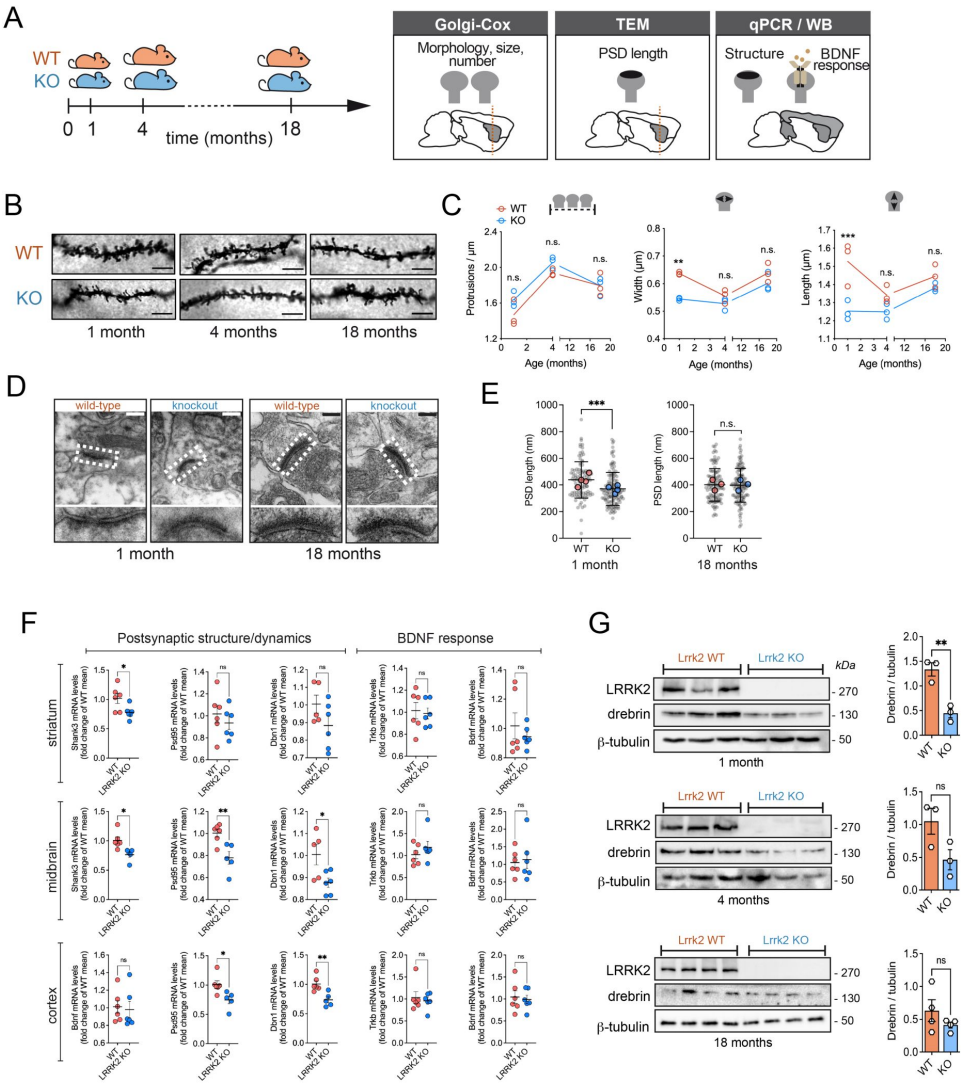


## Figure 5.

### Postsynaptic structural changes in young *Lrrk2* knockout mice.

**(A)** Overview of experimental design. **(B)** Representative images of neurite segments from Golgi-Cox stained neurons of dorsal striatum. Scale bar: 3 µm. **(C)** Quantification of average spine number (top), width (middle) and length (bottom) of *n*=3 animals per group (same segments analyzed in B). Statistical significance was determined by two-way ANOVA with Šídák's multiple comparisons test. Number of protrusions: interaction *P*=0.3820, F (2, 12) = 1.044; age: ****P*<0.0001, F (2, 12) = 27.12; genotype: *P*=0.0840, F (1, 12) = 3.550; WT vs. KO (1 month) *P*=0.2013; WT vs. KO (4 months) *P*=0.5080; WT vs. KO (18 months) *P*>0.9999. Width: interaction *P*=0.0815, F (2, 12) = 3.112; age: ***P*=0.0004, F (2, 12) = 16.14; genotype: ***P*=0.0007, F (1, 12) = 20.77; WT vs. KO (1 month) **P*=0.0017; WT vs. KO (4 months) *P*=0.4602; WT vs. KO (18 months) *P*=0.2489. Length: interaction **P*=0.0345, F (2, 12) = 4.514; age: **P*=0.0203, F (2, 12) = 5.488; genotype: ***P*=0.0006, F (1, 12) = 21.53; WT vs. KO (1 month) ***P*=0.0008; WT vs. KO (4 months) *P*=0.2875; WT vs. KO (18 months) *P*=0.5948. **(D)** Representative transmission electron microscopy (TEM) micrographs of striatal synapses from 1-month and 18-month old WT vs KO mouse brain slices. Scale bar: 200 nm. **(E)** Quantification of post-synaptic density (PSD) length. Graphs show the length of individual synapses (grey dots) and the average PSD length per animal (colored dots). Statistical significance has been calculated with Student's t-test: 1 month-old mice (*n*=4 mice, 95 synapses WT, 118 synapses KO, ***P*=0.0003); 18-month old mice (*n*=3 mice, 108 synapses WT, 119 synapses KO, *P*=0.8502). **(F)** Quantitative PCR of *Bdnf, TrkB, Psd95, Shank3* and *Dbn1* mRNA expression in striatum, cortex and midbrain form *n*=6 *Lrrk2* WT and *n*=6 *Lrrk2* KO one-month old mice. Statistical significance has been calculated with Student's t-test. (**G**) Western blot analysis of brain samples from the same Lrrk2 WT and KO mice where Golgi-Cox staining has been performed. The reduction in drebrin content is significant in Lrrk2 KO mice at 1 month of age. Differences between the two genotypes have been evaluated using Student's t-test (significance **P*<0.01), *n*=3-4 animals per genotype per age.

### LRRK2 knockout in human iPSC-derived neurons increases basal spontaneous activity

To further explore the connection between LRRK2 and BDNF activity in a cell model more relevant for human disease, we differentiated human induced pluripotent stem cells (hiPSCs) into cortical neurons following established protocols.[67] Wild-type and isogenic LRRK2 knockout (KO) hiPSCs[68] were differentiated in parallel for 50, 70 and 90 days (3 independent culture rounds per genotype), prior to subjecting them to patch clamp to assess spontaneous activity in the absence or presence of acute exposure to BDNF (24 hrs, 50 ng/ml) (**Fig. 6A**).

Acute BDNF treatment led to a significant increase in the mean frequency of miniature post-synaptic excitatory currents (mEPSC) in WT cultures (**Fig. 6B-C**). This finding is corroborated by the significant leftward shift in cumulative probability curves of interevent intervals (IEIs) between BDNF-treated neurons versus untreated neurons (**Fig. 6D**). In contrast, KO neurons already display elevated mEPSC frequency, comparable to that of BDNF-treated WT cultures. No significant change in mEPSC frequency was observed in KO neurons upon BDNF treatment (**Fig. 6C-D**). Furthermore, BDNF treatment had no effect on the average peak amplitude in either genotypes, before or after BDNF treatment (**Fig. 6E-F**).

To determine whether this apparent sealing effect of LRRK2 KO is restricted to DIV70 cultures or measurable also in younger or more mature neurons, we quantified the mEPSCs in DIV50 and DIV90 neurons. As illustrated in **Fig. S7 (A-B)**, no significant differences across genotypes or treatments are observed at these timepoints, indicating that the genotype effect is transient during culture maturation.

Since only the frequency, but not the amplitude, of mEPSCs was altered at DIV70, we infer that BDNF primarily affects the presynapse rather than the postsynapse in this experimental paradigm, likely increasing neurotransmitter release in WT neurons. To determine whether the increased release was due to increase in release probability ($P_r$) or a higher number of synaptic contacts, we measured the number of presynaptic Bassoon colocalization with postsynaptic Homer (**Fig. S7C-D**). Confocal imaging of synapses combined with IMARIS volume reconstruction showed no increase in the total number of synapses under BDNF stimulation in neither genotype, suggesting that BDNF increases $P_r$ rather than synapse number.

## Discussion

Understanding the early events that lead to synaptic dysfunction in PD is crucial to design effective therapeutic approaches. Previous work from our laboratories and other groups have shown that the PD-associated kinase LRRK2 regulates important synaptic processes.[69,70] At the presynapse, LRRK2 controls synaptic vesicles cycle through association with its WD40 domain[23,24,71,72] and phosphorylation of a panel of presynaptic proteins, including N-ethylmaleimide sensitive fusion (NSF)[26], synapsin I[27], auxilin[30], synaptojanin[29] and EndophylinA.[28] It has also been shown to regulate neurotransmitter release via modulation of presynaptic vesicular interacting proteins. At the postsynapse, LRRK2 plays key roles in shaping the function of excitatory synapses in the striatum.[33,34,65,66,70] However, the mechanisms underlying LRRK2 synaptic function are still poorly elucidated. In the present study we provide multiple lines of evidence that LRRK2 affects synaptic function in response to BDNF neurotrophic stimulation, which promotes relocalization of LRRK2 to the actin-cytoskeleton in a phosphorylation-dependent manner.

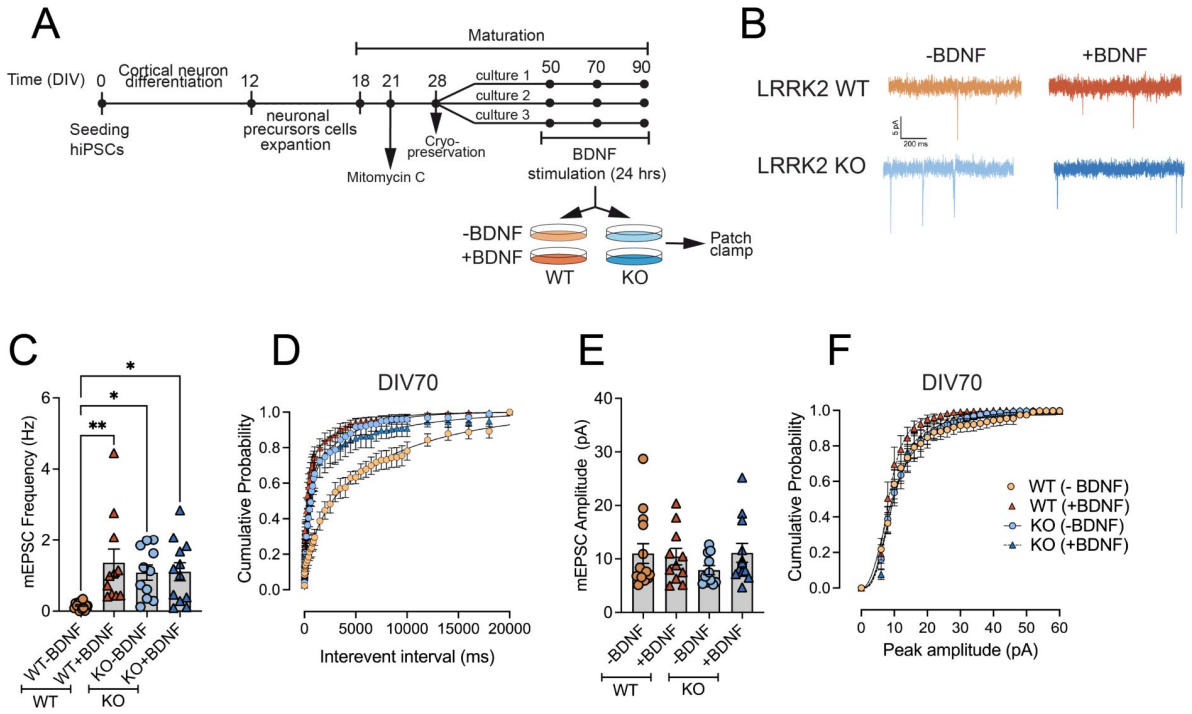


**Figure 6.**

### Effect of BDNF exposure on spontaneous electrical activity recorded in DIV70 LRRK2 WT and KO cortical neurons.

(**A**) Schematic representation of the experimental setup. (**B**) Representative spontaneous traces of hiPSC-derived WT and KO neurons in the presence or absence of 50 ng/ml BDNF for 24 hrs. **(C)** Frequency of miniature postsynaptic excitatory currents (mEPSC) in LRRK2 WT and KO cultures (WT vehicle: 0.16 ± 0.03 Hz (*n*=15, *N*=3); WT BDNF: 1.36 ± 0.38 Hz (*n*=11, *N*=3); KO vehicle: 1.09 ± 0.21 Hz (*n*=11, *N*=3); KO BDNF: 1.11 ± 0.25 Hz (*n*=12, *N*=3). Statistical significance was determined using one-way ANOVA (WT vehicle vs. WT BDNF ***P*<0.01; WT BDNF vs. KO BDNF **P*<0.05; WT vehicle vs. KO BDNF **P*<0.05; *P*>0.05 for all the other comparisons). **(D)** Cumulative probability curves of interevent interval (IEIs) in DIV70 WT and KO -/+ BDNF treated cultures. **(E)** Amplitude of miniature postsynaptic excitatory currents (mEPSC) in DIV70 LRRK2 WT and KO cultures. BDNF treatment has no effect on the average peak amplitude (WT vehicle: 11.00 ± 1.85 pA (*n*=14, *N*=3); WT BDNF: 7.9 ± 0.84 pA (*n*=11, *N*=3); KO vehicle 10.42 ± 1.53 pA (*n*=11, *N*=3); KO BDNF 11.12 ± 1.76 pA (*n*=12, *N*=3)). Statistical significance was determined using one-way ANOVA (*P*>0.05 for all comparisons).

There are several novel findings in our study. First, we identified BDNF as an extracellular stimulus that increases LRRK2 activity. The phosphorylation kinetics are rapid and transient, and both *Lrrk2* KO neurons and differentiated SH-SY5Y LRRK2 KO cells display reduced activation of downstream AKT and ERK1/2, consistent with LRRK2 acting downstream of TrkB/BDNF and upstream of ERK1/2 and AKT. As previously documented, we observed high Ser935 phosphorylation under basal conditions, in agreement with mass spectrometry determination showing nearly complete phosphorylation of this residue in whole brain.[44] In contrast, phosphorylation of RAB substrates, as well as BDNF-downstream kinases ERK and AKT, is minimal at baseline. Thus, the modest increase in Ser935 phosphorylation upon BDNF stimulation may reflect a ceiling effect. Prolonged BDNF exposure leads to a reduction in Ser935 phosphorylation below pre-stimulation levels, likely through negative feedback mechanisms such as phosphatase activity or receptor desensitization.[73] In contrast, phosphorylation of RABs did not drop below pre-stimulation levels. This aligns with the low pRAB stoichiometry in the brain[44] and suggest that these targets remain responsive and largely unsaturated under basal conditions. Taken together, these findings highlight the nuanced regulation of LRRK2 activity and indicate a positive correlation between Ser935 phosphorylation and LRRK2 activity under BDNF signalling, similar to previous observations on microglia cells upon inflammatory stimuli.[74] They also imply that phosphorylated LRRK2 remains incompletely active unless further stimulated (e.g., by BDNF), suggesting a multi-step activation mechanism. Thus, Ser935 phosphorylation status does not always correlate with LRRK2 functional output, potentially reflecting distinct regulatory states or compartment-specific activation dynamics.[75]

Using a literature-based network analysis of LRRK2 PPIs, combined with AP-MS/MS in SH-SY5Y cells and phosphoproteomics of hyperactive Lrrk2 G2019S from brain striatum, we identified a highly interconnected cluster of actin and synaptic proteins linked to LRRK2. Both BDNF-activated LRRK2 and hyperactive LRRK2 G2019S mutant are associated with GO terms related to synaptic function and cytoskeletal organization. The prevalence of synaptic components in the phoshoproteomic study is particularly notable considering that it was performed on total striatal lysates composed of an heterogeneous mixture of cell types. This strengthens the importance of LRRK2-mediated signaling in the synaptic compartment.

The central role of synaptic dysfunction in PD neurodegeneration is increasingly recognized[76] and further supported by the latest and largest meta-analysis of PD genome-wide association studies (GWAS), which identified 134 loci as risk factors for PD.[77] The open reading frames closest to the risk signals showed strong enrichment for neuronal genes involved in dendritic spine and synapse biology (**Fig. S8** and [77]). Even though these data require functional validation (GWAS directly identifies risk loci but not genes), they may further support synaptic impairment as an hallmark of PD.[78]

Of note, while LRRK2 G2019S cases are often characterized by the absence of Lewy bodies[79,80], two recent studies disclosed the presence of widespread alpha-synuclein oligomers in LRRK2-PD brains, suggesting that early-stage presynaptic alpha-synuclein aggregates may contribute to synaptic dysfunction in LRRK2-PD.[81,82] Whether these alpha-synuclein oligomers are enriched in specific dopaminergic subtypes is unknown, and future studies should investigate if there is any correlation with the dopaminergic neuronal subpopulations most vulnerable in PD.[83,84]

Further supporting a contribution of LRRK2 on synaptic function, we found that knockout of mouse *Lrrk2* resulted in blunted BDNF-induced synapse maturation *in vitro*. These findings suggest a mechanism whereby BDNF signaling reshapes the LRRK2 interactome to promote its incorporation into a macromolecular complex required for coordinating actin dynamics during synaptic structural plasticity. Interestingly, in human iPSCs-derived cortical neurons, loss of LRRK2 seems to accelerate synaptic maturation: DIV70 KO neurons exhibit high spontaneous synaptic activity equivalent to BDNF-stimulated WT neurons. This indicates that LRRK2 may act to suppress

premature maturation and temporally gate BDNF responsiveness, aligning with the differences in spine structural dynamics observed in KO mice. While previous evidence has shown that LRRK2 modulates neurotransmitter release,[22] our current findings imply that these changes can be acutely altered by BDNF signalling with loss of LRRK2 removing this plastic capacity.

BDNF is key to reorganize the actin cytoskeleton during long term potentiation (LTP) through the action of Rho GTPases Rac1 and Cdc42.[85] LRRK2 was previously reported to interact with Rac1[86,87] and with other actin-related proteins.[53] Here we demonstrated that LRRK2 association with actin cytoskeleton in dendritic spines increases upon BDNF stimulation. We validated the BDNF-dependency of the interaction between LRRK2 and drebrin, an actin binding protein that promotes stable F-actin formation in dendritic spines.[48] A LRRK2-drebrin link is supported by multiple lines of evidence from our data, including increased phosphorylation at Ser339 in G2019S knockin striata and reduced drebrin levels in Lrrk2 knockout brains during development, which matched with morphological alteration of dendritic protrusions. Ser339 in human drebrin is located in the N-terminal region, which we identified as important for the interaction with LRRK2. This site lies just before the proline-rich (PP) domain of the protein. The N-terminal region is positioned between the actin-binding domains and the C-terminal Homer-binding sequences, and it plays a key role in protein-protein interactions and cytoskeletal regulation.[88] Notably, this region was shown to interact with adafin (ADFN), a protein involved in cytoskeletal-related processes crucial for synapse formation and function. Adafin regulates puncta adherentia junctions, presynaptic differentiation, and cadherin complex assembly, essential for hippocampal excitatory synapses, spine formation, and learning and memory processes.[89] Of note, adafin is listed among LRRK2-interacting proteins (*https://www.ebi.ac.uk/intact/home*), supporting a possible functional relevance of LRRK2-mediated drebrin phosphorylation in adafin-drebrin complex formation.

It has been shown that drebrin knockout results in delayed synaptogenesis and inhibition of postsynaptic PSD95 accumulation, indicating a key role in spine maturation.[48,90,91] During LTP, $Ca^{2+}$ entry through N-methyl-d-aspartate (NMDA) receptors causes drebrin exodus from the spine compartment to allow actin monomers entrance and polymerization to increase the size of the cytoskeleton.[92] We postulate that LRRK2 may favor drebrin exodus at the shaft of the dendrite during plasticity processes. Actin remodeling during spine enlargement is also coordinated by the ARP2/3 complex, which is activated by binding to WAVE family proteins downstream of active Rac1.[93] Strikingly, we found that BDNF stimulates LRRK2 interaction with three out of seven subunits of the ARP2/3 complex (ACTR2, ACTR3 and ARPC2) and LRRK2 was reported to interact with WAVE proteins.[94] Altogether these findings, in agreement with our earlier study,[35] highlight a crucial role for LRRK2 in actin-based dendritic spine remodeling. Clearly, future studies should be directed at clarifying the precise molecular dynamics and kinetics of these processes.

Another interesting aspect disclosed in our study is a developmental phenotype characterized by defects in dendritic protrusions morphogenesis as consequence of loss of LRRK2. Interestingly, this developmental abnormality is rescued with age. This is not surprising considering that the homologous kinase LRRK1 may compensate for LRRK2 deficiency, as suggested by the overt neurodegeneration observed in double *Lrrk1/Lrrk2* KO mice but absent in the single KO[95–97] and the redundant but not overlapping pattern of expression of the two kinases.[98] Indeed, striatal Lrrk2 expression in the rodent brain increases up to postnatal week 4,[35,64,98,99] while Lrrk1 transcript in this region is relatively stable during development.[64]

Several lines of evidence indicate that genetic, biochemical and cellular alterations of BDNF/TrkB signaling are linked to PD. At striatal synapses, BDNF/TrkB signaling enhances both dopamine and glutamate release and ERK1/2 activation.[100,101] BDNF is required for the establishment of the proper number and for the survival of dopaminergic neurons in the SNpc, [102,103] and presynaptic dopamine release in the striatum is enhanced by BDNF.[37] BDNF levels are lower in

peripheral tissues, brain, and blood of sporadic PD patients.[104] Moreover, the V66M polymorphism modifies the risk of sporadic and mutant LRRK2-associated PD.[105,106] Decreased BDNF concentration in serum and brain correlates with an increased degeneration of dopaminergic neurons in PD[107] and with loss of striatal DA transporter (DAT) in patients with striatal dopaminergic neurodegeneration.[108] Thus, robust literature support deregulation of striatal BDNF signaling in PD. Future studies should be directed at investigating possible deregulated mechanisms of BDNF signaling in G2019S mice and hiPSCs-derived neurons with G2019S mutation.

At the onset of PD, loss of dopaminergic axonal terminals largely exceeds loss of cell bodies,[4] implying that early synapse deterioration may be the trigger of axonal degeneration and, ultimately, neuronal death.[109] In contrast to neuronal loss, which is irreversible, disease-associated synaptic dysfunctions could be rescued through the growth of new terminals and/or dendritic spines.[5] Thus, focusing on early, prodromal dysfunction in PD appears key to design effective therapeutic and preventive strategies, and our study uncovered LRRK2 as a promising disease modifying target of early-stage PD.

# Materials and methods

## Mouse strains

C57Bl/6J Lrrk2 knock-out (KO) and G2019S-Lrrk2 knock-in mice were provided by Dr. Heather Melrose (Mayo Clinics, Florida, USA). Housing and handling of mice were done in compliance with national guidelines. All animal procedures were approved by the Ethical Committee of the University of Padova and the Italian Ministry of Health (license 1041/2016-PR and 105/2019) and followed the guidelines approved by the Northwestern University Animal Care and Use Committee. Approximately equal numbers of males and females were used for every experiment.

## Cell cultures

### Generation of LRRK2 KO SH-SY5Y CRISPR/Cas9 edited monoclonal cell line

The KO of LRRK2 was performed using CRISPR/Cas9-mediated genome editing technology following the protocol by Sharma *et al.*[110] Two sgRNAs were selected among those designed by the laboratory of Zhang F (*https://www.genscript.com/gRNA-detail/120892/LRRK2-CRISPR-guide-RNA.html*) and one was designed using the online platform Benchling (*https://www.benchling.com*). All the gRNAs were synthetized by Sigma-Aldrich. The oligos pairs encoding the 20-nt guide sequence were annealed and ligated into the pSpCas9(BB)-2A-Puro (PX459) V2.0 vector (Addgene, Watertown, MA, US) and then amplified in chemically competent E. coli StbI3 cells (ThermoFisher ScientificTM). Human neuroblastoma-derived SH-SY5Y cells were transfected using Lipofectamine 2000 (Invitrogen) and subjected to puromycin selection. The selected cells were diluted to obtain monoclonal cell lines. Approximately one week after plating, the colonies were inspected for a clonal appearance and progressively expanded. Finally, the deletion of LRRK2 was verified in multiple lines by western blot analysis with LRRK2 specific antibody (**Fig. S5**).

### SH-SY5Y cell line maintenance, differentiation and treatments

SH-SY5Y cells (naïve, LRRK2 KO, expressing GFP or GFP-LRRK2 wild type) were cultured in a mixture (1:1) of Dulbecco's Modified Eagle's Medium (DMEM, Biowest) and Ham's F-12 Nutrient Mixture (F12, Biowest), supplemented with 10% (v/v) Fetal Bovine Serum (FBS, Thermo Fisher Scientific) and 1% Penicillin/Streptomycin solution (PS, GIBCO Life Technologies).

To promote N-type (neuronal-like cells) cell differentiation, cells were plated in DMEM/F12 containing 1% PS, 1% FBS and 10μM of all-trans-retinoic acid (RA, Sigma-Aldrich). At regular intervals of 48 hours, RA was newly provided to the medium. Cells were differentiated for 6 days and then subjected to the treatments.

SH-SY5Y cells were starved for 5 hours in DMEM/F12 supplemented with 1% PS and then stimulated with 100ng/mL BDNF (50240-MNAS, Sino Biological) for different time periods (5, 15, 30 and 60 minutes) in serum-free medium. LRRK2 kinase activity was inhibited pre-treating cells with 0.5μM MLi-2 (ab254528, Abcam) for 90 minutes. For the detection of phospho-S935 and phospho-Rabs, 80 μg of total protein were loaded, whereas 30 μg were used for the detection of phospho-AKT and phospho-ERK1/2, as well as for total proteins.

## HEK293T cell line maintenance and transfection

HEK293T cells (Life technologies) were cultured in DMEM (Biowest) supplemented with 10% (v/v) FBS (Thermo Fisher Scientific) and 1% PS (GIBCO Life Technologies). Cells were plated in 100mm dishes and, once they reached 80% confluency, they were transfected with polyethyleneimine (PEI, Polysciences) at 1:2 DNA to PEI ratio (v/w). Flag-LRRK2 was co-expressed with YFP-drebrin full-length, N-terminal domain (1-256 aa), or C-terminal domain (256-649 aa).

## Primary mouse cortical neuron preparation, transfection and treatments

Primary cortical neurons from Lrrk2 WT and KO C57BL/6J mice were derived from postnatal mouse (P0) exploiting the Papain Dissociation System (Worthington Biochemical Corporation). Cortices were incubated in Papain solution (Papain and DNase solution in Earle's Balanced Salt Solution) for 40 minutes at 37°C. Subsequently, tissue was triturated and centrifugated for 5 minutes at 200g. The supernatant was discarded, and the pellet was resuspended in Stop solution [DNase solution and Trypsin inhibitor solution (15,5mg/mL) in Earle's Balanced Salt Solution]. For 10 minutes the tissue was allowed to precipitate and then the supernatant was pipetted drop-by-drop on 5mL of 10/10 solution (10 μg/mL Trypsin inhibitor and 10 μg/mL BSA in Earle's Balanced Salt Solution) and centrifugated for 10 minutes at 100g. The pellet was resuspended in Neurobasal A medium (GIBCO Life Technologies) supplemented with 2% B27 supplement (GIBCO Life Technologies), 0.5 mM L-glutamine (GIBCO Life Technologies), 100 units/mL penicillin, and 100 μg/mL streptomycin (GIBCO Life Technologies). Cells were diluted and counted in 0.4% Trypan blue. Neurons were plated at 1000-1500 cells/$mm^2$ onto 6-well plates or at 200 cells/$mm^2$ on 12mm glass coverslips in 24-well plates and maintained in culture for 14 days prior to the treatments. After 7 days, 50% of the Neurobasal medium was removed and replaced with fresh one.

At DIV14, Lrrk2 WT and KO mature neurons cultured in the 6-well plates for western blot analysis were treated with MLi-2 (0.5μM) for 90 minutes and with BDNF (100ng/mL) for 5, 30, 60 and 180 minutes in Neurobasal completed medium. At DIV4, Lrrk2 WT and KO primary neurons plated in 24-well plates were transfected with lipofectamine (Lipofectamine 2000, Invitrogen) in a 1:2 ratio with DNA (v/w). The transfection was carried in Opti-MEM (GIBCO Life Technologies) for 45 minutes. Transfected neurons were then maintained in culture for additional 9-10 days. At DIV14, neurons were treated for 24 hours with 100ng/mL BDNF to study the spine maturation process.

## Media composition for cortical neuron differentiation from hiPSC

Neuronal maintenance media (NMM): 1:1 mixture of N2 media (DMEM/F12 GlutaMax supplemented with 1X N2, 50 units/mg/ml Penicillin/Streptomycin solution, 1X MEM Non-Essential Amino Acids Solution (100X), 100μM 2-Mercaptoethanol (ThermoFisher Scientific), 1mM sodium pyruvate and 5 μg/ml insulin (Merck)) and B27 media (Neurobasal supplemented with 1X B27 and 2mM L-Glutamine (ThermoFisher Scientific).

Neuronal induction media (NIM): NMM media supplemented with 100nM LDN193189 (Sigma Aldrich) and 10µM SB431542 (Bio-Techne).

### hiPSC cell culture, cortical neuron differentiation and treatments

Isogenic human induced-pluripotent stem cell lines (hiPSC) of WT and LRRK2 KO, made and kindly provided by Mark R Cookson's laboratory,[68] were cultured using E8 media (Thermo Fisher Scientific) in a 6-well plate coated with Cultrex. Cortical neuronal differentiation was carried out according to Shi, *et al.*[67] Briefly, upon reaching 100% confluency, media was changed to neuronal induction media (NIM) and is marked as 0 days *in vitro* (DIV0). Daily NIM media change was carried out till DIV12, upon which neuronal precursor cells (NPCs) are generated. On DIV12, NPCs were expanded via passage at 1:2 ratio, supplemented with neuronal maintenance media (NMM) media and 20 ng/ml FGF2 (Bio-Techne). Neurogenesis was initiated on DIV18 with the removal of FGF2 and the cells supplemented with NMM only changing every 2 days. At DIV25-30, neurons were cryopreserved in CryoStor CS10 solution (Stem Cell technologies).

For electrophysiological recordings and immunocytochemistry/immunofluorescence (ICC/IF), thawed neurons were plated on Cultrex coated 10mm coverslips at a density of 60k/cm[2]. All cells were treated with 1 ug/ml Mitomycin C (Sigma-Aldrich) for 1 hour at 37°C, 48-72 hours after plating to remove any proliferating cells. Neurons were maintained in NMM until used for experiments. BDNF treatment was carried out with cells incubated with 50 ng/ml BDNF (Bio-Techne) for 24 hours prior to use in electrophysiological recordings and ICC/IF.

## Electrophysiological recordings

Whole-cell patch-clamp recordings were performed on cortical neurons at DIV70-75 (mentioned as DIV70 from here on) in voltage clamp at Vh −70 mV and the membrane test function was used to determine intrinsic membrane properties ~1 min after obtaining whole-cell configuration, as described previously.[111] Briefly, coverslip containing neurons were transferred to warner bath (RC-26G) and maintained at 35 ± 2 °C through constant perfusion using in-line heater and controller (Warner Instruments) with extra cellular solution (ECS) containing (in mM unless stated): 145 NaCl, 3 KCl, 2 $MgCl_2$, 2 $CaCl_2$, 10 glucose, 10 HEPES, pH 7.4, 310 mOsm. Tetrodotoxin (TTX 0.2µM), and picrotoxin (PTX 100µM), were added before use to block sodium and $GABA_A$ currents. Pipette resistance (Rp) of glass electrodes was 4–6 MΩ when filled with (in mM): 130 Csmethanesulfonate, 5 CsCl, 4 NaCl, 2 MgCl2, 5 EGTA, 10 HEPES, 5 QX-314, 0.5 GTP, 10 Na2-phosphocreatine, and 5 MgATP, 0.1 spermine, pH 7.2, 300 mOsm. Data was acquired by Multiclamp700B amplifier and digidata 1550B and signals were filtered at 2kHz, digitized at 10 kHz, and analyzed in Clampfit 10 (MolecularDevices). Tolerance for series resistance (Rs) was <35 MΩ and uncompensated; ΔRs tolerance cut-off was <20%. mEPSCs were analyzed using Clampfit10 (threshold 5pA); all events were checked by eye. Data are presented as mean ± s.e.m. where n is cells from a minimum of 3 separate cultures (culture N in brackets).

## Cells and tissues lysis, SDS-PAGE and Western blotting analysis

Immortalized cells, neurons and mouse brain tissues were lysed for 30 minutes on ice in appropriate volume of cold RIPA lysis buffer (Cell Signaling Technologies) supplemented with protease inhibitor cocktail. Protein concentration was assessed by performing BCA assay (Thermo Fisher Scientific). Proteins were solubilized in sample buffer (200mM Tris-HCl pH 6.8, 8% SDS, 400mM DTT, 40% glycerol, q.s. Bromophenol Blue) and resolved by SDS-PAGE on 8% Tris polyacrylamide homemade gels in Tris-glycine-SDS running buffer for the AP-MS experiments, and on 4-20% polyacrylamide gels (GenScript® Express Plus PAGE) in Tris-MOPS-SDS running buffer (GenScript® Running Buffer Powder) for the other cases. Proteins were transferred on PVDF (polyvinylidene difluoride, Bio-Rad) membranes using a semi-dry transfer system (Trans-Blot® Turbo Transfer System, Bio-Rad). Non-specific binding sites were blocked incubating membranes with 5% non-fat dry milk diluted in 0.1% Tween-20 Tris-buffered saline (TBS-T) for 1

hour at room temperature under agitation. Membranes were subsequently incubated overnight at 4°C with primary antibodies in 5% non-fat dry milk in TBS-T or in 5% BSA in TBS-T. After three washes in TBS-T at room temperature, membranes were incubated for 1 hour at room temperature with horseradish peroxidase (HRP)-conjugated goat anti-mouse or anti-rabbit IgG. After three more washes in TBS-T, proteins were visualized using chemiluminescence (Immobilon ECL western HRP substrate, Millipore). Densitometric analysis was carried out using the Image J software. The antibodies used for western blotting are as follows: rabbit α-LRRK2 (MJFF2 c41-2, ab133474, Abcam, 1:300); rabbit α-phospho-Ser935 LRRK2 (ab133450, Abcam, 1:300); mouse α-phospho-Ser473-AKT (sc-293125, Santa Cruz Biotechnology, 1:500); rabbit α-AKT (9272S, Cell Signaling Technology, 1:1000); rabbit α-phospho [(Thr202/Tyr204, Thr185/Tyr187)-ERK1/2 (12-302, Millipore, 1:1500); rabbit α-ERK1/2 (4695, Cell Signaling Technology, 1:1000); mouse α-GAPDH (CSB-MA000195, 1:5000); mouse α-βIII tubulin (T8578, Sigma-Aldrich, 1:40000); mouse α-DREBRIN (MA1-20377, Thermo Fisher Scientific, 1:500); α-Flag M2-HRP (A8592, Sigma-Aldrich, 1:5000); α-mouse IgG-HRP (A9044, Sigma-Aldrich, 1:80000); α-rabbit IgG-HRP (A9169, Sigma-Aldrich, 1:16000).

## Staining on mammalian cells and brain tissue

### Immunocytochemistry and confocal microscopy of primary neurons

Mouse primary cortical neurons derived from Lrrk2 WT C57BL/6 and KO pups (P0) were fixed using 4% paraformaldehyde (PFA, Sigma-Aldrich) in PBS1X pH 7.4 for 20 minutes at room temperature and, after three washes in PBS1X, they were subjected to staining protocol. Cells were firstly permeabilized with 0.3% Triton-X in PBS1X for 5 minutes and then saturated in blocking buffer [1% Bovine serum Albumin (BSA) Fraction V, 0.1% Triton-X, 50mM Glycine, 2% goat serum in PBS1X] for 1 hour at room temperature in agitation. The primary and secondary antibodies incubation steps were carried out in working solution (20% blocking buffer in PBS1X) for 1 hour at room temperature. Both incubations were followed by three washes in working solution. Nuclei staining was performed in Hoechst 33258 (Invitrogen, 1:10000 dilution in PBS1X) for 5 minutes and followed by three rinses in PBS1X. After been cleaning in distilled water, coverslips were mounted on microscope slides with Mowiol® mounting medium. Immunofluorescence z-stack images (z-stack thickness: 0.5 µm x 6 = 3 µm) were obtained on Zeiss LSM700 laser scanning confocal microscope exploiting a 63X oil immersion objective.

The antibodies used for immunocytochemistry are as follows: mouse α-PSD95 (ab2723, Abcam, 1:200), rabbit α-MAP2 (sc-20172, Santa Cruz, 1:200); mouse α-drebrin (MA1-20377, Thermo Fisher Scientific, 1:400); goat anti-mouse-Alexa Fluor 568 (A11004, Invitrogen), goat anti-mouse-Alexa Fluor (A11004, Invitrogen), goat anti-rabbit-Alexa Fluor 488 (A11034, Invitrogen), rabbit-Alexa Fluor 568 (A11036, Invitrogen), goat anti-rabbit-Alexa Fluor 405.

### Immunostaining and Image Analysis of hiPCS-derived cortical neurons

For immunocytochemistry DIV70 cells on coverslips were fixed in 4% paraformaldehyde (PFA) for 10 minutes. Cells were then permeabilized and blocked using 0.4% Tween with 10% normal goat serum (NGS), in PBS1X for 1 hour. Primary antibodies were incubated overnight at 4°C in PBST plus 10% NGS. Cells were washed 3× with PBST before 1 hour incubation at room temperature with secondary antibodies (α-guinea pig Alexa-488, α-rabbit Alexa 568, α-chicken 647 along with DAPI) from Molecular probes and Jackson Laboratories). Primary antibodies were chicken anti-microtubule associated protein 2 (MAP2) (Antibodies A85363, dil. 1:1000), rabbit anti-homer 1 (Synaptic Systems 160003, dil. 1:500), and guinea pig anti-bassoon (Synaptic Systems 141004, dil. 1:500). Coverslips were slide mounted with FluorSave (Sigma-Aldrich) and all images were acquired on Leica confocal microscope as 0.45 µm z-stacks at 60× magnification (flattened with the max projection function for cluster analysis). Single 60× images were used for analyses. Excitation

and acquisition parameters were constrained across all experimental paired (culture) acquisitions. All images were analyzed using IMARIS microscopy image analysis software (v10.0.0 Oxford Instruments). Data are presented as mean ± s.e.m.

### Golgi-Cox staining

Animals were terminally anesthetized and transcardially perfused with 0.9% saline. Half of each brain was incubated with Golgi-Cox solution (Potassium dichromate, Mercuric chloride, Potassium chromate prepared according to Zaqout *et al.*[112]) in the dark at room temperature for 14 days and then transferred in 30% sucrose solution in PBS1X. Brains were cut with a vibratome in 100 µm thick slices. The sections were then blotted by pressing an absorbent paper moistened with sucrose solution onto the slides and dried for 7-10 minutes. The samples were then subjected to color development procedure consisting in the following steps: 1. two 5-minutes washes in distilled water; 2. 5-minutes dehydration step in 50% ethanol; 3. 10-minutes incubation step in 20% ammonium hydroxide; 4. 5-minutes wash in distilled $H_2O$; 5. 8-minutes incubation step in 5% sodium thiosulfate at room temperature in the dark; 6. two additional 1-minute rinses in distilled $H_2O$; 7. dehydration in ascending grades of ethanol (70%, 95% and 100%). After two final 6-minutes incubations with xylene, the slides were covered with Eukitt® mounting medium. Z-stack images (z-stack thickness between 0.5 µm x 30 = 15 µm and 0.5 µm x 80 = 40 µm) were acquired with Zeiss LSM700 laser scanning confocal microscope using 100X/1,40 Oil DIC M27 immersion objective with phase contrast acquisition mode. All images were analyzed using freely available RECONSTRUCT software and according to Risher *et al.*[113]. 3-4 neurons per mice (n=3 per genotype) were acquired in the dorsal striatum and n≅4 segments per neurons were analyzed.

### Electron Microscopy

Coronal brain slices were fixed with 2.5% glutaraldehyde in 0.1M sodium cacodylate pH 7.4 buffer overnight at 4° C, postfixed in 1% osmium tetroxide for 1h at 4° C, ethanol dehydrated, then infiltrated in a mixture of EMbed 812 (Electron Microscopy Sciences) epoxy resin and absolute ethanol 1:1, and then finally embedded in EMbed 812 (Electron Microscopy Sciences) epoxy resin. Ultrathin sections were obtained with a Leica EM UC7 ultramicrotome and subsequently counterstained with uranyl acetate and lead citrate. Samples were then examined with a Tecnai G2 (Fei-Thermo Fisher) transmission electron microscope operating at 120 kV, digital images were acquired using a Veleta (Olympus Soft Imaging Solutions) digital camera. Images were acquired at the level of dorsal striatum in n=4 mice per genotype (1-month old mice) or n=3 mice per genotype (18-months old mice). n≅20 synapses per mice were analyzed in 1-month old mice; n≅40 synapses per mice were analyzed in 18-months old mice. We gratefully thank the DeBio Imaging facility at the University of Padova for their support with the staining procedure.

## Quantitative PCR

Total RNA was isolated from midbrain, striatum, and cortex of 1 month-old animals (n=6 animals per group, Lrrk2 WT and Lrrk2 KO) using Animal Tissue RNA Purification Kit (Norgen), according to manufacturer's instruction. After extraction, RNA concentration was quantified with NanoDrop 2000C spectrophotometer (Thermo Fisher Scientific). After DNAse treatment (Thermo Fisher Scientific, according to manufacturer's protocol), complementary DNA (cDNA) was generated using qRT SuperMix (Bimake). The cDNAs were used for quantitative PCR (qPCR) exploiting iTaq Universal SYBR® Green Supermix and CFX96 RealTime System (BioRad) for 40 cycles. All samples were run in triplicated, and transcripts levels normalized against the geometrical means of RPL27, actin, and GAPDH relative abundance (housekeeping genes). Data shown were produced using Bio-Rad CFX Manager software and analyzed according to ddCt algorithm.

Primers (5'-3') used are:

*Bdnf* FW: GGCTGACACTTTTGAGCACGTC

*Bdnf* REV: CTCCAAAGGCACTTGACTGCTG

*TrkB* FW: TGAGGAGGACACAGGATGTTGA

*Trkb* REV: TTCCAGTGCAAGCCAGTATCTG

*Shank3* FW: ACCTTGAGTCTGTAGATGTGGAAG

*Shank3* REV: GCTTGTGTCCAACCTTCACGAC

*Psd95* FW: GGTGACGACCCATCCATCTTTATC

*Psd95* REV: CGGACATCCACTTCATTGACAAAC

*Arpc2* FW: GAGTCACAGTAGTCTTCAGCACG

*Arpc2* REV: AGGTTCCCTGTGGCTGAAAAGG

*Dbn1* FW: AGAAGTCGGAGTCAGAGGTGGA

*Dbn1* REV: ATGCCACTCGTTCCTGCTGTCT

*Darpp32* FW: AGATTCAGTTCTCTGTGCCCG

*Darpp32* REV: GGTTCTCTGATGTGGAGAGGC

housekeeping genes

*Rpl27* FW: AAGCCGTCATCGTGAAGAACA

*Rpl27* REV: CTTGATCTTGGATCGCTTGGC

*GAPDH* FW: AGGTCGGTGTGAACGGAT TTG

*GAPDH* REV: TGTAGACCATGTAGTTGAGGTCA

*ACTB* FW: CAACGGCTCCGGCATGTG

*ACTB* REV: CTCTTGCTCTGGGCCTCG

## Protein purification from mammalian cells

For the affinity purification (AP) protocol, SH-SY5Y GFP and SH-SY5Y GFP-LRRK2 cells were plated onto 100mm dishes and differentiated for 6 days. SH-SY5Y GFP-LRRK2 cells were treated with BDNF (100ng/mL) or with an equal volume of vehicle for 15 minutes, while SH-SY5Y OE-GFP cells were left untreated. Cells were harvested in lysis buffer (20mM Tris-HCl pH 7.5, 150mM NaCl, 1mM EDTA, 1% Tween 20, 2.5mM sodium pyrophosphate, 1mM β-glycerophosphate, 1mM sodium orthovanadate) supplemented with protease inhibitor cocktail (Sigma-Aldrich). Lysates were incubated end-over-end with GFP-TrapA beads (ChromoTek) overnight at 4°C. Immunocomplexes were subsequently washed ten times with buffers containing a decreasing amount of NaCl and Tween20 and incubated with sample buffer 2X. The eluted proteins were resolved by SDS-PAGE and processed for western blot analysis or Mass Spectrometry (MS).

HEK293T cells were transfected as described above and drebrin constructs were immunoprecipitated with GFP-trap resin following the same protocol used for the SH-SY5Y cells. The eluded samples were resolved by SDS-PAGE and processed for western blot analysis to visualize the co-precipidated LRRK2 using Flag antibodies.

## LC-MS/MS and data analysis

Three biological replicates of GFP-trap purifications of SH-SY5Y cells were processed for the proteomics experiments. Gels were stained with Colloidal Coomassie Brilliant Blue (0.25% Brilliant Blue R-250, 40% ethanol, 10% acetic acid in milli-Q water) for at least 1 hour and then rinsed in destaining solution (10% isopropanol, 10% acetic acid in milli-Q water). Gel slices were cut into small pieces and subjected to reduction with dithiothreitol (DTT 10 mM in 50 mM NH4HCO3, for 1 h at 56 °C), alkylation with iodoacetamide (55 mM in 50 mM NH4HCO3, for 45 min at RT and in the dark), and in-gel digestion with sequencing grade modified trypsin (Promega, 12.5 ng/µL in 50 mM NH4HCO3). Samples were analyzed with a LTQ-Orbitrap XL mass spectrometer (Thermo Fisher Scientific) coupled to a HPLC UltiMate 3000 (Dionex – Thermo Fisher Scientific) through a nanospray interface. Peptides were separated at a flow rate of 250 nL/min using an 11-cm-long capillary column (PicoFrit, 75-µm ID, 15-µm tip, New Objective) packed in house with C18 material (Aeris Peptide 3.6 µm XB C18; Phenomenex). A linear gradient of acetonitrile/0.1% formic acid from 3 to 40% was used for peptide separation and the instrument operated in a data dependent acquisition mode with a Top4 method (one full MS scan at 60,000 resolution in the Orbitrap, followed by the acquisition in the linear ion trap of the MS/MS spectra of the four most intense ions). Two technical replicates were acquired for each biological replicate. Raw data files were analyzed using MaxQuant and Andromeda software package[114] and searched against the human section of the UniProt database (version September 2020, 75093 entries) concatenated with a database of common contaminants found in proteomic experiments. Trypsin was selected as digesting enzyme with up to two missed cleavages allowed, carbamidomethylation of cysteine residues was set as a fixed modification and methionine oxidation as a variable modification. A search against a randomized database was used to assess the false discovery rate (FDR), and data were filtered to remove contaminants and reverse sequences and keep into account only proteins identified with at least two peptides and a FDR ≤ 0.01, both at peptide and protein level.

Intensity values were retrieved for 350 proteins. A single step of data QC was applied to the intensity values: proteins whose intensity value was 0.00 for both the 2 technical replicates in at least 1 of the 3 pull-down experiments performed with LRRK2-GFP were removed. This is a stringent QC step, but it was implemented to remove proteins with no triplicate data available for the LRRK2 pull-down as this could have occurred because of genuine low levels of pull-down (values close to the limit of detection, missing not at random values) or because of technical issues with the single sample (loss/poor quality of sample, missing at random values). QC reduced the number of proteins in the analysis from 350 to 269 entries.

Intensity data were then processed according to Aguilan *et al.*[115] Briefly, intensity data were log2 transformed and normalized to the median of all proteins within the same experiment. Missing data (0.00 intensity values) were considered missing not at random thus they were imputed via probabilistic minimum imputation (random values within less than 2.5 standard deviations from the distribution of intensity values per the single experiment, 0.3 max variability).[115,116]

Finally, fold change (GFP-LRRK2 vs GFP and GFP-LRRK2 BDNF treated vs GFP-LRRK2 untreated) and associated p-value (two-tailed, paired t-test) were calculated and visualized.

## Phosphoproteomics analysis

## Protein processing for MS

Striata from 8 weeks mice were dissected and rapidly homogenized in four volumes of ice-cold Buffer A (0.32 M sucrose, 5 mM HEPES, pH7.4, 1 mM $MgCl_2$, 0.5 mM $CaCl_2$) supplemented with Halt protease and phosphatase inhibitor cocktail (Thermo Fisher Scientific) using a Teflon homogenizer (12 strokes). Homogenized brain extract was centrifuged at 1400g for 10 minutes. Supernatant (S1) was saved and pellet (P1) was homogenized in buffer A with a Teflon homogenizer (five strokes). After centrifugation at 700 g for 10 minutes, the supernatant (S1') was pooled with S1. Pooled S1 and S1' were centrifuged at 13,800 g for 10 minutes to the crude synaptosomal pellet (P2). The crude synaptosomal pellet (P2) was homogenized in buffer B (0.32M sucrose, 6mM Tris, pH 8.0) supplemented with protease and phosphatase inhibitors cocktail with a Teflon homogenizer (five strokes) and was carefully loaded onto a discontinuous sucrose gradient (0.8 M/1 M/1.2 M sucrose solution in 6 mM Tris, pH 8.0) with a Pasteur pippete, followed by centrifugation in a swinging bucket rotor for 2 hours at 82,500g. The synaptic plasma membrane fraction (SPM) in the interphase between 1 M and 1.2 M sucrose fractions was collected using a syringe and transferred to clean ultracentrifuge tubes. 6 mM Tris buffer was added to each sample to adjust the sucrose concentration from 1.2 M to 0.32 M and the samples were centrifuged in a swinging bucket rotor at 200,000g for 30 minutes. The supernatant was removed and discarded. Added to the pellets the lysis solution containing 12 mM sodium deoxycholate, 12 mM sodium lauroyl sarcosinate, 10 mM TCEP, 40 mM CAA, and phosphatase inhibitor cocktail (Millipore-Sigma) in 50 mM Tris·HCl, pH 8.5, and incubated 10 min at 95°C with vigorous shaking. Sonicated the pellets several times with a sonicator probe and boiled again for 5 minutes. Centrifuged at 16,000g for 10 minutes to remove the debris and collected supernatant. The samples were diluted fivefold with 50 mM triethylammonium bicarbonate and analyzed by BCA to determine protein concentration. The samples were then normalized to 300µg protein in each and digested with 6µg Lys-C (Wako) for 3 hours at 37°C. 6µg trypsin was added for overnight digestion at 37°C. The supernatants were collected and acidified with trifluoroacetic acid (TFA) to a final concentration of 1% TFA. Ethyl acetate solution was added at 1:1 ratio to the samples. The mixture was vortexed for 2 minutes and then centrifuged at 16,000g for 2 minutes to obtain aqueous and organic phases. The organic phase (top layer) was removed, and the aqueous phase was collected, dried completely in a vacuum centrifuge, and desalted using Top-Tip C18 tips (Glygen) according to manufacturer's instructions. The samples were dried completely in a vacuum centrifuge and subjected to phosphopeptide enrichment using PolyMAC Phosphopeptide Enrichment kit (Tymora Analytical) according to manufacturer's instructions, and the eluted phosphopeptides dried completely in a vacuum centrifuge.

## LC-MS/MS Analysis

The full phosphopeptide sample was dissolved in 10.5 µL of 0.05% trifluoroacetic acid with 3% (vol/vol) acetonitrile and 10 µL of each sample was injected into an Ultimate 3000 nano UHPLC system (Thermo Fisher Scientific). Peptides were captured on a 2-cm Acclaim PepMap trap column and separated on a 50-cm column packed with ReproSil Saphir 1.8 µm C18 beads (Dr. Maisch GmbH). The mobile phase buffer consisted of 0.1% formic acid in ultrapure water (buffer A) with an eluting buffer of 0.1% formic acid in 80% (vol/vol) acetonitrile (buffer B) run with a linear 90-min gradient of 6–30% buffer B at flow rate of 300 nL/min. The UHPLC was coupled online with a Q-Exactive HF-X mass spectrometer (Thermo Fisher Scientific). The mass spectrometer was operated in the data-dependent mode, in which a full-scan MS (from m/z 375 to 1,500 with the resolution of 60,000) was followed by MS/MS of the 15 most intense ions (30,000 resolution; normalized collision energy - 28%; automatic gain control target (AGC) - 2E4, maximum injection time - 200 ms; 60sec exclusion].

### LC-MS Data Processing

The raw files were searched directly against the mouse database with no redundant entries, using Byonic (Protein Metrics) and Sequest search engines loaded into Proteome Discoverer 2.3 software (Thermo Fisher Scientific). MS1 precursor mass tolerance was set at 10 ppm, and MS2 tolerance was set at 20ppm. Search criteria included a static carbamidomethylation of cysteines (+57.0214 Da), and variable modifications of phosphorylation of S, T and Y residues (+79.996 Da), oxidation (+15.9949 Da) on methionine residues and acetylation (+42.011 Da) at N terminus of proteins. Search was performed with full trypsin/P digestion and allowed a maximum of two missed cleavages on the peptides analyzed from the sequence database. The false-discovery rates of proteins and peptides were set at 0.01. All protein and peptide identifications were grouped and any redundant entries were removed. Only unique peptides and unique master proteins were reported.

### Label-free Quantitation Analysis

All data were quantified using the label-free quantitation node of Precursor Ions Quantifier through the Proteome Discoverer v2.3 (Thermo Fisher Scientific). For the quantification of phosphoproteomic data, the intensities of phosphopeptides were extracted with initial precursor mass tolerance set at 10 ppm, minimum number of isotope peaks as 2, maximum ΔRT of isotope pattern multiplets – 0.2 min, PSM confidence FDR of 0.01, with hypothesis test of ANOVA, maximum RT shift of 5 min, pairwise ratio-based ratio calculation, and 100 as the maximum allowed fold change. For calculations of fold-change between the groups of proteins, total phosphoprotein abundance values were added together, and the ratios of these sums were used to compare proteins within different samples.

## Bioinformatics

The LRRK2 interactome was constructed following the procedure reported in Zhao *et al.*[117] Briefly, protein interactions reported for LRRK2 in peer-reviewed literature were considered if the interaction was replicated in at least 2 different papers or identified with 2 different interaction detection methods. The obtained LRRK2 protein interaction network was analysed in Zhao *et al.*[51] to identify topological clusters using the FastGreed R Package (based on degree centrality). Here we report one of the identified clusters that is enriched for synaptic functions. Functional enrichment was performed using g:Profiler, g:GOSt (*https://biit.cs.ut.ee/gprofiler/gost*)[118] with Gene Ontology Biological Processes (GO-BPs) and SynGO (*https://www.syngoportal.org/*).

## Statistical analysis

Statistical analyses and plotting were performed with GraphPad-Prism9. Unpaired, two-tailed t-test or Shapiro-Wilk test were used for experiments comparing two groups; one-way ANOVA was used for experiments comparing three or more groups; two-way ANOVA was used when multiple groups and two factors (i.e., genotype and treatment) were to be compared. Šídák's multiple comparisons test was used when determining statistical significance for comparisons between groups.

# Data availability

The authors confirm that the data supporting the findings of this study are available within the article and its supplementary material.

Protein composition of the LRRK2 cluster enriched for synaptic functions can be obtained from Zhao *et al.*[117]

# Supplementary figures

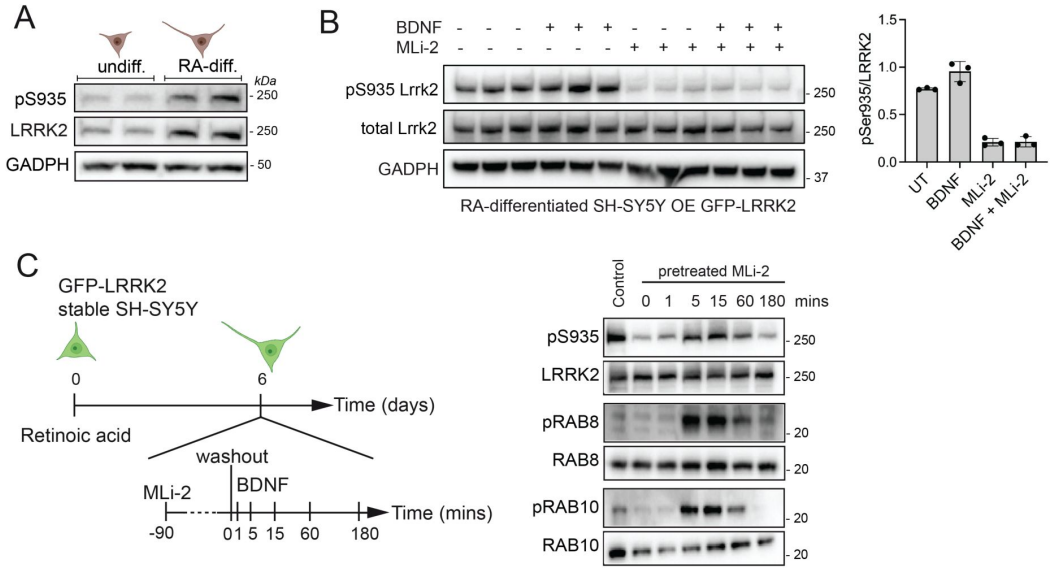


## Figure S1.

**(A)** Western blot analysis of undifferentiated versus differentiated naïve SH-SY5Y and western blot with anti-phospho-Ser935 LRRK2 and total LRRK2 antibodies. **(B)** Cells stably overexpressing GFP-LRRK2 treated with 100 ng/ml BDNF for 5 mins or with 500 nM MLi-2 for 90 mins. **(C)** On the left, schematic representation of experimental setting. On the right, BDNF stimulation of GFP-LRRK2 SH-SY5Y cells prior to MLi-2 (500 nM) treatment for 90 minutes. Western blot were performed using anti LRRK2 (phospho-Ser935 and total), anti-RAB10 (phospho Thr73 and total) and anti-RAB8 (pan-phopho-RABs and total RAB8).

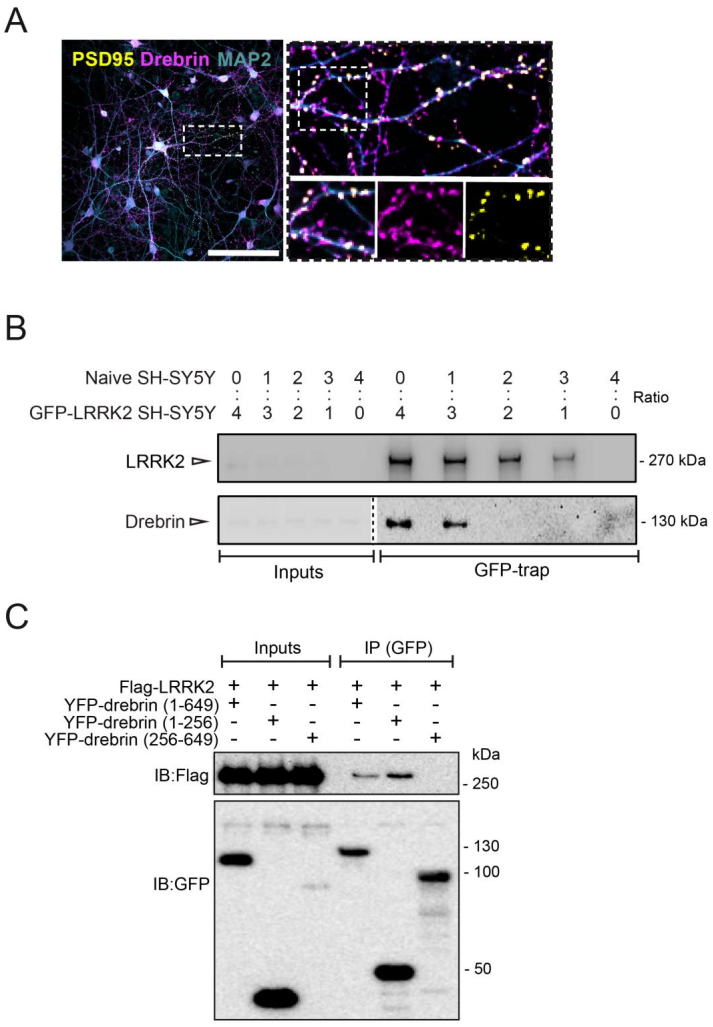


## Figure S2.

### Western blot analysis validating the specificity of LRRK2-Drebrin interaction.

**(A)** Confocal immunofluorescence of DIV14 primary neurons co-stained with MAP2 (neuronal marker), PSD95 (postsynaptic marker) and drebrin. Scale bar: 100 µm; magnifications scale bar: 10 µm. **(B)** To rule out that drebrin does not bind the resin but exclusively GFP-LRRK2 bound to anti-GFP nanobodies, GFP-LRRK2 was purified from cell lysates containing a mix of GFP-LRRK2 OE SH-SY5Y cells and naïve SH-SY5Y cells at different ratios: 4:0, 3:1, 2:2, 1:3, 0:4 (OE:naïve). The levels of drebrin bound to GFP-LRRK2 diminish proportionally with the reduction of LRRK2 purified from the lysate, with a complete lack of signal in the eluate from the resin incubated with naïve cells only (0:4 condition), confirming the specificity of drebrin binding to GFP-LRRK2. **(C)** Co-immunoprecipitation of 3xFlag-LRRK2 with YFP-drebrin domains (full-length, N-terminus and C-terminus; aminoacid boundaries are indicated in the figure). Drebrin constructs were immunoprecipitated with GFP-trap resin and co-precipitated LRRK2 visualized by western blot using anti Flag antibodies.

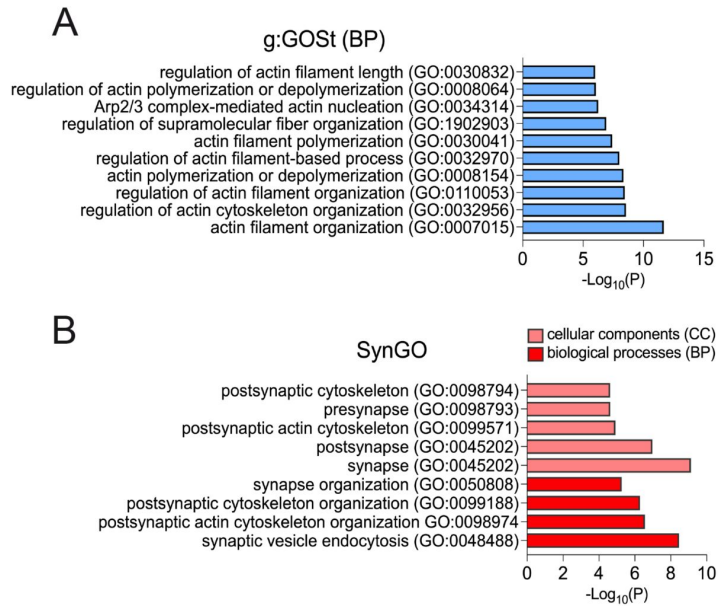


**Figure S3.**

**(A)** Functional enrichment analysis; the analysis was performed using g:Profiler g:GOSt, proteins related to actin cytoskeleton were manually identified and blue-colored, and the first ten GO-BPs categories with term size <500 were graphed. **(B)** SynGO of enriched biological-processes and cellular components; synaptic proteins were red-colored, and significant terms in SynGO-BP and SynGO-CC categories were graphed.

## Figure S4.

### Analysis of the predicted aminoacid pathogenicity in drebrin using AlphaMissense pathogenicity score.

Aminoacid change of S339 or its neighbor S337 is predicted to be benign, suggesting that phosphorylation at this site may play a regulatory function.

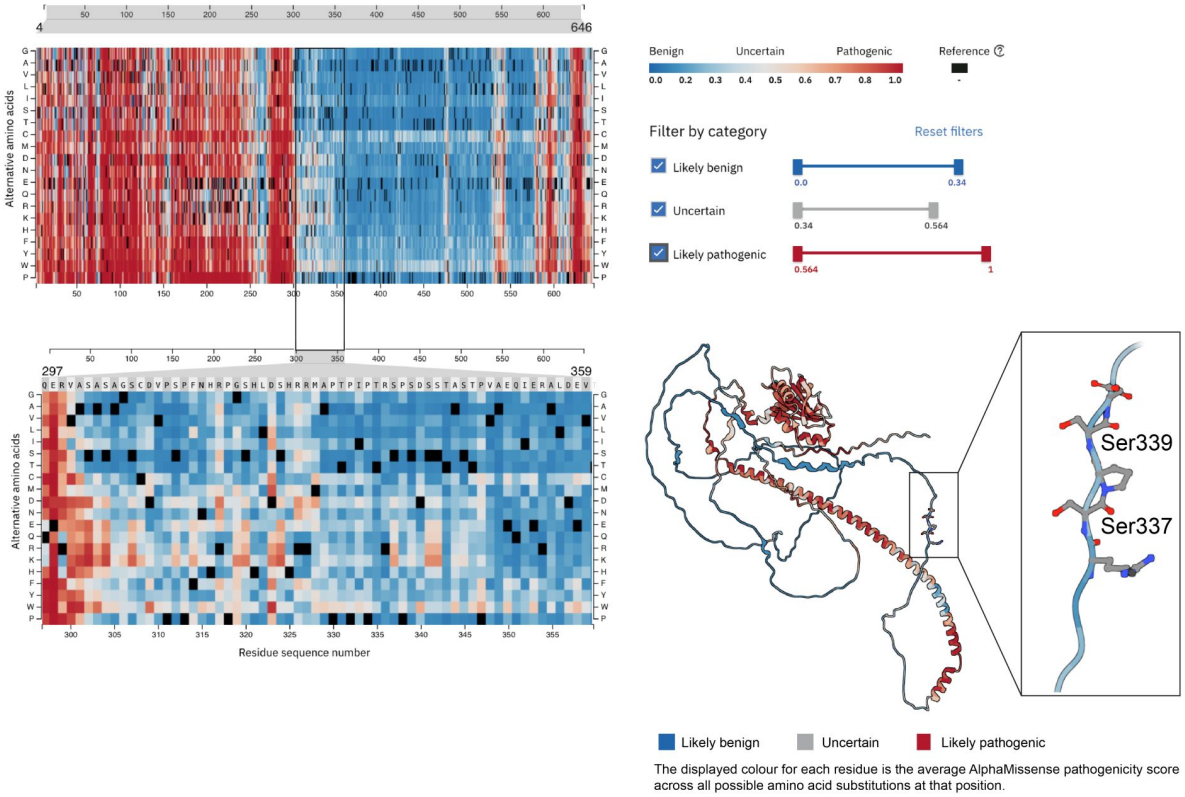


## Figure S5.

Western blot of different monoclonal populations of SH-SY5Y cells transfected with pSpCas9(BB)-2A-Puro (PX459) V2.0 vector (Addgene, Watertown, MA, US) for co-expression of Cas9 and gRNAs (gRNA1, gRNA2 and gRNAB) and subsequent single clone isolation and expansion. The band intensities corresponding to the total amount of endogenous LRRK2 were normalized to GAPDH, used as loading control.

| Guide name | sequence |
|---|---|
| gRNA1 | CACACTCGCGACTCTCATAT |
| gRNA2 | TGTGCCTCTGTTGATCGTCT |
| gRNAB | GAGTCCAAGACGATCAACAG |

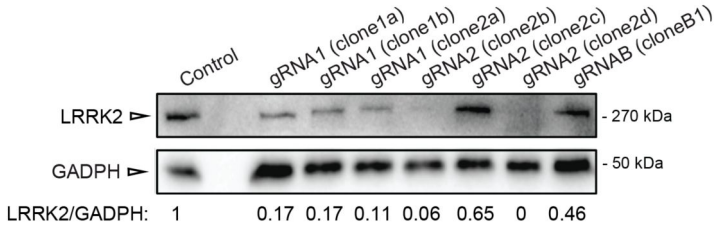

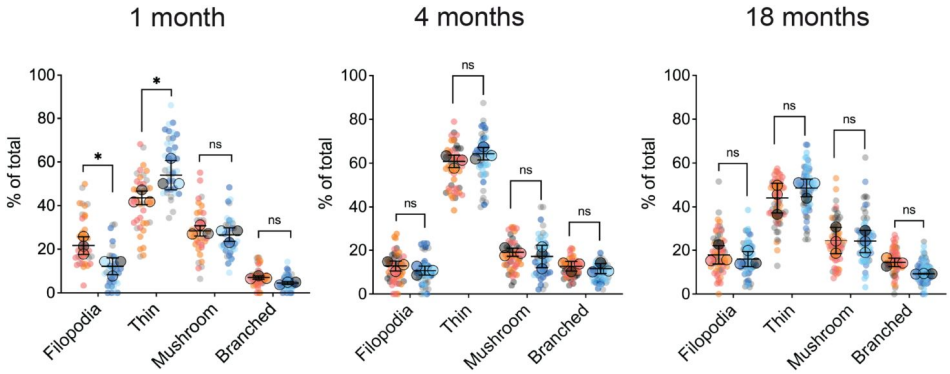


**Figure S6.**

**Morphological classification of protrusions into four classes (filopodia, thin, mushroom, branched) and quantified as % of the total number.**

Each dot represents one segment (*n* ;: 20 segments analyzed per animal; genotype: wild-type vs. *Lrrk2* KO; age: 1, 4, 18 month-old; *n*=3 mice per group) and error bars represent the mean ± SD of *n*=3 mice (color coded). Statistical significance was determined by two-way ANOVA with Šídák's multiple comparisons test on mean values. One-month: interaction: ***P*=0.0017, F (3, 16) = 8.018; genotype: *P*=0.5731, F (1, 16) = 0.3309; class of protrusion: *****P*<0.0001, F (3, 16) = 158.4; filopodia WT vs. KO *P*=0.0201; thin WT vs. KO **P*=0.0102; mushroom WT vs. KO *P*=0.9585; branched WT vs. KO *P*=0.8726. Four-months: interaction: *P*=0.3178, F (3, 16) = 1.271; genotype: *P*=0.7300, F (1, 16) = 0.1233; class of protrusion: *****P*<0.0001, F (3, 16) = 438.9; filopodia WT vs. KO *P*=0.8478; thin WT vs. KO *P*=0.4921; mushroom WT vs. KO *P*=0.8882; branched WT vs. KO *P*=0.9858. Eighteen-months: interaction: *P*=0.3237, F (3, 16) = 1.253; genotype: *P*=0.6880, F (1, 16) = 0.1672; class of protrusion: *****P*<0.0001, F (3, 16) = 69.67; filopodia WT vs. KO *P*=0.9756; thin WT vs. KO *P*=0.6413; mushroom WT vs. KO *P*>0.9999; branched WT vs. KO *P*=0.5290.

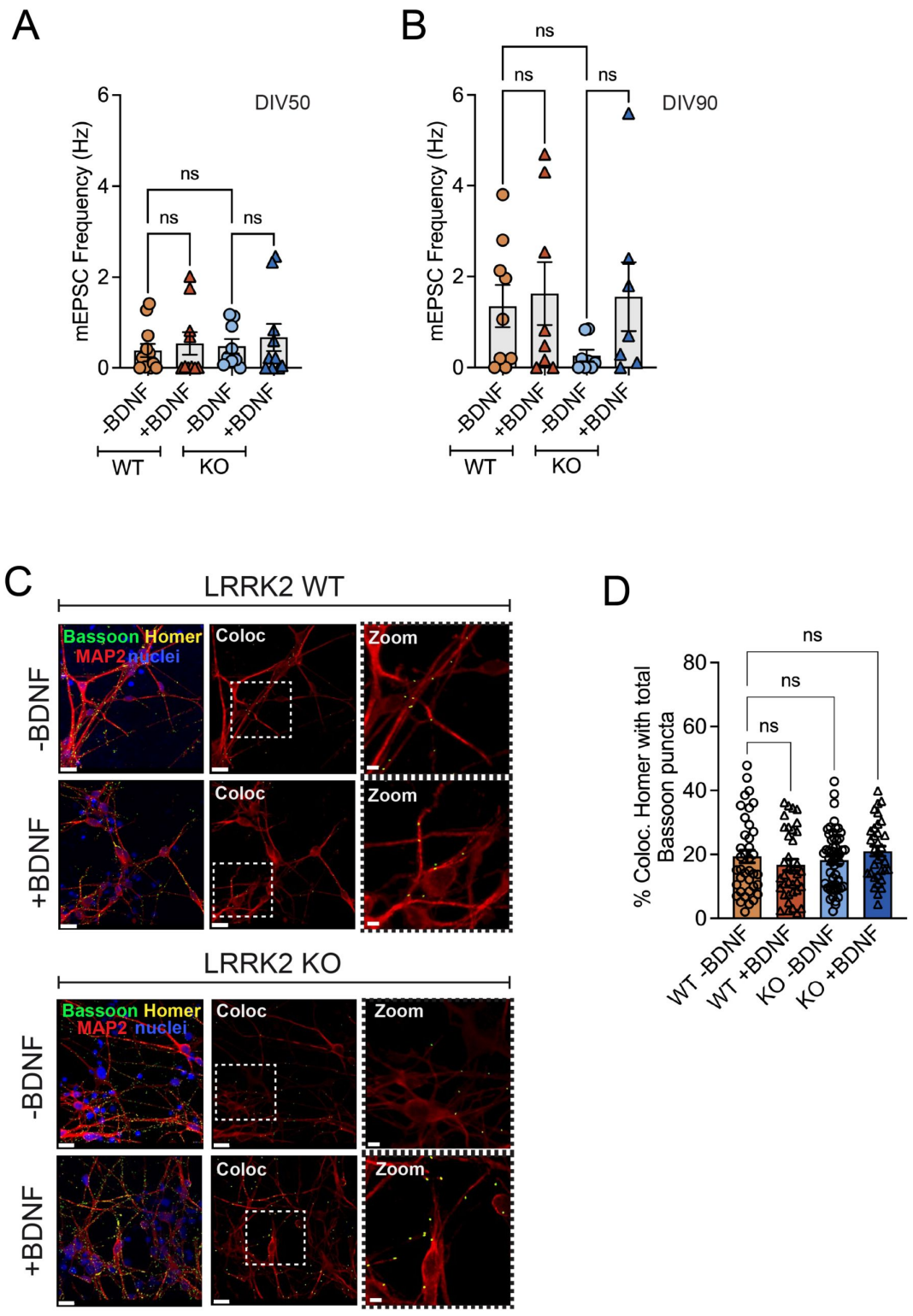


**Figure S7.**

No significant change in the frequency of mEPSC between WT and KO in **(A)** DIV50 and **(B)** DIV90 due to the addition of BDNF (50 mg/ml for 24 hrs). One-way ANOVA with Tukey's post-doc test. P>0.05 for all comparisons (N=2 independent cultures). (**C**) Immunocytochemistry of WT and LRRK2 KO cortical neurons at DIV70 using Bassoon (pre-synaptic marker), Homer (post-synaptic marker), MAP2 (neuronal marker) and DAPI (scale bars 20 µm; zoom 5 µm). (**D**) Quantification of the % of Homer puncta colocalizing with total Bassoon (on MAP2-positive processes). BDNF was applied at 50 mg/ml for 24. One-way ANOVA with Tukey's post-doc test. P>0.05 for all comparisons. N=4 cultures with 5-25 neurons imaged per condition per culture.

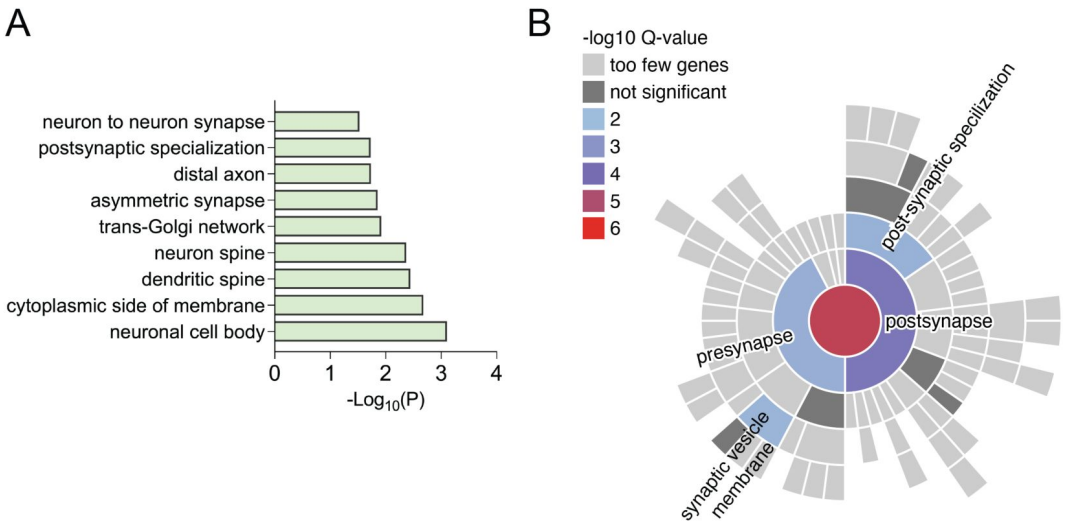


## Figure S8.

**(A)** Functional enrichment analysis of the nearest genes to each of the 134 significant loci (obtained from table S3, column F from *https://doi.org/10.1101/2025.03.14.24319455*) was performed using g:Profiler g:GOSt with term size <500 to increase specificity. (B) SynGO analysis of 32 genes mapped from the input list (from GWAS) revealed significant enrichment of synaptic Cellular Component (5 terms) and Biological Process (6 terms) annotations at 1% FDR. Annotations were based on 31 genes for Cellular Components and 27 for Biological Processes, using a brain-expressed background of 18,035 genes. Experimental-evidence filtering was not applied. SynGO version 20231201 was used.

# Supplemental file 1

## Procedure to check CRISPR-mediated LRRK2 KO in SH-SY5Y cells

Selection of off-targets and primers design

- *http://crispor.gi.ucsc.edu/*
- Copy and paste the sequence of LRRK2 exon we targeted (exon # XX)
- Select the reference genome: Homo sapiens – Human – USCS Dec. 2013 (GRCh38/hg38) + SNPs: dbSNP148, Kaviar
- Select the Protospacer Adjacent Motif (PAM): 20bp-NGG – Sp Cas9, SpCas9-HF1, eSpCas9 1.1
- Submit
- Select the first 8 results exhibiting a CFD (Cutting Frequency Determination) off-target score > 0.2
- Search for the genomic region containing the off-target sequence reported for each of the selected results
- Design forward and reverse primers, respectively upstream to and downstream of the off-target, for each sequence (off-targets and LRRK2 on-target)
- Select the forward primers for the sequencing

Cell culture procedure and sequencing

- Culture SH-SY5Y cells wild-type and LRRK2 KO until reaching confluence in T25 flasks as described in the material and methods
- Detach and centrifuge the cell populations, keeping the pellets in ice
- Deliver pairs of primers and cellular pellets to BMR Genomics (*https://www.bmr-genomics.it/*) for PCR amplification and sequencing
- Compare the sequences obtained from wild-type and LRRK2 KO cells with the reference ones using BLAST in order to find potential mismatches
- If the sequence identity is higher than 99% and the mismatch is placed in the final portion of the sequenced region, it is accepted as equal to the reference sequence

## Results

Disruption of the sequence was observed only in LRRK2 on-target site in the LRRK2 KO SH-SY5Y cells, while the 8 off-target regions were unchanged across the genotypes as well as when compared to the reference sequence

**ontarget_mm0_exon_LRRK2_chr12_40225585**
F_TGCTGGTGTTCACGTACTCC; Tm=59.9
R_GCACACTCGCGACTCTCATA; Tm=59.9

hLRRK2_LRRK2 WT
CTGTGCTTTTATTTTTGCAAACTTTCTCCCCCTCCTTACATTTGCAAATTTTGTCCTCCTCCCCTTGACCCT
GCTCAAACCCGGACTCTTAAGGAGCCGCAAACTCCCATATCCTTTCCTTAGGGCAGAAAGCAGCTGAGA
ATTTCAGGAAGGTCTTCACCTTTTTGACTTTTCTCCCCGTTTCAGACTAAAAAGGAAAGGGGGTGCTGTG
GATTGTGACTTTGCTTCTTTTCCCCACCCACTTGTTTTCCAGCCTCCAAGTTATTTCAAGGCAAAAATATC
CATGTGCCTCTGTTGATCGTCTTGGACTCCTATATGAGAGTCGCAGCAGGTAAAGGCATTGTTTTCACTTC
AACTCATTCTCCCTTCTGTTTGGAAGGAGACGTTTTACTGGCAATGT

hLRRK2_LRRK2 KO
CTGTGCTTTTATTTTTGCAAACTTTCTCCCCCTCCTTACATTTGCAAATTTTGTCCTCCTCCCCTTGACCCT
GCTCAAACCCGGACTCTTAAGGAGCCGCAAACTCCCATATCCTTTCCTTAGGGCAGAAAGCAGCTGAGA
ATTTCAGGAAGGTCTTCACCTTTTTGACTTTTCTCCCCGTTTCAGACTAAAAAGGAAAGGGGGTGCTGTG
GATTGTGACTTTGCTTCTTTTCCCCACCCACTTGTTTTCCAGCCTCCAAGTTATTTCAAGGCAAAAATATC
CATGTGCCTCTGTTGATCGTCTTGGACTCCTATATGAGAGTCGCGGGTTGTGCAAAAGAATATTTTTCTTT
TTCTTTTCTTCCCTTTTTTTTTTTTTTTTTTTTTTTTTTAAAAAGGGGTTTTGGGGCCCCTTTTAAAAAAGCGG
GGAGGGCAAA

1. **mm4_intergenic_APOC1|APOC4/APOC4-APOC2_chr19_44927007**

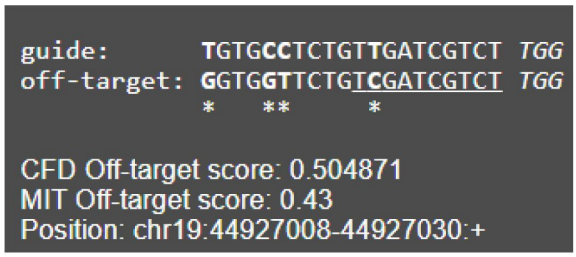


hAPOC1_LRRK2 WT
CGTGGGAGGGAGGGAGGAGGGTGCCACTGATCCCCTGAACCCCTGCCTCCGCCTCCAGGGTGCCCCT
CCGGCCTCGCCATGAGGCTCTTCCTGTCGCTCCCGGTCCTGGTGGTGGTTCTGTCGATGGTCTTGGAA
GGTAAAAGTGGGATGGGAGAATTGCGGAGTTGGAA

hAPOC1_LRRK2 KO
CGTGGGAGGGAGGGAGGAGGGTGCCACTGATCCCCTGAACCCCTGCCTCCGCCTCCAGGGTGCCCCT
CCGGCCTCGCCATGAGGCTCTTCCTGTCGCTCCCGGTCCTGGTGGTGGTTCTGTCGATGGTCTTGGAA
GGTAAAAGTGGGATGGGAGAATTGCGGAGTTGGAA

| Score | Expect | Identities | Gaps | Strand |
|---|---|---|---|---|
| 315 bits(170) | 4e-91 | 170/170(100%) | 0/170(0%) | Plus/Plus |

```
Query  1    CGTGGGAGGGAGGGAGGAGGGTGCCACTGATCCCCTGAACCCCTGCCTCCGCCTCCAGGG  60
            ||||||||||||||||||||||||||||||||||||||||||||||||||||||||||||
Sbjct  1    CGTGGGAGGGAGGGAGGAGGGTGCCACTGATCCCCTGAACCCCTGCCTCCGCCTCCAGGG  60

Query  61   TGCCCCTCCGGCCTCGCCATGAGGCTCTTCCTGTCGCTCCCGGTCCTGGTGGTGGTTCTG  120
            ||||||||||||||||||||||||||||||||||||||||||||||||||||||||||||
Sbjct  61   TGCCCCTCCGGCCTCGCCATGAGGCTCTTCCTGTCGCTCCCGGTCCTGGTGGTGGTTCTG  120

Query  121  TCGATGGTCTTGGAAGGTAAAAGTGGGATGGGAGAATTGCGGAGTTGGAA  170
            ||||||||||||||||||||||||||||||||||||||||||||||||||
Sbjct  121  TCGATGGTCTTGGAAGGTAAAAGTGGGATGGGAGAATTGCGGAGTTGGAA  170
```

2. **mm4_exon_APOE/CTB-129P6.7/APOC1_chr19_44914923**

F_GACAGGACCTCCCAACCAAG; Tm=59.9
R_TCCAACTCCGCAATTCTCCC; Tm=60.0

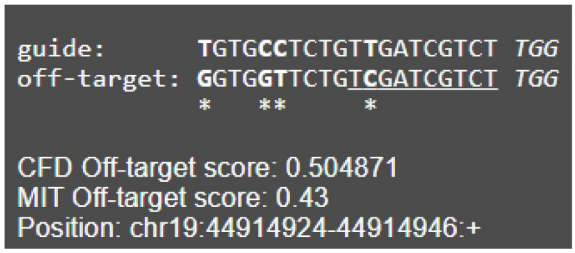


hAPOE_LRRK2 WT
AAGGGATCGAGGGAGGGAGGGAGGAGGGGAGGGATGATGCCCTGAACCCCTGCCTCCGCCTCCAGG
GTGCCCCTCCGGCCTCCCCATGAGGCTCTTCCTGTCGCTCCCGGTCCTGGTGGTGGTTCTGTCGATGG
TCTTGGAAGGTAAAAGTGGGATGGGAGAATTGC

hAPOE_LRRK2 KO
GGAGGGATGATGCCCTGAACCCCTGCCTCCGCCTCCAGGGTGCCCCTCCGGCCTCCCCATGAGGCTCT
TCCTGTCGCTCCCGGTCCTGGTGGTGGTTCTGTCGATGGTCTTGGAAGGTAAAAGTGGGATGGGAGAAT
TGCGGAGTTGGAT

| Score | Expect | Identities | Gaps | Strand |
|---|---|---|---|---|
| 253 bits(280) | 9e-73 | 140/140(100%) | 0/140(0%) | Plus/Plus |

```
Query  1    GGAGGGATGATGCCCTGAACCCCTGCCTCCGCCTCCAGGGTGCCCCTCCGGCCTCCCCAT  60
            ||||||||||||||||||||||||||||||||||||||||||||||||||||||||||||
Sbjct  28   GGAGGGATGATGCCCTGAACCCCTGCCTCCGCCTCCAGGGTGCCCCTCCGGCCTCCCCAT  87

Query  61   GAGGCTCTTCCTGTCGCTCCCGGTCCTGGTGGTGGTTCTGTCGATGGTCTTGGAAGGTAA  120
            ||||||||||||||||||||||||||||||||||||||||||||||||||||||||||||
Sbjct  88   GAGGCTCTTCCTGTCGCTCCCGGTCCTGGTGGTGGTTCTGTCGATGGTCTTGGAAGGTAA  147

Query  121  AAGTGGGATGGGAGAATTGC  140
            ||||||||||||||||||||
Sbjct  148  AAGTGGGATGGGAGAATTGC  167
```

3. **mm4_intergenic_RP11-329N22.1|RRAGC/RP5-864K19.7_chr1_38822106**

F_GCCCTCACCTTACCAAAGCT; Tm=59.9
R_CCGCTTTCATCCTAATGGGGT; Tm=60.1

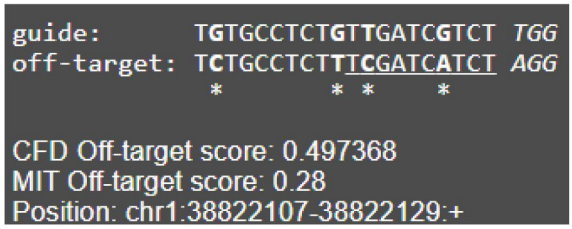


hRP11-329N22.1_LRRK2 WT
GGCTCGCTTGCTAAAGCTCTCCAGAGAGGCACTTTGAATTAAGACCAGAAATGCTTTTAAAAGACTCTGG
TCTCTGGTCTTCTAATGATGACCTCTTCCTTAATTTTGTGATGGCTTCATCTGCCTCTTTCGATCATCTAGG
TAGCTATAAAAAGCTGAACACCTCCTACTAACCCCATTAGGATGAAAGCGG

hRP11-329N22.1_LRRK2 KO
GGCTCGCTTGCTAAAGCTCTCCAGAGAGGCACTTTGAATTAAGACCAGAAATGCTTTTAAAAGACTCTGG
TCTCTGGTCTTCTAATGATGACCTCTTCCTTAATTTTGTGATGGCTTCATCTGCCTCTTTCGATCATCTAGG
TAGCTATAAAAAGCTGAACACCTCCTACTAACCCCATTAGGATGAAAGCGG

| Score | Expect | Identities | Gaps | Strand |
|---|---|---|---|---|
| 357 bits(193) | 8e-104 | 193/193(100%) | 0/193(0%) | Plus/Plus |

```
Query  1    GGCTCGCTTGCTAAAGCTCTCCAGAGAGGCACTTTGAATTAAGACCAGAAATGCTTTTAA  60
            ||||||||||||||||||||||||||||||||||||||||||||||||||||||||||||
Sbjct  1    GGCTCGCTTGCTAAAGCTCTCCAGAGAGGCACTTTGAATTAAGACCAGAAATGCTTTTAA  60

Query  61   AAGACTCTGGTCTCTGGTCTTCTAATGATGACCTCTTCCTTAATTTTGTGATGGCTTCAT  120
            ||||||||||||||||||||||||||||||||||||||||||||||||||||||||||||
Sbjct  61   AAGACTCTGGTCTCTGGTCTTCTAATGATGACCTCTTCCTTAATTTTGTGATGGCTTCAT  120

Query  121  CTGCCTCTTTCGATCATCTAGGTAGCTATAAAAAGCTGAACACCTCCTACTAACCCCATT  180
            ||||||||||||||||||||||||||||||||||||||||||||||||||||||||||||
Sbjct  121  CTGCCTCTTTCGATCATCTAGGTAGCTATAAAAAGCTGAACACCTCCTACTAACCCCATT  180

Query  181  AGGATGAAAGCGG  193
            |||||||||||||
Sbjct  181  AGGATGAAAGCGG  193
```

4. **mm4_intergenic_RP11-295D22.1|AL354931.1_chr9_119731666**

F_GAACTGGCTGCCCAAGGAG; Tm=60.6
R_CAAACACTCCCCAAGTAGACTG; Tm=58.5

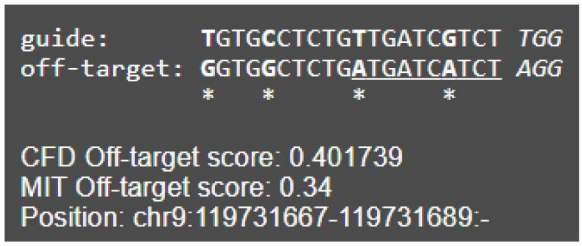


hRP11-295D22.1_LRRK2 WT
TCTTTATTTAGCTCTCAGGCTCTACCTATCCAACTGAAACATTTTCTGAGGTAAGGGCTGAGAATGTGTATT
TTTTTTTTTTTAAAAAAAACAACCCTAGGGGGGTTTTAAAAAAATATAGGTTTGGGAAACTTTTTCCCGGCC
CCCCCTTGGGCCCCCCCTTAAAA

hRP11-295D22.1_LRRK2 KO
TCTTTATTTAGCTCTCAGGCTCTACCTATCCAACTGAAACATTTTCTGAGGTAAGGGCTGAGAATGTGTATT
TTTTTTTTTTTAAAAAAAACAACCCTAGGGGGGTTTTAAAAAAATATAGGTTTGGGAGACTTTTTCCCGGCC
CCCCCTTGGGCCCCCCCTTAAAA

| Score | Expect | Identities | Gaps | Strand |
|---|---|---|---|---|
| 297 bits(329) | 1e-85 | 166/167(99%) | 0/167(0%) | Plus/Plus |

```
Query  1    TCTTTATTTAGCTCTCAGGCTCTACCTATCCAACTGAAACATTTTCTGAGGTAAGGGCTG  60
            ||||||||||||||||||||||||||||||||||||||||||||||||||||||||||||
Sbjct  1    TCTTTATTTAGCTCTCAGGCTCTACCTATCCAACTGAAACATTTTCTGAGGTAAGGGCTG  60

Query  61   AGAATGTGTAttttttttttttttaaaaaaaaCAACCCTAGGGGGGTTTTaaaaaaaTATA  120
            ||||||||||||||||||||||||||||||||||||||||||||||||||||||||||||
Sbjct  61   AGAATGTGTATTTTTTTTTTTTTTAAAAAAAACAACCCTAGGGGGGTTTTAAAAAAATATA  120

Query  121  GGTTTGGGAGACTTTTTCCCGGccccccccttgggcccccccTTAAAA  167
            ||||||||| ||||||||||||||||||||||||||||||||||||||
Sbjct  121  GGTTTGGGAAACTTTTTCCCGGCCCCCCCCTTGGGCCCCCCCCTTAAAA  167
```

5. **mm4_intergenic_RN7SL302P|MIR181A2HG_chr9_124658380**

F_AGTGACTAGAGGCAGCCAGA; Tm=59.9
R_TCTGCTCAGCTCGCATTGAA; Tm=60.0

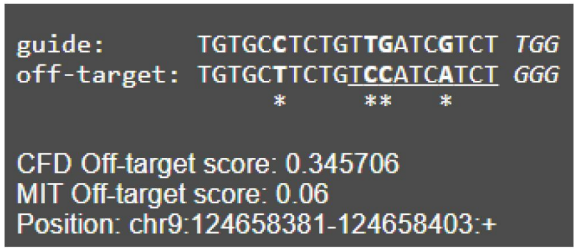


nRN7SL302P_LRRK2 WT
GCCTCTGAATGGTGAGGGCTTCACATTTCACCGATCAGGGCACAGCCCAATCAGAAGACAAACCCCTGC
ACTGCCAGGGACCAGCAAATCCGCTTTCTTCCAGTGTGCACATGACTAAATGTGCTTCTGTCCATCATCT
GGGTCATATATAGTTCAATGCGAGCTGAGCAGAA

nRN7SL302P_LRRK2 KO
GCCTCTGAATGGTGAGGGCTTCACATTTCACCGATCAGGGCACAGCCCAATCAGAAGACAAACCCCTGC
ACTGCCAGGGACCAGCAAATCCGCTTTCTTCCAGTGTGCACATGACTAAATGTGCTTCTGTCCATCATCT
GGGTCATATATAGTTCAATGCGAGCTGAGCAGAA

| Score | Expect | Identities | Gaps | Strand |
|---|---|---|---|---|
| 320 bits(173) | 8e-93 | 173/173(100%) | 0/173(0%) | Plus/Plus |

```
Query  1    GCCTCTGAATGGTGAGGGCTTCACATTTCACCGATCAGGGCACAGCCCAATCAGAAGACA  60
            ||||||||||||||||||||||||||||||||||||||||||||||||||||||||||||
Sbjct  1    GCCTCTGAATGGTGAGGGCTTCACATTTCACCGATCAGGGCACAGCCCAATCAGAAGACA  60

Query  61   AACCCCTGCACTGCCAGGGACCAGCAAATCCGCTTTCTTCCAGTGTGCACATGACTAAAT  120
            ||||||||||||||||||||||||||||||||||||||||||||||||||||||||||||
Sbjct  61   AACCCCTGCACTGCCAGGGACCAGCAAATCCGCTTTCTTCCAGTGTGCACATGACTAAAT  120

Query  121  GTGCTTCTGTCCATCATCTGGGTCATATATAGTTCAATGCGAGCTGAGCAGAA  173
            |||||||||||||||||||||||||||||||||||||||||||||||||||||
Sbjct  121  GTGCTTCTGTCCATCATCTGGGTCATATATAGTTCAATGCGAGCTGAGCAGAA  173
```

6. **mm4_intergenic_RP11-354I10.1|OFCC1_chr6_9603371**

F_AACTCAGGGCTGACATTGGG; Tm=59.9
R_GCTGACAGCTGTTCTTTCAGA; Tm=58.5

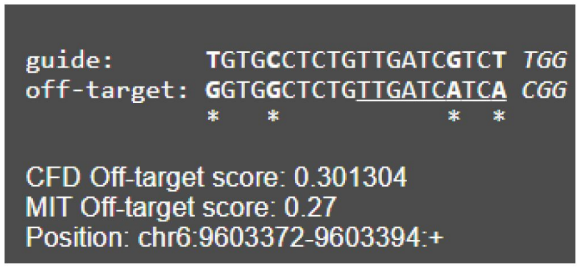


hRP11-354_LRRK2 WT
AATCTTAAGACGTTGAATAGTTTACAACCAAGTAAAGTATACTTTTGCAAAAATGGAAGGACTATGTGCTGT
GGCTTATAATTTTCACAGCCGTGATGATCAACAGAGCCACCACCACCAACACCCAGGATCCCTATATTCCA
GGGAATAAATCCCAATGTCAGCCCTGAGTTA

hRP11-354_LRRK2 KO
TTTAATCTTAAGACGTTGAATAGTTTACAACCAAGTAAAGTATACTTTTGCAAAAATGGAAGGACTATGTGC
TGTGGCTTATAATTTTCACAGCCGTGATGATCAACAGAGCCACCACCACCAACACCCAGGATCCCTATATT
CCAGGGAATAAATCCCAATGTCAGCCCTGAGTTA

| Score | Expect | Identities | Gaps | Strand |
|---|---|---|---|---|
| 322 bits(174) | 2e-93 | 174/174(100%) | 0/174(0%) | Plus/Plus |

```
Query  4    AATCTTAAGACGTTGAATAGTTTACAACCAAGTAAAGTATACTTTTGCAAAAATGGAAGG  63
            ||||||||||||||||||||||||||||||||||||||||||||||||||||||||||||
Sbjct  1    AATCTTAAGACGTTGAATAGTTTACAACCAAGTAAAGTATACTTTTGCAAAAATGGAAGG  60

Query  64   ACTATGTGCTGTGGCTTATAATTTTCACAGCCGTGATGATCAACAGAGCCACCACCACCA  123
            ||||||||||||||||||||||||||||||||||||||||||||||||||||||||||||
Sbjct  61   ACTATGTGCTGTGGCTTATAATTTTCACAGCCGTGATGATCAACAGAGCCACCACCACCA  120

Query  124  ACACCCAGGATCCCTATATTCCAGGGAATAAATCCCAATGTCAGCCCTGAGTTA  177
            ||||||||||||||||||||||||||||||||||||||||||||||||||||||
Sbjct  121  ACACCCAGGATCCCTATATTCCAGGGAATAAATCCCAATGTCAGCCCTGAGTTA  174
```

7. **mm4_intergenic_RP11-566H8.3|RP11-566H8.1_chr8_31391168**

F_TTTGCCACCTCTCTTGCAGT; Tm=59.8
R_CCACAGCTGCTACTATCTGCA; Tm=59.8

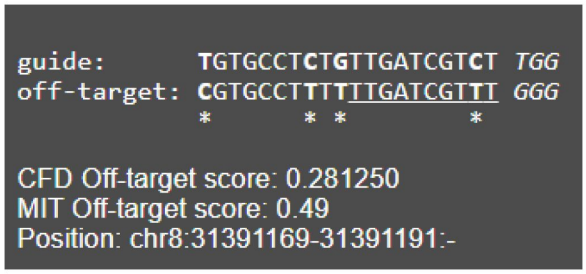


hRP11-566H8.3_LRRK2 WT
CATAAATCGGAATTGCAATTCACATGCAGAAGGGAAGAAGCTATCTTACTTGTCATCTCGATGGAAAGTTG
CTTTTGCTTAGGATTTATTCTTTTATCTTTTTTTCCCCTGACTTTCTGAATAGGTGAGGACACAGATTTCAG
CGTGCCTTTTTTGATCGTTTGGGCTTTTTTGATCTTTTTTGTTGTTGCTTTTTCCCTTTATGTTTTAGGTTAA
CTCACTGCAAGAGAGGTGGGCAAAA

hRP11-566H8.3_LRRK2 KO
TGATTTCTGTCCAGATCATAAATCGGAATTGCAATTCACATGCAGAAGGGAAGAAGCTATCTTACTTGTCAT
CTCGATGGAAAGTTGCTTTTGCTTAGGATTTATTCTTTTATCTTTTTTTCCCCTGACTTTCTGAATAGGTGA
GGACACAGATTTCAGCGTGCCTTTTTTGATCGTTTGGGCTTTTTTGATCTTTTTTGTTGTTGCTTTTTCCCT
TTATGTTTTAGGTTAACTCACTGCAAGAGAGGTGG-CAAAA

| Score | Expect | Identities | Gaps | Strand |
|---|---|---|---|---|
| 438 bits(237) | 5e-128 | 240/241(99%) | 1/241(0%) | Plus/Plus |

```
Query  17   CATAAATCGGAATTGCAATTCACATGCAGAAGGGAAGAAGCTATCTTACTTGTCATCTCG  76
            ||||||||||||||||||||||||||||||||||||||||||||||||||||||||||||
Sbjct  1    CATAAATCGGAATTGCAATTCACATGCAGAAGGGAAGAAGCTATCTTACTTGTCATCTCG  60

Query  77   ATGGAAAGTTGCTTTTGCTTAGGATTTATTCTTTTATCttttttttCCCCTGACTTTCTGA  136
            ||||||||||||||||||||||||||||||||||||||||||||||||||||||||||||
Sbjct  61   ATGGAAAGTTGCTTTTGCTTAGGATTTATTCTTTTATCTTTTTTTCCCCTGACTTTCTGA  120

Query  137  ATAGGTGAGGACACAGATTTCAGCGTGCctttttttgatcgtttgggctttttttgatcttt  196
            ||||||||||||||||||||||||||||||||||||||||||||||||||||||||||||
Sbjct  121  ATAGGTGAGGACACAGATTTCAGCGTGCCTTTTTTGATCGTTTGGGCTTTTTTGATCTTT  180

Query  197  tttgttgttgctttttcccttttatgttttAGGTTAACTCACTGCAAGAGAGGTGG-CAAA  255
            |||||||||||||||||||||||||||||||||||||||||||||||||||||| ||||
Sbjct  181  TTTGTTGTTGCTTTTTCCCTTTATGTTTTAGGTTAACTCACTGCAAGAGAGGTGGGCAAA  240

Query  256  A  256
            |
Sbjct  241  A  241
```

8. **mm4_intron_CDKN3_chr14_54414282**

F_CTCGGATGTCTGTGTCTTTG; Tm=60.0
R_CAATAAGACAGGAGAGGCAG; Tm=60.0

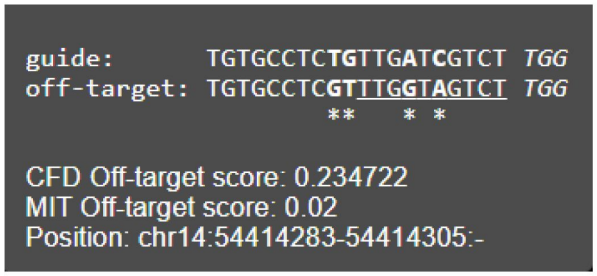


hCDKN3_LRRK2 WT
TAGGATGAGGGCCTGCTCTAATTCGTCTTAACTTGAATATACCTGCAAAGACTCAAATTCTGAATAAGGTC
CCACTCACAGGTACAGGATAAGGACTTCAGCATGTCTTTTGGGGGGACATAATTCAACCAGTAACACCTA
CCGTGTACCACACGCCAAGACTACCAAACGAGGCACAGTCCCCACCTTCGAGGAACCTATAACTAACAC
TACCATTTAACTGCAATAAGACAGGAGAAGGCAGA

hCDKN3_LRRK2 KO
GTAGGAACTAGTCTCTAGGATGAGGGCCTGCTCTAATTCGTCTTAACTTGAATATACCTGCAAAGACTCAA
ATTCTGAATAAGGTCCCACTCACAGGTACAGGATAAGGACTTCAGCATGTCTTTTGGGGGGACATAATTC
AACCAGTAACACCTACCGTGTACCACACGCCAAGACTACCAAACGAGGCACAGTCCCCACCTTCGAGGA
ACCTATAACTAACACTACCATTTAACTGCAATAAGACAGG-GAGGGCAGA

| Score | Expect | Identities | Gaps | Strand |
|---|---|---|---|---|
| 440 bits(238) | 1e-128 | 243/245(99%) | 1/245(0%) | Plus/Plus |

```
Query  16   TAGGATGAGGGCCTGCTCTAATTCGTCTTAACTTGAATATACCTGCAAAGACTCAAATTC  75
            ||||||||||||||||||||||||||||||||||||||||||||||||||||||||||||
Sbjct  1    TAGGATGAGGGCCTGCTCTAATTCGTCTTAACTTGAATATACCTGCAAAGACTCAAATTC  60

Query  76   TGAATAAGGTCCCACTCACAGGTACAGGATAAGGACTTCAGCATGTCTTTTGGGGGGACA  135
            ||||||||||||||||||||||||||||||||||||||||||||||||||||||||||||
Sbjct  61   TGAATAAGGTCCCACTCACAGGTACAGGATAAGGACTTCAGCATGTCTTTTGGGGGGACA  120

Query  136  TAATTCAACCAGTAACACCTACCGTGTACCACACGCCAAGACTACCAAACGAGGCACAGT  195
            ||||||||||||||||||||||||||||||||||||||||||||||||||||||||||||
Sbjct  121  TAATTCAACCAGTAACACCTACCGTGTACCACACGCCAAGACTACCAAACGAGGCACAGT  180

Query  196  CCCCACCTTCGAGGAACCTATAACTAACACTACCATTTAACTGCAATAAGACAGG-GAGG  254
            |||||||||||||||||||||||||||||||||||||||||||||||||||| || |
Sbjct  181  CCCCACCTTCGAGGAACCTATAACTAACACTACCATTTAACTGCAATAAGACAGGAGAAG  240

Query  255  GCAGA  259
            |||||
Sbjct  241  GCAGA  245
```

# Acknowledgements

We are very grateful to Dr. Mark R Cookson and Alexandra Beilina (NIA, NIH, USA) for providing WT and LRRK2 KO human iPSC lines used for electrophysiological measurements.

# Additional information

## Funding

This work was supported by the University of Padova [STARS Grants, LRRKing-Role of the Parkinson's disease kinase LRRK2 in shaping neurites and synapses, EG), the Michael J. Fox Foundation for Parkinson's Research-LRRK2 challenge (EG, LP and CM), NIH R01 NS097901 (LP), UKRI future Leader Fellowship funding MR/T041129/1 (DBK).

## Funding

**University of Padova (STARS Grants, LRRKing-Role of the Parkinson's disease kinase LRRK2 in shaping neurites and synapses)**

**Michael J. Fox Foundation**

**NIH (R01 NS097901)**

# Additional files

***Supplementary .xls table 1***

***Supplementary .xls table 2***

***Supplementary .xls table 3***

# References


1. Fiala JC, Spacek J, Harris KM (2002) **Dendritic spine pathology: Cause or consequence of neurological disorders?** *Brain Res Rev* **39**:29–54 https://doi.org/10.1016/S0165-0173(02)00158-3 | Google Scholar

2. Hong S, Beja-Glasser VF, Nfonoyim BM, et al. (2016) **Complement and microglia mediate early synapse loss in Alzheimer mouse models** *Science* **352**:712–716 https://doi.org/10.1126/science.aad8373 | Google Scholar

3. Milnerwood AJ, Raymond LA (2010) **Early synaptic pathophysiology in neurodegeneration: Insights from Huntington's disease** *Trends Neurosci* **33**:513–523 https://doi.org/10.1016/j.tins.2010.08.002 | Google Scholar

4. Soukup S, Vanhauwaert R, Verstreken P (2018) **Parkinson's disease: convergence on synaptic homeostasis** *EMBO J* **37** https://doi.org/10.15252/embj.201898960 | Google Scholar

5. Picconi B, Piccoli G, Calabresi P (2012) **Synaptic dysfunction in Parkinson's disease** *Adv Exp Med Biol* **970**:553–572 https://doi.org/10.1007/978-3-7091-0932-8_24 | Google Scholar

6. Kordower JH, Olanow CW, Dodiya HB, et al. (2013) **Disease duration and the integrity of the nigrostriatal system in Parkinson's disease** *Brain* **136**:2419–2431 https://doi.org/10.1093/brain/awt192 | Google Scholar

7. Bellucci A, Antonini A, Pizzi M, Spano PF (2017) **The end is the beginning: Parkinson's disease in the light of brain imaging** *Front Aging Neurosci* **9** https://doi.org/10.3389/fnagi.2017.00330 | Google Scholar

8. Chidambaram SB, Rathipriya AG, Bolla SR, et al. (2019) **Dendritic spines: Revisiting the physiological role** *Prog Neuropsychopharmacol Biol Psychiatry* **92**:161–193 https://doi.org/10.1016/j.pnpbp.2019.01.005 | Google Scholar

9. González-Rodríguez P, Zampese E, Stout KA, et al. (2021) **Disruption of mitochondrial complex I induces progressive parkinsonism** *Nature* **599**:650–656 https://doi.org/10.1038/s41586-021-04059-0 | Google Scholar

10. Cookson MR (2015) **LRRK2 Pathways Leading to Neurodegeneration** *Curr Neurol Neurosci Rep* **15** https://doi.org/10.1007/s11910-015-0564-y | Google Scholar

11. Greggio E, Cookson MR (2009) **Leucine-rich repeat kinase 2 mutations and Parkinson's disease: Three questions** *ASN Neuro* **1**:13–24 https://doi.org/10.1042/AN20090007 | Google Scholar

12. Marchand A, Drouyer M, Sarchione A, Chartier-Harlin MC, Taymans JM (2020) **LRRK2 Phosphorylation, More Than an Epiphenomenon** *Front Neurosci* **14** https://doi.org/10.3389/fnins.2020.00527 | Google Scholar

13. Wallings R, Manzoni C, Bandopadhyay R (2015) **Cellular processes associated with LRRK2 function and dysfunction** *FEBS Journal* **282**:2806–2826 https://doi.org/10.1111/febs.13305 | Google Scholar

14. Alessi DR, Pfeffer SR (2024) **Leucine-Rich Repeat Kinases** *Annu Rev Biochem* **93**:261–287 https://doi.org/10.1146/ANNUREV-BIOCHEM-030122-051144 | Google Scholar

15. Civiero L, Cogo S, Biosa A, Greggio E (2018) **The role of LRRK2 in cytoskeletal dynamics** *Biochem Soc Trans* **46**:1653–1663 https://doi.org/10.1042/BST20180469 | Google Scholar

16. Iannotta L, Greggio E (2021) **LRRK2 signaling in neurodegeneration: two decades of progress** *Essays Biochem* **65**:859–872 https://doi.org/10.1042/ebc20210013 | Google Scholar

17. Nichols RJ, Dzamko N, Morrice NA, et al. (2010) **14-3-3 Binding to LRRK2 is disrupted by multiple Parkinson's disease-associated mutations and regulates cytoplasmic localization** *Biochemical Journal* **430**:393–404 https://doi.org/10.1042/BJ20100483 | Google Scholar

18. Dzamko N, Inesta-Vaquera F, Zhang J, et al. (2012) **The IkappaB kinase family phosphorylates the Parkinson's disease kinase LRRK2 at Ser935 and Ser910 during Toll-Like Receptor signaling** *PLoS One* **7** https://doi.org/10.1371/journal.pone.0039132 | Google Scholar

19. Muda K, Bertinetti D, Gesellchen F, et al. (2014) **Parkinson-related LRRK2 mutation R1441C/G/H impairs PKA phosphorylation of LRRK2 and disrupts its interaction with 14-3-3** *Proc Natl Acad Sci U S A* **111** https://doi.org/10.1073/pnas.1312701111 | Google Scholar

20. Chia R, Haddock S, Beilina A, et al. (2014) **Phosphorylation of LRRK2 by casein kinase 1α regulates trans-Golgi clustering via differential interaction with ARHGEF7** *Nat Commun* **5** https://doi.org/10.1038/ncomms6827 | Google Scholar

21. Dzamko N, Deak M, Hentati F, et al. (2010) **Inhibition of LRRK2 kinase activity leads to dephosphorylation of Ser 910/Ser935, disruption of 14-3-3 binding and altered cytoplasmic localization** *Biochemical Journal* **430**:405–413 https://doi.org/10.1042/BJ20100784 | Google Scholar

22. Nazish I, Arber C, Piers TM, et al. (2021) **Abrogation of LRRK2 dependent Rab10 phosphorylation with TLR4 activation and alterations in evoked cytokine release in immune cells** *Neurochem Int* **147** https://doi.org/10.1016/j.neuint.2021.105070 | Google Scholar

23. Maas JW, Yang J, Edwards RH (2017) **Endogenous Leucine-Rich Repeat Kinase 2 Slows Synaptic Vesicle Recycling in Striatal Neurons** *Front Synaptic Neurosci* **9** https://doi.org/10.3389/FNSYN.2017.00005 | Google Scholar

24. Cirnaru MD, Marte A, Belluzzi E, et al. (2014) **LRRK2 kinase activity regulates synaptic vesicle trafficking and neurotransmitter release through modulation of LRRK2 macro-molecular complex** *Front Mol Neurosci* **7** https://doi.org/10.3389/FNMOL.2014.00049 | Google Scholar

25. Pischedda F, Piccoli G (2021) **LRRK2 at the pre-synaptic site: A 16-years perspective** *J Neurochem* **157**:297–311 https://doi.org/10.1111/jnc.15240 | Google Scholar

26. Belluzzi E, Gonnelli A, Cirnaru MD, et al. (2016) **LRRK2 phosphorylates pre-synaptic N-ethylmaleimide sensitive fusion (NSF) protein enhancing its ATPase activity and SNARE complex disassembling rate** *Mol Neurodegener* **11**:1–16 https://doi.org/10.1186/S13024-015-0066-Z | Google Scholar

27. Marte A, Russo I, Rebosio C, et al. (2019) **Leucine-rich repeat kinase 2 phosphorylation on synapsin I regulates glutamate release at pre-synaptic sites** *J Neurochem* **150**:264–281 https://doi.org/10.1111/jnc.14778 | Google Scholar

28. Soukup SF, Kuenen S, Vanhauwaert R, et al. (2016) **A LRRK2-Dependent EndophilinA Phosphoswitch Is Critical for Macroautophagy at Presynaptic Terminals** *Neuron* **92**:829–844 https://doi.org/10.1016/J.NEURON.2016.09.037 | Google Scholar

29. Cao M, Wu Y, Ashrafi G, et al. (2017) **Parkinson Sac Domain Mutation in Synaptojanin 1 Impairs Clathrin Uncoating at Synapses and Triggers Dystrophic Changes in Dopaminergic Axons** *Neuron* **93**:882–896 https://doi.org/10.1016/J.NEURON.2017.01.019 | Google Scholar

30. Nguyen M, Krainc D (2018) **LRRK2 phosphorylation of auxilin mediates synaptic defects in dopaminergic neurons from patients with Parkinson's disease** *Proc Natl Acad Sci U S A* **115**:5576–5581 https://doi.org/10.1073/PNAS.1717590115 | Google Scholar

31. Rassu M, Del Giudice MG, Sanna S, et al. (2017) **Role of LRRK2 in the regulation of dopamine receptor trafficking** *PLoS One* **12** https://doi.org/10.1371/journal.pone.0179082 | Google Scholar

32. Gupta S, Tielemans A, Guevara CA, Huntley GW, Benson DL (2024) **Parkinson's-linked LRRK2-G2019S derails AMPAR trafficking, mobility, and composition in striatum with cell-type and subunit specificity** *Proc Natl Acad Sci U S A* **121** https://doi.org/10.1073/PNAS.2317833121 | Google Scholar

33. Chen C, Soto G, Dumrongprechachan V, et al. (2020) **Pathway-specific dysregulation of striatal excitatory synapses by LRRK2 mutations** *eLife* **9**:1–26 https://doi.org/10.7554/eLife.58997 | Google Scholar

34. Matikainen-Ankney BA, Kezunovic N, Mesias RE, et al. (2016) **Altered development of synapse structure and function in striatum caused by Parkinson's disease-linked LRRK2-G2019S mutation** *Journal of Neuroscience* **36**:7128–7141 https://doi.org/10.1523/JNEUROSCI.3314-15.2016 | Google Scholar

35. Parisiadou L, Yu J, Sgobio C, et al. (2014) **LRRK2 regulates synaptogenesis and dopamine receptor activation through modulation of PKA activity** *Nat Neurosci* **17**:367–376 https://doi.org/10.1038/NN.3636 | Google Scholar

36. Thoenen H. (1995) **Neurotrophins and neuronal plasticity** *Science* **270**:593–598 https://doi.org/10.1126/science.270.5236.593 | Google Scholar

37. Baydyuk M, Xu B (2014) **BDNF signaling and survival of striatal neurons** *Front Cell Neurosci* **8** https://doi.org/10.3389/fncel.2014.00254 | Google Scholar

38. Iannotta L, Biosa A, Kluss JH, et al. (2020) **Divergent Effects of G2019S and R1441C LRRK2 Mutations on LRRK2 and Rab10 Phosphorylations in Mouse Tissues** *Cells* **9** https://doi.org/10.3390/cells9112344 | Google Scholar

39. Skelton PD, Tokars V, Parisiadou L (2022) **LRRK2 at Striatal Synapses: Cell-Type Specificity and Mechanistic Insights** *Cells* **11** https://doi.org/10.3390/cells11010169 | Google Scholar

40. Piccoli G, Condliffe SB, Bauer M, et al. (2011) **LRRK2 controls synaptic vesicle storage and mobilization within the recycling pool** *Journal of Neuroscience* **31**:2225–2237 https://doi.org

/10.1523/JNEUROSCI.3730-10.2011 | Google Scholar

41. Kluss JH, Lewis PA, Greggio E (2022) **Leucine-rich repeat kinase 2 (LRRK2): an update on the potential therapeutic target for Parkinson's disease** *Expert Opin Ther Targets* **26**:537–546 https://doi.org/10.1080/14728222.2022.2082937 | Google Scholar

42. Encinas M, Iglesias M, Liu Y, et al. (2000) **Sequential treatment of SH-SY5Y cells with retinoic acid and brain-derived neurotrophic factor gives rise to fully differentiated, neurotrophic factor-dependent, human neuron-like cells** *J Neurochem* **75**:991–1003 https://doi.org/10.1046/j.1471-4159.2000.0750991.x | Google Scholar

43. Numakawa T, Suzuki S, Kumamaru E, Adachi N, Richards M, Kunugi H (2010) **BDNF function and intracellular signaling in neurons** *Histol Histopathol* **25**:237–258 https://doi.org/10.14670/HH-25.237 | Google Scholar

44. Nirujogi RS, Tonelli F, Taylor M, et al. (2021) **Development of a multiplexed targeted mass spectrometry assay for LRRK2-phosphorylated Rabs and Ser910/Ser935 biomarker sites** *Biochem J* **478**:299–326 https://doi.org/10.1042/BCJ20200930 | Google Scholar

45. Manzoni C, Denny P, Lovering RC, Lewis PA (2015) **Computational analysis of the LRRK2 interactome** *PeerJ* **2** https://doi.org/10.7717/peerj.778 | Google Scholar

46. Tomkins JE, Dihanich S, Beilina A, et al. (2018) **Comparative Protein Interaction Network Analysis Identifies Shared and Distinct Functions for the Human ROCO Proteins** *Proteomics* **18** https://doi.org/10.1002/pmic.201700444 | Google Scholar

47. Koopmans F, van Nierop P, Andres-Alonso M, et al. (2019) **SynGO: An Evidence-Based, Expert-Curated Knowledge Base for the Synapse** *Neuron* **103**:217–234 https://doi.org/10.1016/j.neuron.2019.05.002 | Google Scholar

48. Koganezawa N, Hanamura K, Sekino Y, Shirao T (2017) **The role of drebrin in dendritic spines** *Molecular and Cellular Neuroscience* **84**:85–92 https://doi.org/10.1016/j.mcn.2017.01.004 | Google Scholar

49. Shirao T, Hanamura K, Koganezawa N, Ishizuka Y, Yamazaki H, Sekino Y (2017) **The role of drebrin in neurons** *J Neurochem* **141**:819–834 https://doi.org/10.1111/JNC.13988 | Google Scholar

50. Martin ER, Gandawijaya J, Oguro-Ando A (2022) **A novel method for generating glutamatergic SH-SY5Y neuron-like cells utilizing B-27 supplement** *Front Pharmacol* **13** https://doi.org/10.3389/FPHAR.2022.943627 | Google Scholar

51. Zhao Y, Harvey K, Escott-Price V, Lewis PA, Manzoni C (2023) **Transcriptomics analyses of the LRRK2 protein interactome reveal distinct molecular signatures for sporadic and LRRK2 Parkinson's Disease** *bioRxiv* https://doi.org/10.1101/2023.09.12.557373 | Google Scholar

52. Spirin V, Mirny LA (2003) **Protein complexes and functional modules in molecular networks** *Proc Natl Acad Sci U S A* **100**:12123–12128 https://doi.org/10.1073/PNAS.2032324100 | Google Scholar

53. Meixner A, Boldt K, Van Troys M, et al. (2011) **A QUICK screen for Lrrk2 interaction partners-leucine-rich repeat kinase 2 is involved in actin cytoskeleton dynamics** *Mol Cell Proteomics* **10** https://doi.org/10.1074/MCP.M110.001172 | Google Scholar

54. Liu Z, Lee J, Krummey S, Lu W, Cai H, Lenardo MJ (2011) **The kinase LRRK2 is a regulator of the transcription factor NFAT that modulates the severity of inflammatory bowel disease** *Nat Immunol* **12**:1063–1070 https://doi.org/10.1038/NI.2113 | Google Scholar

55. Chen C, Masotti M, Shepard N, et al. (2025) **LRRK2 mediates haloperidol-induced changes in indirect pathway striatal projection neurons** *Mol Psychiatry* https://doi.org/10.1038/S41380-025-03030-Z | Google Scholar

56. Cheng J, Novati G, Pan J, et al. (2023) **Accurate proteome-wide missense variant effect prediction with AlphaMissense** *Science* :381–6664 https://doi.org/10.1126/SCIENCE.ADG7492 | Google Scholar

57. Kellner Y, Gödecke N, Dierkes T, Thieme N, Zagrebelsky M, Korte M (2014) **The BDNF effects on dendritic spines of mature hippocampal neurons depend on neuronal activity** *Front Synaptic Neurosci* **6** https://doi.org/10.3389/fnsyn.2014.00005 | Google Scholar

58. Zagrebelsky M, Korte M (2014) **Form follows function: BDNF and its involvement in sculpting the function and structure of synapses** *Neuropharmacology* **76**:628–638 https://doi.org/10.1016/j.neuropharm.2013.05.029 | Google Scholar

59. Lai KO, Wong ASL, Cheung MC, et al. (2012) **TrkB phosphorylation by Cdk5 is required for activity-dependent structural plasticity and spatial memory** *Nat Neurosci* **15**:1506–1515 https://doi.org/10.1038/nn.3237 | Google Scholar

60. Ji Y, Pang PT, Feng L, Lu B (2005) **Cyclic AMP controls BDNF-induced TrkB phosphorylation and dendritic spine formation in mature hippocampal neurons** *Nat Neurosci* **8**:164–172 https://doi.org/10.1038/nn1381 | Google Scholar

61. Lendvai B, Stern EA, Chen B, Svoboda K (2000) **Experience-dependent plasticity of dendritic spines in the developing rat barrel cortex in vivo** *Nature* **404**:876–881 https://doi.org/10.1038/35009107 | Google Scholar

62. Koleske AJ (2013) **Molecular mechanisms of dendrite stability** *Nat Rev Neurosci* **14**:536–550 https://doi.org/10.1038/nrn3486 | Google Scholar

63. Surmeier DJ, Obeso JA, Halliday GM (2017) **Selective neuronal vulnerability in Parkinson disease** *Nat Rev Neurosci* **18**:101–113 https://doi.org/10.1038/nrn.2016.178 | Google Scholar

64. Westerlund M, Belin AC, Anvret A, Bickford P, Olson L, Galter D (2008) **Developmental regulation of leucine-rich repeat kinase 1 and 2 expression in the brain and other rodent and human organs: Implications for Parkinson's disease** *Neuroscience* **152**:429–436 https://doi.org/10.1016/j.neuroscience.2007.10.062 | Google Scholar

65. Tong Y, Pisani A, Martella G, et al. (2009) **R1441C mutation in LRRK2 impairs dopaminergic neurotransmission in mice** *Proc Natl Acad Sci U S A* **106**:14622–14627 https://doi.org/10.1073/pnas.0906334106 | Google Scholar

66. Volta M, Beccano-Kelly DA, Paschall SA, et al. (2017) **Initial elevations in glutamate and dopamine neurotransmission decline with age, as does exploratory behavior, in LRRK2 G2019S knock-in mice** *eLife* **6** https://doi.org/10.7554/ELIFE.28377 | Google Scholar

67. Shi Y, Kirwan P, Livesey FJ (2012) **Directed differentiation of human pluripotent stem cells to cerebral cortex neurons and neural networks** *Nature Protocols* **7**:1836–1846 https://doi.org/10.1038/nprot.2012.116 | Google Scholar

68. Beylina A, Langston RG, Rosen D, Reed X, Cookson MR (2021) **Generation of fourteen isogenic cell lines for Parkinson's disease-associated leucine-rich repeat kinase (LRRK2)** *Stem Cell Res* **53**:102354 https://doi.org/10.1016/J.SCR.2021.102354 | Google Scholar

69. Beccano-Kelly DA, Kuhlmann N, Tatarnikov I, et al. (2014) **Synaptic function is modulated by LRRK2 and glutamate release is increased in cortical neurons of G2019S LRRK2 knock-in mice** *Front Cell Neurosci* **8**:1–11 https://doi.org/10.3389/FNCEL.2014.00301 | Google Scholar

70. Beccano-Kelly DA, Volta M, Lise LN, et al. (2015) **LRRK2 overexpression alters glutamatergic presynaptic plasticity, striatal dopamine tone, postsynaptic signal transduction, motor activity and memory** *Hum Mol Genet* **24**:1336–1349 https://doi.org/10.1093/HMG/DDU543 | Google Scholar

71. Piccoli G, Onofri F, Cirnaru MD, et al. (2014) **Leucine-Rich Repeat Kinase 2 Binds to Neuronal Vesicles through Protein Interactions Mediated by Its C-Terminal WD40 Domain** *Mol Cell Biol* **34**:2147–2161 https://doi.org/10.1128/mcb.00914-13 | Google Scholar

72. Arranz AM, Delbroek L, van Kolen K, et al. (2015) **LRRK2 functions in synaptic vesicle endocytosis through a kinasedependent mechanism** *J Cell Sci* **128**:541–552 https://doi.org/10.1242/jcs.158196 | Google Scholar

73. Hupfeld CJ, Olefsky JM (2007) **Regulation of receptor tyrosine kinase signaling by GRKs and beta-arrestins** *Annu Rev Physiol* **69**:561–577 https://doi.org/10.1146/ANNUREV.PHYSIOL.69.022405.154626 | Google Scholar

74. Nazish I, Mamais A, Mallach A, et al. (2023) **Differential LRRK2 signalling and gene expression in WT-LRRK2 and G2019S-LRRK2 mouse microglia treated with zymosan and MLi2** *bioRxiv* https://doi.org/10.1101/2023.09.14.557532 | Google Scholar

75. Jeremy Nichols R. (2017) **LRRK2 Phosphorylation** *Adv Neurobiol* **14**:51–70 https://doi.org/10.1007/978-3-319-49969-7_3 | Google Scholar

76. Chen YJ, Xie MR, Zhou SQ, Liu F (2025) **Synapses-associated research in Parkinson's disease: an explored trends analysis** *Front Aging Neurosci* **17** https://doi.org/10.3389/FNAGI.2025.1537119 | Google Scholar

77. (GP2) TGPGP, Leonard HL (2025) **Novel Parkinson's Disease Genetic Risk Factors Within and Across European Populations** *medRxiv* https://doi.org/10.1101/2025.03.14.24319455 | Google Scholar

78. Uytterhoeven V, Verstreken P, Nachman E (2025) **Synaptic sabotage: How Tau and α-Synuclein undermine synaptic health** *J Cell Biol* **224** https://doi.org/10.1083/JCB.202409104 | Google Scholar

79. Gaig C, Martí MJ, Ezquerra M, Rey MJ, Cardozo A, Tolosa E. G (2007) **2019S LRRK2 mutation causing Parkinson's disease without Lewy bodies** *J Neurol Neurosurg Psychiatry* **78**:626–628 https://doi.org/10.1136/JNNP.2006.107904 | Google Scholar

80. Jackson LM, Woodruff BK, Tremblay C, et al. (2024) **Parkinson's Disease Associated with G2019S LRRK2 Mutations without Lewy Body Pathology** *Mov Disord Clin Pract* **11**:874–

878 https://doi.org/10.1002/MDC3.14068 | Google Scholar

81. Sekiya H, Franke L, Hashimoto Y, et al. (2025) **Widespread distribution of α-synuclein oligomers in LRRK2-related Parkinson's disease** *Acta Neuropathol* **149**:42 https://doi.org/10.1007/S00401-025-02872-9 | Google Scholar

82. Jensen NM, Vitic Z, Antorini MR, Viftrup TB, Parkkinen L, Jensen PH (2025) **Abundant non-inclusion α-synuclein pathology in Lewy body-negative LRRK2-mutant cases** *Acta Neuropathol* **149** https://doi.org/10.1007/S00401-025-02871-W | Google Scholar

83. Gaertner Z, Azcorra M, Dombeck DA, Awatramani R (2022) **Molecular heterogeneity in the substantia nigra: A roadmap for understanding PD motor pathophysiology** *Neurobiol Dis* **175** https://doi.org/10.1016/J.NBD.2022.105925 | Google Scholar

84. Gaertner Z, Oram C, Schneeweis A, et al. (2024) **Molecular and spatial transcriptomic classification of midbrain dopamine neurons and their alterations in a LRRK2G2019S model of Parkinson's disease** *bioRxiv* https://doi.org/10.1101/2024.06.06.597807 | Google Scholar

85. Hedrick NG, Harward SC, Hall CE, Murakoshi H, McNamara JO, Yasuda R (2016) **Rho GTPase complementation underlies BDNF-dependent homo- and heterosynaptic plasticity** *Nature* **538**:104–108 https://doi.org/10.1038/nature19784 | Google Scholar

86. Chan D, Citro A, Cordy JM, Shen GC, Wolozin B (2011) **Rac1 protein rescues neurite retraction caused by G2019s leucine-rich repeat kinase 2 (LRRK2)** *Journal of Biological Chemistry* **286**:16140–16149 https://doi.org/10.1074/jbc.M111.234005 | Google Scholar

87. Feng M, Hu X, Li N, et al. (2018) **Distinctive roles of Rac1 and Rab29 in LRRK2 mediated membrane trafficking and neurite outgrowth** *J Biomed Res* **32**:145–156 https://doi.org/10.7555/JBR.31.20170039 | Google Scholar

88. Worth DC, Daly CN, Geraldo S, Oozeer F, Gordon-Weeks PR (2013) **Drebrin contains a cryptic F-actin-bundling activity regulated by Cdk5 phosphorylation** *J Cell Biol* **202**:793–806 https://doi.org/10.1083/JCB.201303005 | Google Scholar

89. Beaudoin GMJ, Schofield CM, Nuwal T, et al. (2012) **Afadin, a Ras/Rap effector that controls cadherin function, promotes spine and excitatory synapse density in the hippocampus** *J Neurosci* **32**:99–110 https://doi.org/10.1523/JNEUROSCI.4565-11.2012 | Google Scholar

90. Takahashi H, Sekino Y, Tanaka S, Mizui T, Kishi S, Shirao T (2003) **Drebrin-dependent actin clustering in dendritic filopodia governs synaptic targeting of postsynaptic density-95 and dendritic spine morphogenesis** *Journal of Neuroscience* **23**:6586–6595 https://doi.org/10.1523/jneurosci.23-16-06586.2003 | Google Scholar

91. Aoki C, Kojima N, Sabaliauskas N, et al. (2009) **Drebrin a knockout eliminates the rapid form of homeostatic synaptic plasticity at excitatory synapses of intact adult cerebral cortex** *Journal of Comparative Neurology* **517**:105–121 https://doi.org/10.1002/cne.22137 | Google Scholar

92. Sekino Y, Tanaka S, Hanamura K, et al. (2006) **Activation of N-methyl-d-aspartate receptor induces a shift of drebrin distribution: Disappearance from dendritic spines and**

**appearance in dendritic shafts** *Molecular and Cellular Neuroscience* **31**:493–504 https://doi.org/10.1016/j.mcn.2005.11.003 | Google Scholar

93. Spence EF, Kanak DJ, Carlson BR, Soderling SH (2016) **The Arp2/3 complex is essential for distinct stages of spine synapse maturation, including synapse unsilencing** *Journal of Neuroscience* **36**:9696–9709 https://doi.org/10.1523/JNEUROSCI.0876-16.2016 | Google Scholar

94. Kim KS, Marcogliese PC, Yang J, et al. (2018) **Regulation of myeloid cell phagocytosis by LRRK2 via WAVE2 complex stabilization is altered in Parkinson's disease** *Proc Natl Acad Sci U S A* **115**:E5164–E5173 https://doi.org/10.1073/pnas.1718946115 | Google Scholar

95. Giaime E, Tong Y, Wagner LK, Yuan Y, Huang G, Shen J (2017) **Age-Dependent Dopaminergic Neurodegeneration and Impairment of the Autophagy-Lysosomal Pathway in LRRK-Deficient Mice** *Neuron* **96**:796–807 https://doi.org/10.1016/j.neuron.2017.09.036 | Google Scholar

96. Huang G, Bloodgood DW, Kang J, et al. (2022) **Motor Impairments and Dopaminergic Defects Caused by Loss of Leucine-Rich Repeat Kinase Function in Mice** *J Neurosci* **42**:4755–4765 https://doi.org/10.1523/JNEUROSCI.0140-22.2022 | Google Scholar

97. Kang J, Huang G, Ma L, et al. (2024) **Cell-autonomous role of leucine-rich repeat kinase in the protection of dopaminergic neuron survival** *eLife* **12** https://doi.org/10.7554/ELIFE.92673 | Google Scholar

98. Biskup S, Moore DJ, Rea A, et al. (2007) **Dynamic and redundant regulation of LRRK2 and LRRK1 expression** *BMC Neurosci* **8** https://doi.org/10.1186/1471-2202-8-102 | Google Scholar

99. Cogo S, Ho FY, Tosoni E, et al. (2022) **The Roc domain of LRRK2 as a hub for protein-protein interactions: a focus on PAK6 and its impact on RAB phosphorylation** *Brain Res* :1778 https://doi.org/10.1016/j.brainres.2022.147781 | Google Scholar

100. Narita M, Aoki K, Takagi M, Yajima Y, Suzuki T (2003) **Implication of brain-derived neurotrophic factor in the release of dopamine and dopamine-related behaviors induced by methamphetamine** *Neuroscience* **119**:767–775 https://doi.org/10.1016/S0306-4522(03)00099-X | Google Scholar

101. Morella I, Hallum H, Brambilla R (2020) **Dopamine D1 and Glutamate Receptors Co-operate With Brain-Derived Neurotrophic Factor (BDNF) and TrkB to Modulate ERK Signaling in Adult Striatal Slices** *Front Cell Neurosci* **14** https://doi.org/10.3389/fncel.2020.564106 | Google Scholar

102. Hyman C, Hofer M, Barde YA, et al. (1991) **BDNF is a neurotrophic factor for dopaminergic neurons of the substantia nigra** *Nature* **350**:230–232 https://doi.org/10.1038/350230a0 | Google Scholar

103. Baquet ZC, Bickford PC, Jones KR (2005) **Brain-derived neurotrophic factor is required for the establishment of the proper number of dopaminergic neurons in the substantia nigra pars compacta** *Journal of Neuroscience* **25**:6251–6259 https://doi.org/10.1523/JNEUROSCI.4601-04.2005 | Google Scholar

104. Rahmani F, Saghazadeh A, Rahmani M, et al. (2019) **Plasma levels of brain-derived neurotrophic factor in patients with Parkinson disease: A systematic review and meta-analysis** *Brain Res* **1704**:127–136 https://doi.org/10.1016/j.brainres.2018.10.006 | Google Scholar

105. Lin CH, Wu RM, Tai CH, Chen ML, Hu FC (2011) **Lrrk2 S1647T and BDNF V66M interact with environmental factors to increase risk of Parkinson's disease** *Parkinsonism Relat Disord* **17**:84–88 https://doi.org/10.1016/j.parkreldis.2010.11.011 | Google Scholar

106. Liu J, Zhou Y, Wang C, Wang T, Zheng Z, Chan P (2012) **Brain-derived neurotrophic factor (BDNF) genetic polymorphism greatly increases risk of leucine-rich repeat kinase 2 (LRRK2) for Parkinson's disease** *Parkinsonism Relat Disord* **18**:140–143 https://doi.org/10.1016/j.parkreldis.2011.09.002 | Google Scholar

107. Siuda J, Patalong-Ogiewa M, Żmuda W, et al. (2017) **Cognitive impairment and BDNF serum levels** *Neurol Neurochir Pol* **51**:24–32 https://doi.org/10.1016/j.pjnns.2016.10.001 | Google Scholar

108. Ziebell M, Khalid U, Klein AB, et al. (2012) **Striatal dopamine transporter binding correlates with serum BDNF levels in patients with striatal dopaminergic neurodegeneration** *Neurobiol Aging* **33**:):428.e1–428 https://doi.org/10.1016/j.neurobiolaging.2010.11.010 | Google Scholar

109. Tagliaferro P, Burke RE (2016) **Retrograde Axonal Degeneration in Parkinson Disease** *J Parkinsons Dis* **6**:1–15 https://doi.org/10.3233/JPD-150769 | Google Scholar

110. Sharma A, Toepfer CN, Ward T, et al. (2018) **CRISPR/Cas9-Mediated Fluorescent Tagging of Endogenous Proteins in Human Pluripotent Stem Cells** *Curr Protoc Hum Genet* **96**:21–21 https://doi.org/10.1002/CPHG.52 | Google Scholar

111. Beccano-Kelly DA, Cherubini M, Mousba Y, et al. (2023) **Calcium dysregulation combined with mitochondrial failure and electrophysiological maturity converge in Parkinson's iPSC-dopamine neurons** *iScience* **26**:107044 https://doi.org/10.1016/J.ISCI.2023.107044 | Google Scholar

112. Zaqout S, Kaindl AM (2016) **Golgi-cox staining step by step** *Front Neuroanat* **10**:181342 https://doi.org/10.3389/FNANA.2016.00038 | Google Scholar

113. Risher WC, Ustunkaya T, Alvarado JS, Eroglu C (2014) **Rapid Golgi Analysis Method for Efficient and Unbiased Classification of Dendritic Spines** *PLoS One* **9**:e107591 https://doi.org/10.1371/JOURNAL.PONE.0107591 | Google Scholar

114. Tyanova S, Temu T, Cox J (2016) **The MaxQuant computational platform for mass spectrometry-based shotgun proteomics** *Nature Protocols* **11**:2301–2319 https://doi.org/10.1038/nprot.2016.136 | Google Scholar

115. Aguilan JT, Kulej K, Sidoli S (2020) **Guide for protein fold change and: P-value calculation for non-experts in proteomics** *Mol Omics* **16**:573–582 https://doi.org/10.1039/d0mo00087f | Google Scholar

116. Lazar C, Gatto L, Ferro M, Bruley C, Burger T. (2016) **Accounting for the Multiple Natures of Missing Values in Label-Free Quantitative Proteomics Data Sets to Compare Imputation Strategies** *J Proteome Res* **15**:1116–1125 https://doi.org/10.1021/acs.jproteome.5b00981 | Google Scholar

117. Zhao Y, Vavouraki N, Lovering RC, et al. (2023) **Tissue specific LRRK2 interactomes reveal a distinct striatal functional unit** *PLoS Comput Biol* **19**:e1010847 https://doi.org/10.1371/JOURNAL.PCBI.1010847 | Google Scholar

118. Raudvere U, Kolberg L, Kuzmin I, et al. (2019) **g:Profiler: a web server for functional enrichment analysis and conversions of gene lists (2019 update)** *Nucleic Acids Res* **47**:W191–W198 https://doi.org/10.1093/NAR/GKZ369 | Google Scholar

## Author information

**Giulia Tombesi**
Department of Biology, University of Padova, Padua, Italy
ORCID iD: 0000-0003-0683-8050

**Shiva Kompella**
School of Pharmacy and UK Dementia Research Institute, Cardiff University, Cardiff, United Kingdom

**Giulia Favetta**
Department of Biology, University of Padova, Padua, Italy
ORCID iD: 0009-0002-2397-9218

**Chuyu Chen**
Northwest University, Chicago, United States
ORCID iD: 0000-0001-5666-5173

**Marta Ornaghi**
Institute for Biochemistry, Charité Universitätsmedizin Berlin, Berlin, Germany, Freie Universität Berlin, Berlin, Germany

**Yibo Zhao**
School of Pharmacy, University College London, London, United Kingdom

**Ester Morosin**
Department of Biology, University of Padova, Padua, Italy

**Martina Sevegnani**
School of Pharmacy, University College London, London, United Kingdom

**Adriano Lama**
CIBIO, University of Trento, Trento, Italy

**Antonella Marte**
Experimental Medicine, University of Genova, Genoa, Italy, IRCCS, Ospedale Policlinico San Martino, Genova, Italy

**Ilaria Battisti**
Department of Biomedical Sciences, University of Padova, Padua, Italy

**Lucia Iannotta**
Department of Biology, University of Padova, Padua, Italy

**Nicoletta Plotegher**
Department of Biology, University of Padova, Padua, Italy, Centro Studi per la Neurodegenerazione (CESNE), University of Padova, Padua, Italy
ORCID iD: 0000-0001-7421-8705

**Laura Civiero**
Department of Biology, University of Padova, Padua, Italy, Centro Studi per la Neurodegenerazione (CESNE), University of Padova, Padua, Italy, IRCCS San Camillo Hospital, Venice, Italy
ORCID iD: 0000-0002-5334-155X

**Franco Onofri**
Experimental Medicine, University of Genova, Genoa, Italy, IRCCS, Ospedale Policlinico San Martino, Genova, Italy
ORCID iD: 0000-0001-5595-0036

**Britta J Eickholt**
Institute for Biochemistry, Charité Universitätsmedizin Berlin, Berlin, Germany

**Giovanni Piccoli**
CIBIO, University of Trento, Trento, Italy
ORCID iD: 0000-0001-5262-7903

**Giorgio Arrigoni**
Department of Biomedical Sciences, University of Padova, Padua, Italy
ORCID iD: 0000-0002-4103-2733

**Dayne Beccano-Kelly**
School of Pharmacy and UK Dementia Research Institute, Cardiff University, Cardiff, United Kingdom

**For correspondence:** Beccano-KellyD@cardiff.ac.uk

**Claudia Manzoni**
School of Pharmacy, University College London, London, United Kingdom
ORCID iD: 0000-0001-5367-4023

**Loukia Parisiadou**
Northwest University, Chicago, United States
ORCID iD: 0000-0002-2569-4200

**Elisa Greggio**
Department of Biology, University of Padova, Padua, Italy, Centro Studi per la Neurodegenerazione (CESNE), University of Padova, Padua, Italy
ORCID iD: 0000-0002-8172-3598

**For correspondence:** elisa.greggio@unipd.it

## Editors

Reviewing Editor
**Andrew West**
Duke University, Durham, United States of America

Senior Editor
**John Huguenard**
Stanford University School of Medicine, Stanford, United States of America

**Reviewer #1 (Public review):**

Summary:

LRRK2 protein is familially linked to Parkinson's disease by the presence of several gene variants that all confer a gain-of-function effect on LRRK2 kinase activity.

The authors examine the effects of BDNF stimulation in immortalized neuron-like cells, cultured mouse primary neurons, hIPSC-derived neurons, and brain tissue from genetically modified mice. They examine a LRRK2 regulatory phosphorylation residue, LRRK2 binding relationships, and measures of synaptic structure and function.

Strengths:

The study addresses an important research question: how does a PD-linked protein interact with other proteins, and contribute to responses to a well-characterized neuronal signalling pathway involved in the regulation of synaptic function and cell health.

They employ a range of good models and techniques to fairly convincingly demonstrate that BDNF stimulation alters LRRK2 phosphorylation and binding to many proteins. IN this revised manuscript, aspects are well validated e.g., drebrin binding, but there is a disconnect between these findings and alterations to LRRK2 substrates. A convincing phosphoproteomic analysis of PD mutant Knock-in mouse brain is included. Overall the links between LRRK2, LRRK2 activity, and the changes to synaptic molecules, structures, and activity are intriguing.

Weaknesses:

The data sets remain disjointed, conclusions are sweeping, and not always in line with what the data is showing. Validation of 'omics' data is light. Some inconsistencies with the major conclusions are ignored. Several of the assays employed (western blotting especially) are underpowered, findings key to their interpretation are addressed in only one or other of the several models employed, and supporting observations are lacking.

Main Conclusions of Abstract:

(1) Increase in pLRRK2 Ser935 and pRAB after BDNF in SH-SY5Y & mouse neurons

Well supported, but only for pLRRK2 in neurons, why not pERK pAkt & pRab?

(2) Omics Proteome remodelling of LRRK2 interactome with BDNF & different in G2019S mouse neurons.

Supports that the phosphoproteome of G2019S is different. Drebrin interaction with LRRK2 very well supported. Link between drebrin and LRRK2 activity somewhat supported (pS935 site), but the consequence (non-specific pRab8) not supported, as there is no evidence of a change in LRRK2 substrate(s).

(3) Golgi 1 month LKO mouse altered dendritic spines, transient at 1m not older.

Supported but very small transient change in spines, disconnected to other results (e.g., drebrin).

(4) iPSC-derived neurons BDNF increases mEPSC frequency (transient at 70 not 50 or 90 days) in WT not KO "which appear to bypass this regulation through developmental compensation"

Weak, not clear what is being bypassed.

Main Conclusions Based on Old and New Figure / Data:

(1) Increase in pLRRK2 Ser935 and pRAB after BDNF in SH-SY5Y & mouse neurons

Well supported, but only for pLRRK2 in neurons, why not ERK Akt & Rab?

(2) BDNF promotes LRRK2 interaction with "post-synaptic actin cytoskeleton components"

Tone down, only one postsynaptic validated - drebrin strong BUT CONTRADICTORY; link between drebrin and LRRK2 activity (pS935 site) supported, consequence (non-specific pRab8) broken, no evidence of change in LRRK2 substrate.

(3) LRRK2 G2019S striatal phosphoproteome is different from WT.

It is different. Where is link to BDNF or Drebrin?

(4) BDNF signaling is impaired in Lrrk2 knockout neurons

TrkB changes seem higher in SHSY5Y. pAKT impaired, pERK not convincing. Primary neurons Akt slower but it and Erk mostly intact. MLi-2 did not block pAkt or pErk in WT or KO (higher in latter). Whatever is happening in KO, Mli-2 not really blocking effect in WT. If we are to assume that studying the KO was a means to understand LRRK2 function, the authors data should explain why we care if an effect is absent in LKO, if LRRK2 isn't doing the same job in WT?

BDNF increases synaptic puncta in WT not LKO (which start higher?). Is this BDNF increase blocked by LRRK2 inhibition?

(5) Postsynaptic structural changes in Lrrk2 knockout neurons

Golgi impregnation shows some very small spine changes at 1m. Not sustained over age. mRNA changes are very small (10% not even a fold... very weak and should be written as so). Derbrin levels reduced clearly at 1m, but probably also at 4 & 18. Underpowered, disconnected time course from the spine changes.

(6) An effect on "spontaneous electrical activity" at Div70

Weak. What is so special at 70 days that means we should be confident in the differences, or be satisfied that the other time points are legitimately ignored? These are 10-11 cells from 3 cultures assayed at 3 time points but only one is presented (rest in supplement). This should be a 2 (time) or 3 way (+culture RM) ANOVA. As it stands, in WT there is a little - no activity at 50 days, little to no at 70 days, and variable to lots or none at 90. BDNF did nothing at 50 or 90 but may have at 70. In KO low activity stable at 50 & 70, tanks at 90. BDNF would seem to have a similar effect on KO at 90 as WT at 70, but as there are only 7 cells it remains inconclusive. Thus the conclusion that BDNF signalling is broken in LKO is not well supported by the ephys data, nor is the BDNF effect in WT cells (even at the 70 day time point) shown to be susceptible to LRRK2 inhibition.

https://doi.org/10.7554/eLife.95987.2.sa2

**Reviewer #2 (Public review):**

The data show that BDNF regulates the PD-associated kinase LRRK2, they place LRRK2 within well-described BDNF pathways biochemically, and they show that LRRK2 can play a role mediating BDNF-driven synaptic outcomes at excitatory synapses. The chief strength is that the data provide a potential focal point for multiple observations that have been made across many labs. The findings will be of broad interest because LRRK2 has emerged as a protein that is likely to be part of Parkinson's pathology and its normal and pathological actions remain poorly understood.

A major strength of the study is the multiple approaches that were used (biochemistry, bioinformatics, light and electron microscopy and electrophysiology) across different experimental models (cells, primary neurons, human neurons, mice) to identify and examine the impact of BDNF on LRRK2 signaling and functions. Noteworthy is also the employment of LRRK2KO preparations to validate outcomes and to place LRRK2 actions up or downstream.

The demonstration that LRRK2 and drebrin interact directly is important and suggests that other interacting proteins identified biochemically and bioinformatically in the paper will be important to pursue.

Some data from different models do not fit well with one another (like mouse and human neurons). This is likely due to inherent differences in the preparations. Since different experiments were carried out on the different preps, however, it is not possible to cross compare. The lack of this information is viewed more as an open question than a cause for concern.

https://doi.org/10.7554/eLife.95987.2.sa1

**Author response:**

The following is the authors' response to the original reviews.

> ***Reviewer #1 (Public Review):***
>
> *Summary:*
>
> *LRRK2 protein is familially linked to Parkinson's disease by the presence of several gene variants that all confer a gain-of-function effect on LRRK2 kinase activity.*
>
> *The authors examine the effects of BDNF stimulation in immortalized neuron-like cells, cultured mouse primary neurons, hIPSC-derived neurons, and synaptosome preparations from the brain. They examine an LRRK2 regulatory phosphorylation residue, LRRK2 binding relationships, and measures of synaptic structure and function.*
>
> *Strengths:*
>
> *The study addresses an important research question: how does a PD-linked protein interact with other proteins, and contribute to responses to a well-characterized neuronal signalling pathway involved in the regulation of synaptic function and cell health?*
>
> *They employ a range of good models and techniques to fairly convincingly demonstrate that BDNF stimulation alters LRRK2 phosphorylation and binding to many proteins. Some effects of BDNF stimulation appear impaired in (some of the) LRRK2 knock-out scenarios (but not all). A phosphoproteomic analysis of PD mutant Knock-in mouse brain synaptosomes is included.*

We thank this Reviewer for pointing out the strengths of our work.

> *Weaknesses:*
>
> *The data sets are disjointed, conclusions are sweeping, and not always in line with what the data is showing. Validation of 'omics' data is very light. Some inconsistencies with the major conclusions are ignored. Several of the assays employed (western blotting especially) are likely underpowered, findings key to their interpretation are addressed in only one or other of the several models employed, and supporting observations are lacking.*

We appreciate the Reviewer's overall evaluaVon. In this revised version, we have provided several novel results that strengthen the omics data and the mechanisVc experiments and make the conclusions in line with the data.

> *As examples to aid reader interpretation: (a) pS935 LRRK2 seems to go up at 5 minutes but goes down below pre-stimulation levels after (at times when BDNF-induced phosphorylation of other known targets remains very high). This is ignored in favour of discussion/investigation of initial increases, and the fact that BDNF does many things (which might indirectly contribute to initial but unsustained changes to pLRRK2) is not addressed.*

We thank the Reviewer for raising this important point, which we agree deserves additional investigation. Although phosphorylation does decrease below pre-stimulation levels, a reduction is also observed for ERK/AKT upon sustained exposure to BDNF in our experimental paradigm (figure 1F-G). This phenomenon is well known in response to a number of extracellular stimuli and can be explained by mechanisms related to cellular negative feedback regulation, receptor desensitization (e.g. phosphorylation or internalization), or cellular adaptation. The effect on pSer935, however, is peculiar as phosphorylation goes below the unstimulated level, as pointed by the reviewer. In contrast to ERK and AKT whose phosphorylation is almost absent under unstimulated conditions (Figure 1F-G), the stoichiometry of Ser935 phosphorylation under unstimulated conditions is high. This observation is consistent with MS determination of relative abundance of pSer935 (e.g. in whole brain LRRK2 is nearly 100% phosphorylated at Ser935, see Nirujogi et al., Biochem J 2021). Thus we hypothesized that the modest increase in phosphorylation driven by BDNF likely reflects a saturation or ceiling effect, indicating that the phosphorylation level is already near its maximum under resting conditions. Prolonged BDNF stimulation would bring phosphorylation down below pre-stimulation levels, through negative feedback mechanisms (e.g. phosphatase activity) explained above. To test this hypothesis, we conducted an experiment in conditions where LRRK2 is pretreated for 90 minutes with MLi-2 inhibitor, to reduce basal phosphorylation of S935. After MLi-2 washout, we stimulated with BDNF at different time points. We used GFP-LRRK2 stable lines for this experiment, since the ceiling effect was particularly evident (Figure S1A) and this model has been used for the interactomic study. As shown below (and incorporated in Fig. S1B in the manuscript), LRRK2 responds robustly to BDNF stimulation both in terms of pSer935 and pRABs. Phosphorylation peaks at 5-15 mins, while it decreases to unstimulated levels at 60 and 180 minutes. Notably, while the peak of pSer935 at 5-15 mins is similar to the untreated condition (supporting that Ser935 is nearly saturated in unstimulated conditions), the phosphorylation of RABs during this time period exceeds unstimulated levels. These findings support the notion that, under basal conditions, RAB phosphorylation is far from saturation. The antibodies used to detect RAB phosphorylation are the following: RAB10 Abcam # ab230261 e RAB8 (pan RABs) Abcam # ab230260.

Given the robust response of RAB10 phosphorylation upon BDNF stimulation, we further investigated RAB10 phosphorylation during BDNF stimulation in naïve SH-SY5Y cells. We confirmed that the increase in pSer935 is coupled to increase in pT73-RAB10. Also in this case, RAB10 phosphorylation does not go below the unstimulated level, which aligns with the low pRAB10 stoichiometry in brain (Nirujogi et al., Biochem J 2021). This experiment adds the novel and exciting finding that BDNF stimulation increases LRRK2 kinase activity (RAB phosphorylation) in neuronal cells.

Note that new supplemental figure 1 now includes: A) a comparison of LRRK2 pS935 and total protein levels before and after RA differentiation; B) differentiated GFP-LRRK2 SH-SY5Y (unstimulated, BDNF, MLi-2, BDNF+MLi-2); C) the kinetic of BDNF response in differentiated GFP-LRRK2 SH-SY5Y.

> *(b) Drebrin coIP itself looks like a very strong result, as does the increase after BDNF, but this was only demonstrated with a GFP over-expression construct despite several mouse and neuron models being employed elsewhere and available for copIP of endogenous LRRK2. Also, the coIP is only demonstrated in one direction. Similarly, the decrease in drebrin levels in mice is not assessed in the other model systems, coIP wasn't done, and mRNA transcripts are not quantified (even though others were). Drebrin phosphorylation state is not examined.*

We appreciate the Reviewer suggestions and provided additional experimental evidence supporting the functional relevance of LRRK2-drebrin interaction.

(1) As suggested, we performed qPCR and observed that 1 month-old KO midbrain and cortex express lower levels of Dbn1 as compared to WT brains (Figure 5G). This result is in agreement with the western blot data (Figure 5H).

(2)To further validate the physiological relevance of LRRK2-drebrin interaction we performed two experiments:

i) Western blots looking at pSer935 and pRab8 (pan Rab) in Dbn1 WT and knockout brains. As reported and quantified in Figure 2I, we observed a significant decrease in pSer935 and a trend decrease in pRab8 in Dbn1 KO brains. This finding supports the notion that Drebrin forms a complex with LRRK2 that is important for its activity, e.g. upon BDNF stimulation.

ii) Reverse co-immunoprecipitation of YFP-drebrin full-length, N-terminal domain (1-256 aa) and C-terminal domain (256-649 aa) (plasmids kindly received from Professor Phillip R. Gordon-Weeks, Worth et al., J Cell Biol, 2013) with Flag-LRRK2 co-expressed in HEK293T cells. As shown in supplementary Fig. S2C, we confirm that YFP-drebrin binds LRRK2, with the Nterminal region of drebrin appearing to be the major contributor to this interaction. This result is important as the N-terminal region contains the ADF-H (actin-depolymerising factor homology) domain and a coil-coil region known to directly bind actin (Shirao et al., J Neurochem 2017; Koganezawa et al., Mol Cell Neurosci. 2017). Interestingly, both full-length Drebrin and its truncated C-terminal construct cause the same morphological changes in Factin, indicating that Drebrin-induced morphological changes in F-actin are mediated by its N-terminal domains rather than its intrinsically disordered C-terminal region (Shirao et al., J Neurochem, 2017; Koganezawa et al., Mol Cell Neurosci. 2017). Given the role of LRRK2 in actin-cytoskeletal dynamics and its binding with multiple actin-related protein binding (Fig. 2 and Meixner et al., Mol Cell Proteomics. 2011; Parisiadou and Cai, Commun Integr Biol 2010), these results suggest the possibility that LRRK2 controls actin dynamics by competing with drebrin binding to actin and open new avenues for futures studies.

(3) To address the request for examining drebrin phosphorylation state, we decided to perform another phophoproteomic experiment, leveraging a parallel analysis incorporated

in our latest manuscript (Chen et al., Mol Theraphy 2025). In this experiment, we isolated total striatal proteins from WT and G2019S KI mice and enriched the phospho-peptides. Unlike the experiment presented in Fig. 7, phosphopeptides were enriched from total striatal lysates rather than synaptosomal fractions, and phosphorylation levels were normalized to the corresponding total protein abundance. This approach was intended to avoid bias toward synaptic proteins, allowing for the analysis of a broader pool of proteins derived from a heterogeneous ensemble of cell types (neurons, glia, endothelial cells, pericytes etc.). We were pleased to find that this new experiment confirmed drebrin S339 as a differentially phosphorylated site, with a 3.7 fold higher abundance in G2019S Lrrk2 KI mice. The fact that this experiment evidenced an increased phosphorylation stoichiometry in G2019S mice rather than a decreased is likely due to the normalization of each peptide by its corresponding total protein. Gene ontology analysis of differentially phosphorylated proteins using stringent term size (<200 genes) showed post-synaptic spines and presynaptic active zones as enriched categories (Fig. 3F). A SynGO analysis confirms both pre and postsynaptic categories, with high significance for terms related to postsynaptic cytoskeleton (Fig. 3G). As pointed, this is particularly interesting as the starting material was whole striatal tissue – not synaptosomes as previously – indicating that most significant phosphorylation differences occur in synaptic compartments. This once again reinforces our hypothesis that LRRK2 has a prominent role in the synapse. Overall, we confirmed with an independent phosphoproteomic analysis that LRRK2 kinase activity influences the phosphorylation state of proteins related to synaptic function, particularly postsynaptic cytoskeleton. For clarity in data presentation, as mentioned by the Reviewers, we removed Figure 7 and incorporated this new analysis in figure 3, alongside the synaptic cluster analysis.

Altogether, three independent OMICs approaches – (i) experimental LRRK2 interactomics in neuronal cells, (ii) a literature-based LRRK2 synaptic/cytoskeletal interactor cluster, and (iii) a phospho-proteomic analysis of striatal proteins from G2019S KI mice (to model LRRK2 hyperactivity) – converge to synaptic actin-cytoskeleton as a key hub of LRRK2 neuronal function.

> *(c) The large differences in the CRISPR KO cells in terms of BDNF responses are not seen in the primary neurons of KO mice, suggesting that other differences between the two might be responsible, rather than the lack of LRRK2 protein.*

Considering that some variability is expected for these type of cultures and across different species, any difference in response magnitude and kinetics could be attributed to the levels of TrKB and downstream components expressed by the two cell types.

We are confident that differentiated SH-SY5Y cells provide a reliable model for our study as we could translate the results obtained in SH-SY5Y cells in other models. However, to rule out the possibility that the more pronounced effect observed in SH-SY5Y KO cells as respect to Lrrk2 KO primary neurons was due to CRISPR off-target effect, we performed an off-target analysis. Specifically, we selected the first 8 putative off targets exhibiting a CDF (Cutting Frequency Determination) off-target-score >0.2.

As shown in supplemental file 1, sequence disruption was observed only in the LRRK2 ontarget site in LRRK2 KO SH-SY5Y cells, while the 8 off-target regions remained unchanged across the genotypes and relative to the reference sequence.

> *(d) No validation of hits in the G2019S mutant phosphoproteomics, and no other assays related to the rest of the paper/conclusions. Drebrin phosphorylation is different but unvalidated, or related to previous data sets beyond some discussion. The fact that LRRK2 binding occurs, and increases with BDNF stimulation, should be compared to its phosphorylation status and the effects of the G2019S mutation.*

As illustrated in the response to point (b), we performed a new phosphoproteomics investigation – with total striatal lysates instead of striatal synaptosomes and normalization phospho-peptides over total proteins – and found that S339 phosphorylation increases when LRRK2 kinase activity increases (G2019S). To address the request of validating drebrin phosphorylation, the main limitation is that there are no available antibodies against Ser339. While we tried phos-Tag gels in striatal lysates, we could not detect any reliable and specific signal with the same drebrin antibody used for western blot (Thermo Fisher Scientific: MA120377) due to technical limitations of the phosTag method. We are confident that phosphorylation at S339 has a physiological relevance, as it was identified 67 times across multiple proteomic discovery studies and they are placed among the most frequently phosphorylated sites in drebrin (https://www.phosphosite.org/proteinAction.action?id=2675&showAllSites=true).

To infer a possible role of this phosphorylation, we looked at the predicted pathogenicity of using AlphaMissense (Cheng et al., Science 2023). included as supplementary figure (Fig. S3), aminoacid substitutions within this site are predicted not to be pathogenic, also due to the low confidence of the AlphaFold structure.

Ser339 in human drebrin is located just before the proline-rich region (PP domain) of the protein. This region is situated between the actin-binding domains and the C-terminal Homerbinding sequences and plays a role in protein-protein interactions and cytoskeletal regulation (Worth et al., J Cell Biol, 2013). Of interest, this region was previously shown to be the interaction site of adafin (ADFN), a protein involved in multiple cytoskeletal-related processes, including synapse formation and function by regulating puncta adherentia junctions, presynaptic differentiation, and cadherin complex assembly, which are essential for hippocampal excitatory synapses, spine formation, and learning and memory processes (Beaudoin, G. M., 3rd et al., J Neurosci, 2013). Of note, adafin is in the list of LRRK2 interacting proteins (https://www.ebi.ac.uk/intact/home), supporting a possible functional relevance of LRRK2-mediated drebrin phosphorylation in adafin-drebrin complex formation. This has been discussed in the discussion section.

The aim of this MS analysis in G2019S KI mice – now included in figure 3 – was to further validate the crucial role of LRRK2 kinase activity in the context of synaptic regulation, rather than to discover and characterize novel substrates. Consequently, Figure 7 has been eliminated.

> ***Reviewer #2 (Public Review):***
>
> *Taken as a whole, the data in the manuscript show that BDNF can regulate PD-associated kinase LRRK2 and that LRRK2 modifies the BDNF response. The chief strength is that the data provide a potential focal point for multiple observations across many labs. Since LRRK2 has emerged as a protein that is likely to be part of the pathology in both sporadic and LRRK2 PD, the findings will be of broad interest. At the same time, the data used to imply a causal throughline from BDNF to LRRK2 to synaptic function and actin cytoskeleton (as in the title) are mostly correlative and the presentation often extends beyond the data. This introduces unnecessary confusion. There are also many methodological details that are lacking or difficult to find. These issues can be addressed.*

We appreciate the Reviewer's positive feedback on our study. We also value the suggestion to present the data in a more streamlined and coherent way. In response, we have updated the title to better reflect our overall findings: "LRRK2 Regulates Synaptic Function through Modulation of Actin Cytoskeletal Dynamics." Additionally, we have included several experiments that we believe enhance and unify the study.

> *(1) The writing/interpretation gets ahead of the data in places and this was confusing. For example, the abstract highlights prior work showing that Ser935 LRRK2 phosphorylation changes LRRK2 localization, and Figure 1 shows that BDNF rapidly increases LRRK2 phosphorylation at this site. Subsequent figures highlight effects at synapses or with synaptic proteins. So is the assumption that LRRK2 is recruited to (or away from) synapses in response to BDNF? Figure 2H shows that LRRK2-drebrin interactions are enhanced in response to BDNF in retinoic acid-treated SH-SY5Y cells, but are synapses generated in these preps? How similar are these preps to the mouse and human cortical or mouse striatal neurons discussed in other parts of the paper (would it be anticipated that BDNF act similarly?) and how valid are SHSY5Y cells as a model for identifying synaptic proteins? Is drebrin localization to synapses (or its presence in synaptosomes) modified by BDNF treatment +/- LRRK2? Or do LRRK2 levels in synaptosomes change in response to BDNF? The presentation requires re-writing to stay within the constraints of the data or additional data should be added to more completely back up the logic.*

We thank the Reviewer for the thorough suggestions and comments. We have extensively revised the text to accurately reflect our findings without overinterpreting. In particular, we agree with the Reviewer that differentiated SH-SY5Y cells are not identical to primary mouse or human neurons; however both neuronal models respond to BDNF. Supporting our observations, it is known that SH-SY5Y cells respond to BDNF. In fact, a common protocol for differentiating SH-SY5Y cells involve BDNF in combination with retinoic acid (Martin et al., Front Pharmacol, 2022; Kovalevich et al., Methods in mol bio, 2013). Additionally, it has been reported that SH-SY5Y cells can form functional synapses (Martin et al., Front Pharmacol, 2022). While we are aware that BDNF, drebrin or LRRK2 can also affect non-synaptic pathways, we focused on synapses when moved to mouse models since: (i) MS and phosphoMS identified several cytoskeletal proteins enriched at the synapse, (ii) we and others have previously reported a role for LRRK2 in governing synaptic and cytoskeletal related processes; (iii) the synapse is a critical site that becomes dysfunctional in the early stages of PD. We have now clarified and adjusted the text as needed. We have also performed additional experiments to address the Reviewer's concern:

(1) "Is the assumption that LRRK2 is recruited to (or away from) synapses in response to BDNF"? This is a very important point. There is consensus in the field that detecting endogenous LRRK2 in brain slices or in primary neurons via immunofluorescence is very challenging with the commercially available antibodies (Fernandez et al., J Parkinsons Dis, 2022). We established a method in our previous studies to detect LRRK2 biochemically in synaptosomes (Cirnaru et al., Front Mol Neurosci, 2014; Belluzzi et al., Mol Neurodegener., 2016). While these data indicate LRRK2 is present in the synaptic compartments, it would be quite challenging to apply this method to the present study. In fact, applying acute BDNF stimulation in vivo and then isolate synaptosomes is a complex experiment beyond the timeframe of the revision due to the need of mouse ethical approvals. However, this is definitely an intriguing angle to explore in the future.

> *(2)"Is drebrin localization to synapses (or its presence in synaptosomes) modified by BDNF treatment +/- LRRK2?" To try and address this question, we adapted a previously published assay to measure drebrin exodus from dendritic spines. During calcium entry and LTP, drebrin exits dendritic spines and accumulates in the dendritic shafts and cell body (Koganezawa et al., 2017). This facilitates the reorganization of the actin cytoskeleton (Shirao et al., 2017). Given the known role of drebrin and its interaction with LRRK2, we hypothesized that LRRK2 loss might affect drebrin relocalization during spine maturation.*

To test this, we treated DIV14 primary cortical neurons from Lrrk2 WT and KO mice with BDNF for 5, 15, and 24 hours, then performed confocal imaging of drebrin localization (Author response image 1). Neurons were transfected at DIV4 with GFP (cell filler) and PSD95 (dendritic spines) for visualization, and endogenous drebrin was stained with an anti-drebrin antibody. We then measured drebrin's overlap with PSD95-positive puncta to track its localization at the spine.

In Lrrk2 WT neurons, drebrin relocalized from spines after BDNF stimulation, peaking at 15 minutes and showing higher co-localization with PSD95 at 24 hours, indicating the spine remodeling occurred. In contrast, Lrrk2 KO neurons showed no drebrin exodus. These findings support the notion that LRRK2's interaction with drebrin is important for spine remodeling via BDNF. However, additional experiments with larger sample sizes are needed, which were not feasible within the revision timeframe (here n=2 experiments with independent neuronal preparations, n=4-7 neurons analyzed per experiment). Thus, we included the relevant figure as Author response image 1 but chose not to add it in the manuscript (figure 3).

**Author response image 1.**

Lrrk2 affects drebrin exodus from dendritic spines. After the exposure to BDNF for different times (5 minutes, 15 minutes and 24 hours), primary neurons from Lrrk2 WT and KO mice have been transfected with GFP and PSD95 and stained for endogenous drebrin at DIV4. The amount of drebrin localizing in dentritic spines outlined by PSD95 has been assessed at DIV14. The graph shows a pronounced decrease in drebrin content in WT neurons during short time treatments and an increase after 24 hours. KO neurons present no evident variations in drebrin localization upon BDNF stimulation. Scale bar: 4 µm.

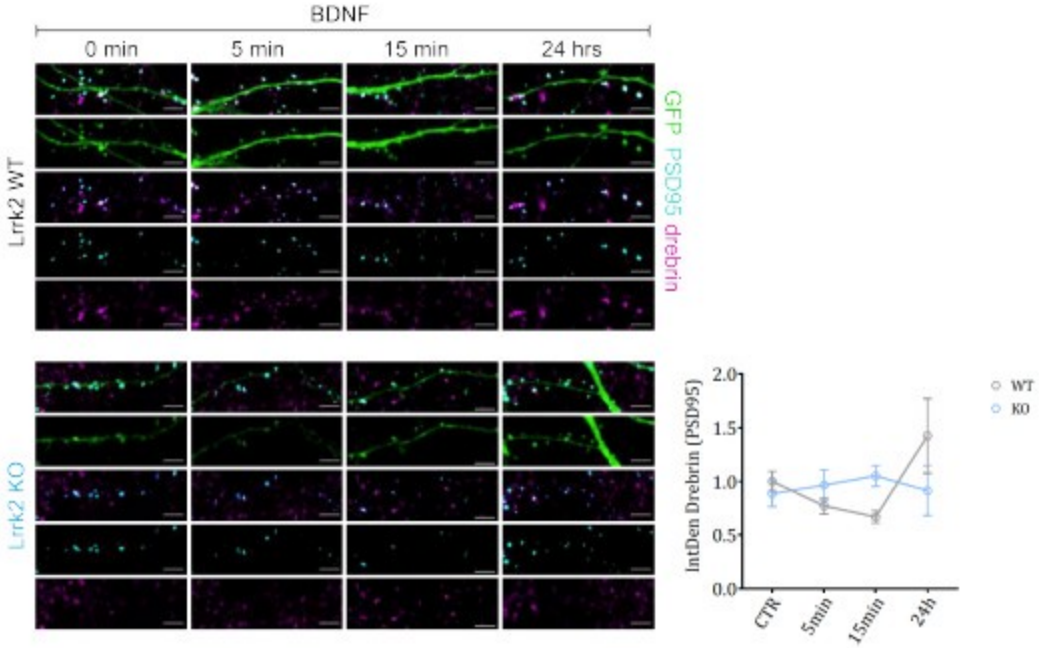


> *(2) The experiments make use of multiple different kinds of preps. This makes it difficult at times to follow and interpret some of the experiments, and it would be of great benefit to more assertively insert "mouse" or "human" and cell type (cortical, glutamatergic, striatal, gabaergic) etc.*

We thank the Reviewer for pointing this out. We have now more clearly specified the cell type and species identity throughout the text to improve clarity and interpretation.

> *(3) Although BDNF induces quantitatively lower levels of ERK or Akt phosphorylation in LRRK2KO preps based on the graphs (Figure 4B, D), the western blot data in Figure 4C make clear that BDNF does not need LRRK2 to mediate either ERK or Akt activation in mouse cortical neurons and in 4A, ERK in SH-SY5Y cells. The presentation of the data in the results (and echoed in the discussion) writes of a "remarkably weaker response". The data in the blots demand more nuance. It seems that LRRK2 may potentiate a response to BDNF that in neurons is independent of LRRK2 kinase activity (as noted). This is more of a point of interpretation, but the words do not match the images.*

We thank the Reviewer for pointing this out. We have rephrased our data presentation to better convey our findings. We were not surprised to find that loss of LRRK2 causes only a reduction of ERK and AKT activation upon BDNF rather than a complete loss. This is because these pathways are complex and redundant and are activated by a number of cellular effectors. The fact that LRRK2 is one among many players whose function can be compensated by other signaling molecules is also supported by the phenotype of Lrrk2 KO mice that is measurable at 1 month but disappears with adulthood (4 and 18 months) (figure 5).

Moreover, we removed the sentence “Of note, 90 mins of Lrrk2 inhibition (MLi-2) prior to BDNF stimulation did not prevent phosphorylation of Akt and Erk1/2, suggesting that LRRK2 participates in BDNF-induced phosphorylation of Akt and Erk1/2 independently from its kinase activity but dependently from its ability to be phosphorylated at Ser935 (Fig. 4C-D and Fig. 1B-C)” since the MLi-2 treatment prior to BDNF stimulation was not quantified and our new data point to an involvement of LRRK2 kinase activity upon BDNF stimulation.

> *(4) Figure 4F/G shows an increase in PSD95 puncta per unit length in response to BDNF in mouse cortical neurons. The data do not show spine induction/dendritic spine density/or spine morphogenesis as suggested in the accompanying text (page 8). Since the neurons are filled/express gfp, spine density could be added or spines having PSD95 puncta. However, the data as reported would be expected to reflect spine and shaft PSDs and could also include some nonsynaptic sites.*

The Reviewer is right. We have rephrased the text to reflect an increase in postsynaptic density (PSD) sites, which may include both spine and shaft PSDs, as well as potential nonsynaptic sites.

> *(5) Experimental details are missing that are needed to fully interpret the data. There are no electron microscopy methods outside of the figure legend. And for this and most other microscopy-based data, there are few to no descriptions of what cells/sites were sampled, how many sites were sampled, and how regions/cells were chosen. For some experiments (like Figure 5D), some detail is provided in the legend (20 segments from each mouse), but it is not clear how many neurons this represents, where in the striatum these neurons reside, etc. For confocal z-stacks, how thick are the optical sections and how thick is the stack? The methods suggest that data were analyzed as collapsed projections, but they cite Imaris, which usually uses volumes, so this is confusing. The guide (sgRNA) sequences that were used should be included. There is no mention of sex as a biological variable.*

We thank the Reviewer for pointing out this missing information. We have now included:

(1) EM methods (page 24)

(2) Methods for ICC and confocal microscopy now incorporates the Z-stack thickness (0.5 µm x 6 = 3 µm) on page 23.

(3) Methods for Golgi-Cox staining now incorporates the Z-stack thickness and number of neurons and segments per neuron analyzed.

(4) The sex of mice is mentioned in the material and methods (page 17): “Approximately equal numbers of males and females were used for every experiment”.

> *(6) For Figures 1F, G, and E, how many experimental replicates are represented by blots that are shown? Graphs/statistics could be added to the supplement. For 1C and 1I, the ANOVA p-value should be added in the legend (in addition to the post hoc value provided).*

The blots relative to figure 1F,G and E are representative of several blots (at least n=5). The same redouts are part of figure 4 where quantifications are provided. We added the ANOVA p-value in the legend for figure 1C, 1I and 1K.

> *(7) Why choose 15 minutes of BDNF exposure for the mass spec experiments when the kinetics in Figure 1 show a peak at 5 mins?*

This is an important point. We repeated the experiment in GFP-LRRK2 SH-SY5Y cells (figure S1C) and included the 15 min time point. In addition to confirming that pSer935 increases similarly at 5 and 15 minutes, we also observed an increase in RAB phosphorylation at these time points. As mentioned in our response to Reviewer’s 1, we pretreated with MLi-2 for 90 minutes in this experiment to reduce the high basal phosphorylation stoichiometry of pSer935.

> *(8) The schematic in Figure 6A suggests that iPSCs were plated, differentiated, and cultured until about day 70 when they were used for recordings. But the methods suggest they were differentiated and then cryopreserved at day 30, and then replated and cultured for 40 more days. Please clarify if day 70 reflects time after re-plating (30+70) or total time in culture (70). If the latter, please add some notes about re-differentiation, etc.*

We thank the reviewer for providing further clarity on the iPSC methodology. In the submitted manuscript 70DIV represents the total time in vitro and the process involved a cryostorage event at 30DIV, with a thaw of the cells and a further 40 days of maturation before measurement. We have adjusted the methods in both the text and figure (new schematic) to clarify this. The cryopreservation step has been used in other iPSC methods to great effect (Drummond et al., Front Cell Dev Biol, 2020). Due to the complexity and length of the iPSC neuronal differentiation process, cryopreservation represents a useful method with which to shorten and enhance the ability to repeat experiments and reduce considerable variation between differentiations. User defined differences in culture conditions for each batch of neurons thawed can usefully be treated as a new and separate N compared to the next batch of neurons.

> *(9) When Figures 6B and 6C are compared it appears that mEPSC frequency may increase earlier in the LRRK2KO preps than in the WT preps since the values appear to be similar to WT + BDNF. In this light, BDNF treatment may have reached a ceiling in the LRRK2KO neurons.*

We thank the reviewer for his/her comment and observations about the ceiling effects. It is indeed possible that the loss of LRRK2 and the application of BDNF could cause the same

elevation in synaptic neurotransmission. In such a situation, the increased activity as a result of BDNF treatment would be masked by the increased activity observed as a result of LRRK2 KO. To better visualize the difference between WT and KO cultures and the possible ceiling effect, we merged the data in one single graph.

> *(10) Schematic data in Figures 5A and C and Figures 5B and E are too small to read/see the data.*

We thank the Reviewer for this suggestion. We have now enlarged figure 5A and moved the graph of figure 5D in supplemental figure S5, since this analysis of spine morphology is secondary to the one shown in figure 5C.

> ***Reviewer #1 (Recommendations For The Authors):***
>
> *Please forgive any redundancy in the comments, I wanted to provide the authors with as much information as I had to explain my opinion.*
>
> *Primary mouse cortical neurons at div14, 20% transient increase in S935 pLRRK2 5min after BDNF, which then declines by 30 minutes (below pre-stim levels, and maybe LRRK2 protein levels do also).*
>
> *In differentiated SHSY5Y cells there is a large expected increase in pERK and pAKT that is sustained way above pre-stim for 60 minutes. There is a 50% initial increase in pLRRK2 (but the blot is not very clear and no double band in these cells), which then looks like reduced well below pre-stim by 30 & 60 minutes.*

We thank the Reviewer for bring up this important point. We have extensively addressed this issue in the public review rebuttal. In essence, the phosphorylation of Ser935 is near saturation under unstimulated conditions, as evidenced by its high basal stoichiometry, whereas Rab phosphorylation is far from saturation, showing an increase upon BDNF stimulation before returning to baseline levels. This distinction highlights that while pSer935 exhibits a ceiling effect due to its near-maximal phosphorylation at rest, pRab responds dynamically to BDNF, indicating low basal phosphorylation and a significant capacity for increase. Figure 1 in the rebuttal summarizes the new data collected.

> *GFP-fused overexpressed LRRK2 coIPs with drebrin, and this is double following 15 min BDNF. Strong result.*

We thank the Reviewer.

> *BDNF-induced pAKT signaling is greatly impaired, and pERK is somewhat impaired, in CRISPR LKO SHSY5Y cells. In mouse primaries, both AKT and Erk phosph is robustly increased and sustained over 60 minutes in WT and LKO. This might be initially less in LKO for Akt (hard to argue on a WB n of 3 with huge WT variability), regardless they are all roughly the same by 60 minutes and even look higher in LKO at 60. This seems like a big disconnect and suggests the impairment in the SHSy5Y cells might have more to do with the CRISPR process than the LRRK2. Were the cells sequenced for off-target CRISPR-induced modifications?*

Following the Reviewer suggestion – and as discussed in the public review section - we performed an off-target analysis. Specifically, we selected the first 8 putative off targets exhibiting a CDF (Cutting Frequency Determination) off-target-score >0.2. As shown in supplemental file 1, sequence disruption was observed only in the LRRK2 on-target site in LRRK2 KO SH-SY5Y cells, while the 8 off-target regions remained unchanged across the genotypes and relative to the reference sequence.

> *No difference in the density of large PSD-95 puncta in dendrites of LKO primary relative to WT, and the small (10%) increase seen in WT after BDNF might be absent in LKO (it is not clear to me that this is absent in every culture rep, and the data is not highly convincing). This is also referred to as spinogenesis, which has not been quantified. Why not is confusing as they did use a GFP fill…*

The Reviewer is right that spinogenesis is not the appropriate term for the process analyzed. We replaced “spinogenesis” with “morphological alternation of dendritic protrusions” or “synapse maturation” which is correlated with the number of PSD95 positive puncta (ElHusseini et al., Science, 2000) .

> *There is a difference in the percentage of dendritic protrusions classified as filopodia to more being classified as thin spines in LKO striatal neurons at 1 month, which is not seen at any other age, The WT filopodia seems to drop and thin spine percent rise to be similar to LKO at 4 months. This is taken as evidence for delayed maturation in LKO, but the data suggest the opposite. These authors previously published decreased spine and increased filopodia density at P15 in LKO. Now they show that filopodia density is decreased and thin spine density increased at one month. How is that shift from increased to decreased filopodia density in LKO (faster than WT from a larger initial point) evidence of impaired maturation? Again this seems accelerated?*

We agree with the Reviewer that the initial interpretation was indeed confusing. To adhere closely to our data and avoid overinterpretation – as also suggested by Reviewer 2 – we revised the text and moved figure 5D to supplementary materials. In essence, our data point out to alterations in the structural properties of dendritic protrusions in young KO mice, specifically a reduction in their size (head width and neck height) and a decrease in postsynaptic density (PSD) length, as observed with TEM. These findings suggest that LRRK2 is involved in morphological processes during spine development.

> *Shank3 and PSD95 mRNA transcript levels were reduced in the LKO midbrain, only shank3 was reduced in the striatum and only PSD was reduced in the cortex. No changes to mRNA of BDNF-related transcripts. None of these mRNA changes protein-validated. Drebrin protein (where is drebrin mRNA?) levels are reduced in LKO at 1&4 but not clearly at 18 months (seems the most robust result but doesn't correlate with other measures, which here is basically a transient increase (1m) in thin striatal spines).*

As illustrated before, we performed qPCR for Dbn1 and found that its expression is significantly reduced in the cortex and midbrain and non-significantly reduced in the striatum (1 months old mice, a different cohort as those used for the other analysis in figure 5).

> *24h BDNF increases the frequency of mEPSCs on hIPSC-derived cortical-like neurons, but not LKO, which is already high. There are no details of synapse number or anything for these cultures and compares 24h treatment. BDNF increases mEPSC frequency within minutes PMC3397209, and acute application while recording on cells may be much more informative (effects of BDNF directly, and no issues with cell-cell / culture variability). Calling mEPSC "spontaneous electrical activity" is not standard.*

We thank the reviewer for this point. We provided information about synapse number (Bassoon/Homer colocalization) in supplementary figure S7. The lack of response of LRRK2 KO cultures in terms of mEPSC is likely due to increase release probability as the number of synapses does not change between the two genotypes.

> *The pattern of LRRK2 activation is very disconnected from that of BDNF signalling onto other kinases. Regarding pLRRK2, s935 is a non-autophosph site said to be required for LRRK2 enzymatic activity, that is mostly used in the field as a readout of successful LRRK2 inhibition, with some evidence that this site regulates LRRK2 subcellular localization (which might be more to do with whether or not it is p at 935 and therefor able to act as a kinase).*
>
> *The authors imply BDNF is activating LRRK2, but really should have looked at other sites, such as the autophospho site 1292 and 'known' LRRK2 substrates like T73 pRab10 (or other e.g., pRab12) as evidence of LRRK2 activation. One can easily argue that the initial increase in pLRRK2 at this site is less consequential than the observation that BDNF silences LRRK2 activity based on p935 being sustained to being reduced after 5 minutes, and well below the prestim levels... not that BDNF activates LRRK2.*

As described above, we have collected new data showing that BDNF stimulation increases LRRK2 kinase activity toward its physiological substrates Rab10 and Rab8 (using a panphospho-Rab antibody) (Figure 1 and Figure S1). Additionally, we have also extensively commented the ceiling effect of pS935.

> *BDNF does a LOT. What happens to network activity in the neural cultures with BDNF application? Should go up immediately. Would increasing neural activity (i.e., through depolarization, forskolin, disinhibition, or something else without BDNF) give a similar 20% increase in pS935 LRRK2? Can this be additive, or occluded? This would have major implications for the conclusions that BDNF and pLRRK2 are tightly linked (as the title suggests).*

These are very valuable observations; however, they fall outside the scope and timeframe of this study. We agree that future research should focus on gaining a deeper mechanistic understanding of how LRRK2 regulates synaptic activity, including vesicle release probability and postsynaptic spine maturation, independently of BDNF.

> *Figures 1A & H "Western blot analysis revealed a rapid (5 mins) and transient increase of Ser935 phosphorylation after BDNF treatment (Fig. 1B and 1C). Of interest, BDNF failed to stimulate Ser935 phosphorylation when neurons were pretreated with the LRRK2 inhibitor MLi-2" . The first thing that stands out is that the pLRRK2 in WB is not very clear at all (although we appreciate it is 'a pig' to work with, I'd hope some replicates are clearer); besides that, the 20% increase only at 5min post-BDNF stimulation seems like a much less profound change than the reduction from base at 60 and more at 180 minutes (where total LRRK2 protein is also going down?). That the blot at 60 minutes in H is representative of a 30% reduction seems off... makes me wonder about the background subtraction in quantification (for this there is much less pLRRK2 and more total LRRK2 than at 0 or 5). LRRK2 (especially) and pLRRK2 seem very sketchy in H. Also, total LRRK2 appears to increase in the SHSY5Y cell not the neurons, and this seems even clearer in 2 H.*

To better visualize the dynamics of pS935 variation relative to time=0, we presented the data as the difference between t=0 and t=x. It clearly shows that pSe935 goes below prestimulation levels, whereas pRab10 does not. The large difference in the initial stoichiometry of these two phosphorylation is extensively discussed above.

> *That MLi2 eliminates pLRRK2 (and seems to reduce LRRK2 protein?) isn't surprising, but a 90min pretreatment with MLi-2 should be compared to MLi-2's vehicle alone (MLi-2 is notoriously insoluble and the majority of diluents have bioactive effects like changing*

> *activity)... especially if concluding increased pLRRK2 in response to BDNF is a crucial point (when comparing against effects on other protein modifications such as pAKT). This highlights a second point... the changes to pERK and pAKT are huge following BDNF (nothing to massive quantities), whereas pLRRK2 increases are 20-50% at best. This suggests a very modest effect of BDNF on LRRK in neurons, compared to the other kinases. I worry this might be less consequential than claimed. Change in S1 is also unlikely to be significant...*

These comments have been thoroughly addressed in the previous responses. Regarding fig. S1, we added an additional experiment (Figure S1C) in GFP-LRRK2 cells showing robust activation of LRRK2 (pS935, pRabs) at the timepoint of MS (15 min).

> *"As the yields of endogenous LRRK2 purification were insufficient for AP-MS/MS analysis, we generated polyclonal SH-SY5Y cells stably expressing GFP-LRRK2 wild-type or GFP control (Supplementary Fig. 1)" . I am concerned that much is being assumed regarding 'synaptic function' from SHSY5Y cells... also overexpressing GFP-LRRK2 and looking at its binding after BDNF isn't synaptic function.*

We appreciate the reviewer's comment. We would like to clarify that the interactors enriched upon BDNF stimulation predominantly fall into semantic categories related to the synapse and actin cytoskeleton. While this does not imply that these interactors are exclusively synaptic, it suggests that this tightly interconnected network likely plays a role in synaptic function. This interpretation is supported by several lines of evidence: (1) previous studies have demonstrated the relevance of this compartment to LRRK2 function; (2) our new phosphoproteomics data from striatal lysate highlight enrichment of synaptic categories; and (3) analysis of the latest GWAS gene list (134 genes) also indicates significant enrichment of synapse-related categories. Taken together, these findings justify further investigation into the role of LRRK2 in synaptic biology, as discussed extensively in the manuscript's discussion section.

> *Figure 2A isn't alluded to in text and supplemental table 1 isn't about LRRK2 binding, but mEPSCs.*

We have added Figure 2A and added supplementary .xls table 1, which refers to the excel list of genes with modulated interaction upon BDNF (uploaded in the supplemental material).

We added the extension .xls also for supplementary table 2 and 3.

> *Figure 2A is useless without some hits being named, and the donut plots in B add nothing beyond a statement that "35% of 'genes' (shouldn't this be proteins?) among the total 207 LRRK2 interactors were SynGO annotated" might as well [just] be the sentence in the text.*

We have now included the names of the most significant hits, including cytoskeletal and translation-related proteins, as well as known LRRK2 interactors. We decided to retain the donut plots, as we believe they simplify data interpretation for the reader, reducing the need to jump back and forth between the figures and the text.

> *Validation of drebrin binding in 2H is great... although only one of 8 named hits; could be increased to include some of the others. A concern alludes to my previous point... there is no appreciable LRRK2 in these cells until GFP-LRRK2 is overexpressed; is this addressed in the MS? Conclusions would be much stronger if bidirectional coIP of these binding candidates were shown with endogenous (GFP-ve) LRRK2 (primaries or hIPSCs, brain tissue?)*

To address the Reviewer's concerns to the best of our abilities, we have added a blot in Supplemental figure S1A showing how the expression levels of LRRK2 increase after RA differentiation. Moreover, we have included several new data further strengthening the functional link between LRRK2 and drebrin, including qPCR of Dbn1 in one-month old Lrrk2 KO brains, western blots of Lrrk2 and Rab in Dbn1 KO brains, and co-IP with drebrin N- and Cterm domains.

> *Figures 3 A-C are not informative beyond the text and D could be useful if proteins were annotated.*

To avoid overcrowding, proteins were annotated in A and the same network structure reported for synaptic and actin-related interactors.

> *Figure 4. Is this now endogenous LRRK2 in the SHSY5Y cells? Again not much LRRK2 though, and no pLRRK shown.*

We confirm that these are naïve SH-SY5Y cells differentiated with RA and LRRK2 is endogenous. We did not assess pS935 in this experiment, as the primary goal was to evaluate pAKT and pERK1/2 levels. To avoid signal saturation, we loaded less total protein (30 µg instead of the 80 µg typically required to detect pS935). pS935 levels were extensively assessed in Figure 1. This experimental detail has now been added in the material and methods section (page 18).

> *In C (primary neurons) There is very little increase in pLRRK2 / LRRK2 at 5 mins, and any is much less profound a change than the reduction at 30 & 60 mins. I think this is interesting and may be a more substantial consequence of BDNF treatment than the small early increase. Any 5 min increase is gone by 30 and pLRRK2 is reduced after. This is a disconnect from the timing of all the other pProteins in this assay, yet pLRRK2 is supposed to be regulating the 'synaptic effects'?*

The first part of the question has already been extensively addressed. Regarding the timing, one possibility is that LRRK2 is activated upstream of AKT and ERK1/2, a hypothesis supported by the reduced activation of AKT and ERK1/2 observed in LRRK2 KO cells, as discussed in the manuscript, and in MLi-2 treated cells (Author response image 2). Concerning the synaptic effects, it is well established that synaptic structural and functional plasticity occurs downstream of receptor activation and kinase signaling cascades. These changes can be mediated by both rapid mechanisms (e.g., mobilization of receptor-containing endosomes via the actin cytoskeleton) and slower processes involving gene transcription of immediate early genes (IEGs). Since structural and functional changes at the synapse generally manifest several hours after stimulation, we typically assessed synaptic activity and structure 24 hours post-stimulation.

> *Akt Erk1&2 both go up rapidly after BDNF in WT, although Akt seems to come down with pLRRK2. If they aren't all the same Akt is probably the most different between LKO and WT but I am very concerned about an n=3 for wb, wb is semi-quantitative at best, and many more than three replicates should be assessed, especially if the argument is that the increases are quantitively different between WT v KO (huge variability in WT makes me think if this were done 10x it would all look same). Moreover, this isn't similar to the LKO primaries "pulled pups" pooled presumably.*

Despite some variability in the magnitude of the pAKT/pERK response in naïve SH-SY5Y cells, all three independent replicates consistently showed a reduced response in LRRK2 KO cells, yielding a highly significant result in the two-way ANOVA test. In contrast, the difference in

response magnitude between WT and LRRK2 KO primary cultures was less pronounced, which justified repeating the experiments with n=9 replicates. We hope the Reviewer acknowledges the inherent variability often observed in western blot experiments, particularly when performed in a fully independent manner (different cultures and stimulations, independent blots).

To further strengthen the conclusion that this effect is reproducible and dependent on LRRK2 kinase activity upstream of AKT and ERK, we probed the membranes in figure 1H with pAKT/total AKT and pERK/total ERK. All things considered and consistent with our hypothesis, MLi-2 significantly reduced BDNF-mediated AKT and ERK1/2 phosphorylation levels (Author response image 2).

**Author response image 2.**

Western blot (same experiments as in figure 1) was performed using antibodies against phospho-Thr202/185 ERK1/2, total ERK1/2 and phospho-Ser473 AKT, total AKT protein levels Retinoic acid-differentiated SH-SY5Y cells stimulated with 100 ng/mL BDNF for 0, 5, 30, 60 mins. MLi-2 was used at 500 nM for 90 mins to inhibit LRRK2 kinase activity.

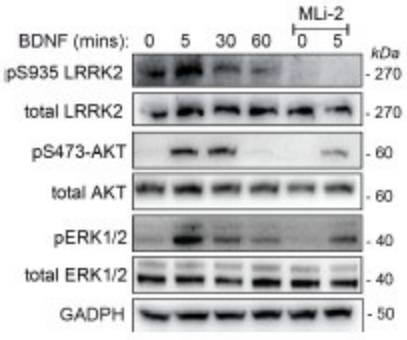


> *G lack of KO effect seems to be skewed from one culture in the plot (grey). The scatter makes it hard to read, perhaps display the culture mean +/- BDNF with paired bars. The fact that one replicate may be changing things is suggested by the weirdly significant treatment effect and no genotype effect. Also, these are GFP-filled cells, the dendritic masks should be shown/explained, and I'm very surprised no one counted the number (or type?) of protrusions, especially as the text describes this assay (incorrectly) as spinogenesis...*

As suggested by the Reviewer we have replotted the results as bar graphs. Regarding the number of protrusions, we initially counted the number of GFP+ puncta in the WT and did not find any difference (Author response image 3). Due to our imaging setup (confocal microscopy rather than super-resolution imaging and Imaris 3D reconstruction), we were unable to perform a fine morphometric analysis. However, this was not entirely unexpected, as BDNF is known to promote both the formation and maturation of dendritic spines. Therefore, we focused on quantifying PSD95+ puncta as a readout of mature postsynaptic compartments. While we acknowledge that we cannot definitively conclude that each PSD95+ punctum is synaptically connected to a presynaptic terminal, the data do indicate an increase in the number of PSD95+ structures following BDNF stimulation.

**Author response image 3.**

GFP+ puncta per unit of neurite length (μm) in DIV14 WT primary neurons untreated or upon 24 hour of BDNF treatment (100 ng/ml). No significant difference were observed (n=3).

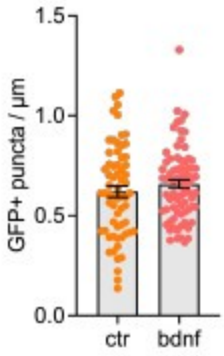


> *Figure 5. "Dendritic spine maturation is delayed in Lrrk2 knockout mice". The only significant change is at 1 month in KO which shows fewer filopodia and increased thin spines (50% vs wt). At 4 months the % of thin spines is increased to 60% in both... Filopodia also look like 4m in KO at 1m... How is that evidence for delayed maturation? If anything it suggests the KO spines are maturing faster. "the average neck height was 15% shorter and the average head width was 27% smaller, meaning that spines are smaller in Lrrk2 KO brains" - it seems odd to say this before saying that actually there are just MORE thin spines, the number of mature "mushroom' is same throughout, and the different percentage of thin comes from fewer filopodia. This central argument that maturation is delayed is not supported and could be backwards, at least according to this data. Similarly, the average PSD length is likely impacted by a preponderance of thin spines in KO... which if mature were fewer would make sense to say delayed KO maturation, but this isn't the case, it is the fewer filopodia (with no PSD) that change the numbers. See previous comments of the preceding manuscript.*

We agree that thin spines, while often considered more immature, represent an intermediate stage in spine development. The data showing an increase in thin spines at 1 month in the KO mice, along with fewer filopodia, could suggest a faster stabilization of these spines, which might indeed be indicative of premature maturation rather than delayed maturation. This change in spine morphology may indicate that the dynamics of synaptic plasticity are affected. Regarding the PSD length, as the Reviewer pointed out, the increased presence of thin spines in KO might account for the observed changes in PSD measurements, as thin spines typically have smaller PSDs. This further reinforces the idea that the overall maturation process may be altered in the KO, but not necessarily delayed.

We rephrase the interpretation of these data, and moved figure 5D as supplemental figure S4.

"To establish whether loss of Lrrk2 in young mice causes a reduction in dendritic spines size by influencing BDNF-TrkB expression" - there is no evidence of this.

We agree and reorganized the text, removing this sentence.

Shank and PSD95 mRNA changes being shown without protein adds very little. Why is drebrin RNA not shown? Also should be several housekeeping RNAs, not one (RPL27)?

We measured Dbn1 mRNA, which shows a significant reduction in midbrain and cortex. Moreover we have now normalized the transcript levels against the geometrical means of three housekeeping genes (RPL27, actin, and GAPDH) relative abundance.

> *Drebrin levels being lower in KO seems to be the strongest result of the paper so far (shame no pLRRK2 or coIP of drebrin to back up the argument). DrebrinA KO mice have*

> *normal spines, what about haploinsufficient drebrin mice (LKO seem to have half derbrin, but only as youngsters?)*

As extensively explained in the public review, we used Dbn1 KO mouse brains and were able to show reduced Lrrk2 activity.

> *Figure 6. hIPSC-derived cortical neurons. The WT 'cortical' neurons have a very low mEPSC frequency at 0.2Hz relative to KO. Is this because they are more or less mature? What is the EPSC frequency of these cells at 30 and 90 days for comparison? Also, it is very very hard to infer anything about mEPSC frequency in the absence of estimates of cell number and more importantly synapse number. Furthermore, where are the details of cell measures such as capacitance, resistance, and quality control e.g., Ra? Table s1 seems redundant here, besides suggesting that the amplitude is higher in KO at base.*

We agree that the developmental trajectory of iPSC-derived neurons is critical to accurately interpreting synaptic function and plasticity. In response, we have included additional data now presented in the supplementary figure S7 and summarize key findings below:

At DIV50, both WT and LRRK2 KO neurons exhibit low basal mEPSC activity (~0.5 Hz) and no response to 24 h BDNF stimulation (50 ng/mL).

At DIV70 WT neurons show very low basal activity (~0.2 Hz), which increases ~7.5-fold upon BDNF treatment (1.5 Hz; $p < 0.001$), and no change in synapse number. KO neurons display elevated basal activity (~1 Hz) similar to BDNF-treated WT neurons, with no further increase upon BDNF exposure (~1.3 Hz) and no change in synapse number.

At DIV90, no significant effect of BDNF in both WT and KO, indicating a possible saturation of plastic responses. The lack of BDNF response at DIV90 may be due to endogenous BDNF production or culture-based saturation effects. While these factors warrant further investigation (e.g., ELISA, co-culture systems), they do not confound the key conclusions regarding the role of LRRK2 in synaptic development and plasticity:

LRRK2 Enables BDNF-Responsive Synaptic Plasticity. In WT neurons, BDNF induces a significant increase in neurotransmitter release (mEPSC frequency) with no reduction in synapse number. This dissociation suggests BDNF promotes presynaptic functional potentiation. KO neurons fail to show changes in either synaptic function or structure in response to BDNF, indicating that LRRK2 is required for activity-dependent remodeling.

LRRK2 Loss Accelerates Synaptic Maturation. At DIV70, KO neurons already exhibit high spontaneous synaptic activity equivalent to BDNF-stimulated WT neurons. This suggests that LRRK2 may act to suppress premature maturation and temporally gate BDNF responsiveness, aligning with the differences in maturation dynamics observed in KO mice (Figure 5).

As suggested by the reviewer we reported the measurement of resistance and capacitance for all DIV (Table 1, supplemental material). A reduction in capacitance was observed in WT neurons at DIV90, which may reflect changes in membrane complexity. However, this did not correlate with differences in synapse number and is unlikely to account for the observed differences in mEPSC frequency. To control for cell number between groups, cell count prior to plating was performed (80k/cm2; see also methods) on the non-dividing cells to keep cell number consistent.

> *The presence of BDNF in WT seems to make them look like LKO, in the rest of the paper the suggestion is that the LKO lack a response to BDNF. Here it looks like it could be that BDNF signalling is saturated in LKO, or they are just very different at base and lack a response.*

> *Knowing which is important to the conclusions, and acute application (recording and BDNF wash-in) would be much more convincing.*

We agree with the Reviewer's point that saturation of BDNF could influence the interpretation of the data if it were to occur. However, it is important to note that no BDNF exists in the media in base control and KO neuronal culture conditions. This is different from other culture conditions and allows us to investigate the effects of BDNF treatment. Thus, the increased mEPSC frequency observed in KO neurons compared to WT neurons is defined only by the deletion of the gene and not by other extrinsic factors which were kept consistent between the groups. The lack of response or change in mEPSC frequency in KO is proposed to be a compensatory mechanism due to the loss of LRRK2. Of Note, LRRK2 as a "synaptic break" has already been described (Beccano-Kelly et al., Hum Mol Gen, 2015). However, a comprehensive analysis of the underlying molecular mechanisms will require future studies beyond with the scope of this paper.

> *"The LRRK2 kinase substrates Rabs are not present in the list of significant phosphopeptides, likely due to the low stoichiometry and/or abundance" Likely due to the fact mass spec does not get anywhere near everything.*

We removed this sentence in light of the new phosphoproteomic analysis.

> *Figure 7 is pretty stand-alone, and not validated in any way, hard to justify its inclusion?*

As extensively explained we removed figure 7 and included the new phospho-MS as part of figure. 3

> *Writing throughout shows a very selective and shallow use of the literature.*

We extensively reviewed the citations.

> *"while Lrrk1 transcript in this region is relatively stable during development" The authors reference a very old paper that barely shows any LRRK1 mRNA, and no protein. Others have shown that LRRK1 is essentially not present postnatally PMC2233633. This isn't even an argument the authors need to make.*

We thank the reviewer and included this more appropriate citation.

> ***Reviewer #2 (Recommendations For The Authors):***
>
> *Cyfip1 (Fig 3A) is part of the WAVE complex (page 13).*

We thank the reviewer and specified it.

> *The discussion could be more focused.*

We extensively revised the discussion to keep it more focused.

Note that we updated the GO ontology analyses to reflect the updated information present in g:Profiler.

References.

Nirujogi, R. S., Tonelli, F., Taylor, M., Lis, P., Zimprich, A., Sammler, E., & Alessi, D. R. (2021). Development of a multiplexed targeted mass spectrometry assay for LRRK2phosphorylated

Rabs and Ser910/Ser935 biomarker sites. The Biochemical journal, 478(2), 299–326. https://doi.org/10.1042/BCJ20200930

Worth, D. C., Daly, C. N., Geraldo, S., Oozeer, F., & Gordon-Weeks, P. R. (2013). Drebrin contains a cryptic F-actin-bundling activity regulated by Cdk5 phosphorylation. The Journal of cell biology, 202(5), 793–806. https://doi.org/10.1083/jcb.201303005

Shirao, T., Hanamura, K., Koganezawa, N., Ishizuka, Y., Yamazaki, H., & Sekino, Y. (2017). The role of drebrin in neurons. Journal of neurochemistry, 141(6), 819–834. https://doi.org/10.1111/jnc.13988

Koganezawa, N., Hanamura, K., Sekino, Y., & Shirao, T. (2017). The role of drebrin in dendritic spines. Molecular and cellular neurosciences, 84, 85–92. https://doi.org/10.1016/j.mcn.2017.01.004

Meixner, A., Boldt, K., Van Troys, M., Askenazi, M., Gloeckner, C. J., Bauer, M., Marto, J. A., Ampe, C., Kinkl, N., & Ueffing, M. (2011). A QUICK screen for Lrrk2 interaction partners--leucine-rich repeat kinase 2 is involved in actin cytoskeleton dynamics. Molecular & cellular proteomics: MCP, 10(1), M110.001172. https://doi.org/10.1074/mcp.M110.001172

Parisiadou, L., & Cai, H. (2010). LRRK2 function on actin and microtubule dynamics in Parkinson disease. Communicative & integrative biology, 3(5), 396–400. https://doi.org/10.4161/cib.3.5.12286

Chen, C., Masotti, M., Shepard, N., Promes, V., Tombesi, G., Arango, D., Manzoni, C., Greggio, E., Hilfiker, S., Kozorovitskiy, Y., & Parisiadou, L. (2024). LRRK2 mediates haloperidol-induced changes in indirect pathway striatal projection neurons. bioRxiv : the preprint server for biology, 2024.06.06.597594. https://doi.org/10.1101/2024.06.06.597594

Cheng, J., Novati, G., Pan, J., Bycroft, C., Žemgulytė, A., Applebaum, T., Pritzel, A.,Wong, L. H., Zielinski, M., Sargeant, T., Schneider, R. G., Senior, A. W., Jumper, J., Hassabis, D., Kohli, P., & Avsec, Ž. (2023). Accurate proteome-wide missense variant effect prediction with AlphaMissense. Science (New York, N.Y.), 381(6664), eadg7492. https://doi.org/10.1126/science.adg7492

Beaudoin, G. M., 3rd, Schofield, C. M., Nuwal, T., Zang, K., Ullian, E. M., Huang, B., & Reichardt, L. F. (2012). Afadin, a Ras/Rap effector that controls cadherin function, promotes spine and excitatory synapse density in the hippocampus. The Journal of neuroscience : the official journal of the Society for Neuroscience, 32(1), 99–110. https://doi.org/10.1523/JNEUROSCI.4565-11.2012

Fernández, B., Chittoor-Vinod, V. G., Kluss, J. H., Kelly, K., Bryant, N., Nguyen, A. P. T., Bukhari, S. A., Smith, N., Lara Ordóñez, A. J., Fdez, E., Chartier-Harlin, M. C., Montine, T. J., Wilson, M. A., Moore, D. J., West, A. B., Cookson, M. R., Nichols, R. J., & Hilfiker, S. (2022). Evaluation of Current Methods to Detect Cellular Leucine-Rich Repeat Kinase 2 (LRRK2) Kinase Activity. Journal of Parkinson's disease, 12(5), 1423–1447. https://doi.org/10.3233/JPD-213128

Cirnaru, M. D., Marte, A., Belluzzi, E., Russo, I., Gabrielli, M., Longo, F., Arcuri, L., Murru, L., Bubacco, L., Matteoli, M., Fedele, E., Sala, C., Passafaro, M., Morari, M., Greggio, E., Onofri, F., & Piccoli, G. (2014). LRRK2 kinase activity regulates synaptic vesicle trafficking and neurotransmitter release through modulation of LRRK2 macromolecular complex. Frontiers in molecular neuroscience, 7, 49. https://doi.org/10.3389/fnmol.2014.00049

Belluzzi, E., Gonnelli, A., Cirnaru, M. D., Marte, A., Plotegher, N., Russo, I., Civiero, L., Cogo, S., Carrion, M. P., Franchin, C., Arrigoni, G., Beltramini, M., Bubacco, L., Onofri, F., Piccoli, G., & Greggio, E. (2016). LRRK2 phosphorylates pre-synaptic Nethylmaleimide sensitive fusion

(NSF) protein enhancing its ATPase activity and SNARE complex disassembling rate. Molecular neurodegeneration, 11, 1. https://doi.org/10.1186/s13024-015-0066-z

Martin, E. R., Gandawijaya, J., & Oguro-Ando, A. (2022). A novel method for generating glutamatergic SH-SY5Y neuron-like cells utilizing B-27 supplement. Frontiers in pharmacology, 13, 943627. https://doi.org/10.3389/fphar.2022.943627

Kovalevich, J., & Langford, D. (2013). Considerations for the use of SH-SY5Y neuroblastoma cells in neurobiology. Methods in molecular biology (Clifton, N.J.), 1078, 9–21. https://doi.org/10.1007/978-1-62703-640-5_2

Drummond, N. J., Singh Dolt, K., Canham, M. A., Kilbride, P., Morris, G. J., & Kunath, T. (2020). Cryopreservation of Human Midbrain Dopaminergic Neural Progenitor Cells Poised for Neuronal Differentiation. Frontiers in cell and developmental biology, 8, 578907. https://doi.org/10.3389/fcell.2020.578907

Tao, X., Finkbeiner, S., Arnold, D. B., Shaywitz, A. J., & Greenberg, M. E. (1998). Ca2+ influx regulates BDNF transcription by a CREB family transcription factor-dependent mechanism. Neuron, 20(4), 709–726. https://doi.org/10.1016/s0896-6273(00)810107

El-Husseini, A. E., Schnell, E., Chetkovich, D. M., Nicoll, R. A., & Bredt, D. S. (2000). PSD95 involvement in maturation of excitatory synapses. Science (New York, N.Y.), 290(5495), 1364–1368.

Glebov OO, Cox S, Humphreys L, Burrone J. Neuronal activity controls transsynaptic geometry. Sci Rep. 2016 Mar 8;6:22703. doi: 10.1038/srep22703. Erratum in: Sci Rep. 2016 May 31;6:26422. doi: 10.1038/srep26422. PMID: 26951792; PMCID: PMC4782104.

Beccano-Kelly DA, Volta M, Munsie LN, Paschall SA, Tatarnikov I, Co K, Chou P, Cao LP, Bergeron S, Mitchell E, Han H, Melrose HL, Tapia L, Raymond LA, Farrer MJ, Milnerwood AJ. LRRK2 overexpression alters glutamatergic presynaptic plasticity, striatal dopamine tone, postsynaptic signal transduction, motor activity and memory. Hum Mol Genet. 2015 Mar 1;24(5):1336-49. doi: 10.1093/hmg/ddu543. Epub 2014 Oct 24. PMID: 25343991.

https://doi.org/10.7554/eLife.95987.2.sa0